COMPUTATIONAL APPROACHES FOR THE ANALYSIS OF CROP MONITORING USING SATELLITE IMAGES

Thesis Submitted for the Award of the Degree of

DOCTOR OF PHILOSOPHY

in

Electronics Communication Engineering

By

Dhande Akshay Pramodrao

Registration Number: 41900395

Supervised By

Dr. Rahul Malik (23360)

Department of Computer Science and Engineering (Assistant Professor)

Lovely Professional University, Punjab, India

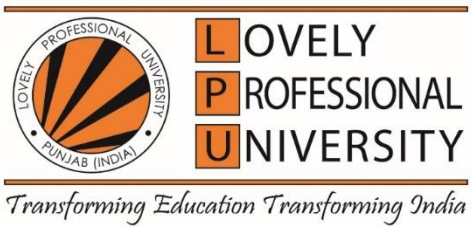

LOVELY PROFESSIONAL UNIVERSITY, PUNJAB

2023

DECLARATION

I, hereby declared that the presented work in the thesis entitled **"Computational approaches for the analysis of crop monitoring using satellite images"** in fulfilment of degree of **Doctor of Philosophy (Ph. D.)** is outcome of research work carried out by me under the supervision Dr. Rahul Malik, working as Assistant Professor, in the Department of Computer Science and Engineering of Lovely Professional University, Punjab, India. In keeping with general practice of reporting scientific observations, due acknowledgements have been made whenever work described here has been based on findings of another investigator. This work has not been submitted in part or full to any other University or Institute for the award of any degree.

(Signature of Scholar)
Dhande Akshay Pramodrao
41900395
Department of Electronics Communication Engineering
Lovely Professional University, Punjab, India

CERTIFICATE

This is to certify that the work reported in the Ph. D. thesis entitled "**Computational approaches for the analysis of crop monitoring using satellite images**" submitted in fulfillment of the requirement for the reward of degree of **Doctor of Philosophy (Ph.D.)** in the Department of Electronics Communication Engineering, is a research work carried out by Dhande Akshay Pramodrao, 41900395, is bonafede record of his original work carried out under my supervision and that no part of thesis has been submitted for any other degree, diploma or equivalent course.

(Signature of Supervisor)
Name of supervisor: Dr. Rahul Malik
Designation: Assistant Professor
Department of Computer Science and Engineering
Lovely Professional University, Punjab

Abstract

There are many different ways in which crops might be damaged, some of the most common of which being natural catastrophes, improper fertilization or treatment, and improper handling. In order to plan and put into action strategies for corrective action, it is required to first create an assessment of the amount of damage that has been incurred. In order to perform this estimate with a high degree of precision, it is essential to obtain images from both the satellite and the near-field perspective. Near-field imagery can be used to aid in assessing damage from crop diseases, while satellite imagery can be used to aid in assessing damage from natural disasters. The processing of these images necessitates the building of different models, which limits the amount of time that can be spent on their correlative analysis and, as a consequence, affects the accuracy of damage diagnosis on an overall basis.

This thesis suggests architecture based on a Deep Convolutional Network (DCN) which successfully perform the correlation between near-field and far-field images. This is done as a method of limiting the effect of the weakness that was previously highlighted. Because of this correlative analysis, the system is able to forecast crop losses with a degree of accuracy that is superior to that of individual models. This is because individual models can only make predictions based on their own data. The model is taught to detect locations that are polluted by natural catastrophes, therefore aiding agricultural experts in implementing corrective steps based on a specific site. The model is taught to search for regions that are contaminated in order to achieve this goal. After comparing the results of the recommended architecture with some newly developed techniques, we found that model achieves 8% better precision, 10% more accuracy, 8% accuracy and 5.1% better recall. performance than the previous model. The assessment is done on a large number of data sets, which helps to validate the model and offers an estimate of its applicability to a wide range of crop kinds. This study also includes suggestions for prospective future research topics that may be explored in order to better the underlying model's overall performance. These recommendations are included at the conclusion of the thesis.

In light of these findings, we have come to the conclusion that satellite image processing is a job that spans multiple domains. A wide variety of models for the processing of satellite pictures have been established by researchers, and each of these models has specific requirements for the kinds of data and procedures that should be employed. For instance, the picture capture module may be given images in a layered format, but the module that extract the feature can need information in a 3D or 2D format. As the performance of these models changes in response to variation in both data set parameters and internal process parameters, when they are applied to real-time settings, their performance is restricted in terms of both their accuracy and their scalability. There is sufficient evidence to say that model reported till date have limitation on their scalability for multiple application as they are application specific.

This thesis offers and analyzes a unique temporal engine with excellent efficiency that takes use of enhanced incremental transfer learning for real-time satellite picture categorization. The engine was developed by we of this thesis have objective to decrease the possibility that these limits may be triggered in operation. The model begins by gathering real-time satellite data via the use of Google Earth Engine. This data is then processed through the using CNN that is based on transfer learning through use of backscatter coefficient analysis. When assessed across a dispersed target, these factors represent the average value of intensity of precision image. As a result of the extraction of the backscatter coefficients, the model can display cropped images in HV and VV modes. As a result, the CNN model can extract a significant number of features from the provided satellite image and divide the datasets into three groups based on crop.

After the images have been sorted into their appropriate categories, they are subjected to further processing that includes a layer of incremental learning. This makes it much easier to visually identify regions that have been destroyed. The suggested model demonstrated an accuracy of 97.66% for identifying crop type and damage severity for various classes of images. This is made possible by its utilization of incremental learning in conjunction with a CNN for the classification process. The use of incremental learning and a CNN were essential in achieving this goal. When it was put through its paces, the performance of the model was found to be stable over a wide range of geographic locations in the neighborhood of where we are now located. This result was also compared with many latest methods, and we come to the conclusion that recommended model had 4.6% better precision, 7.9% higher

recall value and 5% better accuracy, in comparison with them. Because of this, proposed TRSATL model may be used in a manner that is particularly helpful for applications involving real-time satellite-based crop categorization scenarios.

Preface

I am thankful to the Lovely Professional University, Phagwara Punjab for giving me an opportunity to pursue my Ph.D. It has been a great experience for me to pursue my research in this esteemed Organization. I am grateful to Electronics and communication department for providing the facilities during my research. I take this opportunity to thank all people who have helped me and supported me during my research. I am thankful to all the faculty and non-teaching staff within the department as well as outside the department for all the help that I have received during my Ph. D at Lovely Professional University, Phagwara Punjab.

Whenever I reach a milestone in life, I realize how little my effort would have meant without the support of so many people. I would like to start by thanking to my supervisor Dr. Rahul Malik, Assistant Professor, Lovely Professional University, Phagwara Punjab, for his valuable guidance and inputs towards my research work. I am indebted to my supervisor Dr. Rahul Malik; under whose supervision I had started my research work. I am thankful to him for the patience he has shown and the encouragement he has provided. The intelligence and approach to research of Dr. Rahul Malik have been source of inspiration for me. I would like to thank him for his dedicated support, timely advice, inspiration, encouragement, and continuous support throughout my Ph.D.

I would like to thank the members of my RRC Committee, Ms. Nishi Madaan, Dr. Deepika Ghai and Dr. Renu Dhir for their valuable comments and suggestions.

I would also like to thank Dr. S. K. Nanda, and Mr. Pravin Soni for their immense support and guidance while doing my research publications. I would also like to thank colleague Mr. Rupesh Sushir, Mr. Aniket Pawade, Dr. Vishal Padole, Mr. P. N. Pusdekar and my friend Mr. Dipen Saini for his technical support at various stages during my research.

I am very grateful to Dr. Varsha Hutke, Associate Professor at S. G. B. A. U. Amravati, for the kind help. I thank all others who have helped and supported me during the past four years. I would also like to thank my friends from outside LPU Ravindra, Bhushan, Rishikesh, Ankush for their support in everything.

I am grateful to my mother Savita, wife Kiran, Sisters Sheetal and Pooja and all my family members who always inspired me to do this work and for their blessings and good wishes. I would not have reached anywhere without their confidence and backing.

On the successful completion of the research work and this thesis, I would like to pay all praise to the almighty God. In this thesis the work presented would not have been possible without my close association with many people. With utmost humbleness, I would like to take this opportunity to extend my deep sense of gratitude to all those who have directly or indirectly made this research thesis possible.

Dhande Akshay Pramodrao

Contents

List of Figures

List of Tables

Glossary

AI	…….…….. Artificial Intelligence
ML	…….…….. Machine Learning
ANN	…….…….. Artificial Neural Network
CNN	…….…….. Convolutional Neural Network
DCNN	…….…….. Deep Convolutional Neural Network
RNN	…….…….. Recurrent Neural Network
RBFNN	…….…….. Radial Basis Function Neural Network
YOLO	…….…….. You Only Look Once
SVM	…….…….. Support Vector Machine
LSTM	…….…….. Long Short-Term Memory
PDA	…….…….. Personal Digital Assistant
DTM	…….…….. Digital Transaction Management
GIS	…….…….. Geographic Information Systems
NLP	…….…….. Natural Language Processing
CAP	…….…….. Common Agricultural Policy
PSE	…….…….. Pixel Set Encoder
MLP	…….…….. Multi-Layer Perceptron
UAVs	…….…….. Unmanned Aerial Vehicles
GLCM	…….…….. Grey-Level Co-Occurrence Matrix
DVDI	…….…….. Disaster Vegetation Damage Index
NDWI	…….…….. Normalized Difference Water Index
NDVI	…….…….. Normalized Difference Vegetation Index
MODIS	…….…….. Moderate Resolution Imaging Spectroradiometer
MaxEnt	…….…….. Maximum Entropy
MLP	…….…….. Multi Layer Perceptron
IoT	…….…….. Internet Of Things
VGGNet	…….…….. Very Deep Convolutional Networks

NIR …….…….. Near-Infrared

PSO …….…….. Particle Swarm Optimization

GA …….…….. Genetic Algorithm

MDE …….…….. Modified Differential Evolution

SIFT …….…….. Scale Invariant Feature Transform

CRFs …….…….. Conditional Random Fields

MRF …….…….. Markov Random Field

SVR …….…….. Synthetic Variable Ratio

PSNR …….…….. Peak Signal-To-Noise Ratio

LCS …….…….. Linear Contrast Stretching

DBN …….…….. Deep Belief Networks

RBM …….…….. Restricted Boltzmann Machine

SPP …….…….. Spatial Pyramid Pooling

SAR …….…….. Synthetic aperture radar

NDWI …….…….. Normalized Difference Water Index

ACO …….…….. Ant Colony Optimizer

MDFN …….…….. Multitemporal Deep Fusion Network

SSADN …….…….. Semi-Supervised Adversarial Deep Network

ADMS …….…….. Automated Decision-Making Systems

GSA …….…….. Global Sensitivity Analysis

GFM …….…….. Gaussian Filtering Model

CASA …….…….. Carnegie-Ames-Stanford approach

Chapter No 1

Introduction

Chapter No 1

Introduction

Outline

This chapter describes the role of various remote-sensing techniques in agriculture. The inspiration behind this particular research work is discussed here. Followed by the gaps in literature, problem definition, and objectives of this research work are also discussed.

1.1 Satellite Image Processing

Images of the earth and other satellites that were taken using artificial satellites are part of the field of study and development known as satellite image processing. This is a crucial and expanding field of research. The information may be recovered from the images once they have been taken in digital format and uploaded to the computers. The multiple distinct surfaces may be identified by looking at the pixel values after statistical methods have been applied to the digital images.

The development of infrastructure, the monitoring of environmental conditions, and the early identification of the consequences of approaching natural disasters all make substantial use of satellite imagery. Broadly speaking, we could say that satellite imagery is a type of remote sensing that uses pixel resolutions to collect consistent data about the Earth's surface. We are able to state this because of the definition we have given. As a result, there are many different industries where satellite image processing may be used, including research and development, remote sensing, astronomy, and now, large-scale cloud computing. A true and up-to-date representation of earth and its surroundings may be found in satellite images. A broad range of applications that benefit mankind are made possible by the huge network of remote sensing satellites

that orbit the globe and provide regular observation about the Earth's surface. Satellite images have been an invaluable resource for decision-makers, scientists, and planners in the private and public sectors for the purpose of efficient policy and decision-making. It may be mapping the devastation left behind by earthquakes and hurricanes or the examination of slow morphological changes in the urban expansion of a city over period of time.

There are currently about 80 earth observation satellites in orbit above the globe, launched by as many as 20 different countries as part of their civilian space programs. These will be used to map the retreat of polar ice and glacial cover to increase desertification; monitoring drought; and increasing desertification. To monitor the earth's surface, these satellites are fitted with of cutting-edge remote sensing tools. QuickBird satellite, which was originally made commercially accessible in November 2000, has a resolution of less than one meter. Since then, an amazing growth rate is observed in the market for high-resolution satellite imagery, and several private companies are now vying for clients in this fiercely competitive sector. In addition to Maxar (WorldView/QuickBird), GeoEye, SIIS (Kompsat), Airbus (Pleiades), Spot Image, ImageSat International (Eros), BlackBridge (RapidEye), China Siwei (SuperView-1, 2, 3, 4, TripleSat DMC3 Constellation), and PlanetLabs, are some of the most well-known companies also own a large collection of satellites that can collect high resolution satellite pictures on, under different scenarios.

One may download several satellite photos with a medium resolution for free. Sentinel 1 and 2 photos taken at 10 meters, Landsat 8 images taken at 15 meters pan and 30 meters MS, and more. This provides access to extremely high-quality photographs that may be utilized for their particular area or project for scholars and enterprises. A range of monitoring applications, including land cover classification image fusion, and change detection, may benefit from data gathered through remote sensing. In order to gather information about the earth's resources and ecosystem, remote sensing is an essential technique. The availability of high-resolution satellite photos, as well as mapping apps like Bing Maps and Google Earth, have considerably facilitated the dissemination of satellite imaging information. The extensive usage of satellite images is a result of both of these phenomena.

The data and images that satellites collect via remote sensing may have different resolved. The four common resolutions associated with satellite imagery are as follows.

• Resolution of Space

It is described as pixels in a picture that can be seen by the naked eye and is gauged on the ground. The sensor's Instantaneous Field of View (IFoV) controls it. It is said to have a high spatial resolution because it has a high resolving power, also known as the ability to discriminate. Important elements that affecting the precision of ground objects detection is spatial resolution, refers to the size of an entity that can be understood evidently in an image. Figure 1.1 is an example of medium resolution satellites images

Figure 1.1. Images Captured from Medium Resolution Satellites

• Resolution of Spectral

This resolution specifies the number of wavelength intervals that the sensor is capable of sensing, as well as the internal wavelength size. The term "spectral resolution" for an image describes a sensor's ability to distinguish minute wavelength intervals, and it plays a role in certain areas of classifying remotely sensed pictures.

• Resolution of Time

The term "temporal" describes the interval between various imaging cloud phases and is often used to allude to the passing of time or days. The length of time needed to return to the same area and collect data is known as temporal resolution.

• Resolution via radiometry

This resolution, which is often expressed in terms of bits size, communicates the true characteristics of the image. It offers the actual bit depth in addition to recording the various brightness levels of the imaging system.

The detecting land use variation, and making of land cover maps for urban planning, as well as planning scenarios for transportation and the environment, benefits from temporal resolution Figure 1.2 depicts an example of one of these image sets and demonstrates how it may be used in transportation and change detection scenarios.

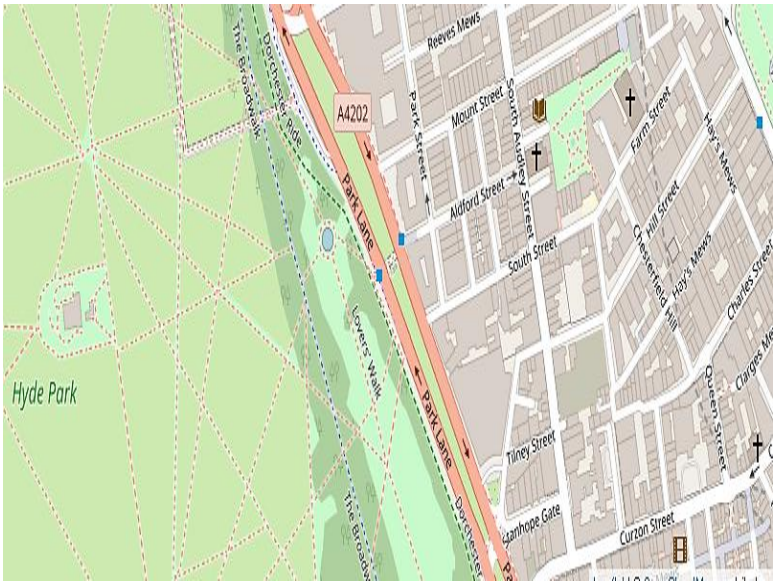

Figure 1.2. Satellite Image for Transportation and Change Detection

Highly detailed ortho-images obtained from high resolution satellite data may be used to build a graphical image of the area of interest and the area around it. In addition to offering a wealth of information, these georeferenced maps also provide a general image of the area.

Urban planning, site selection for new airports and railways, site selection for new airports, property tax surveys, and transportation planning, are just a few of the many

uses for base maps. business and industry are a few examples. One of the quickest and most economical methods is probably using satellite imagery to map out the land use and land cover of an area. Figure 1.3, which gives a realistic image of the situation, shows the current condition of how the property is being utilized clearly. A change detection examination of the zone using pictures taken over time periods may reveal trends in urban development, changes in the amount of forest cover, and the severity of flood and drought damage.

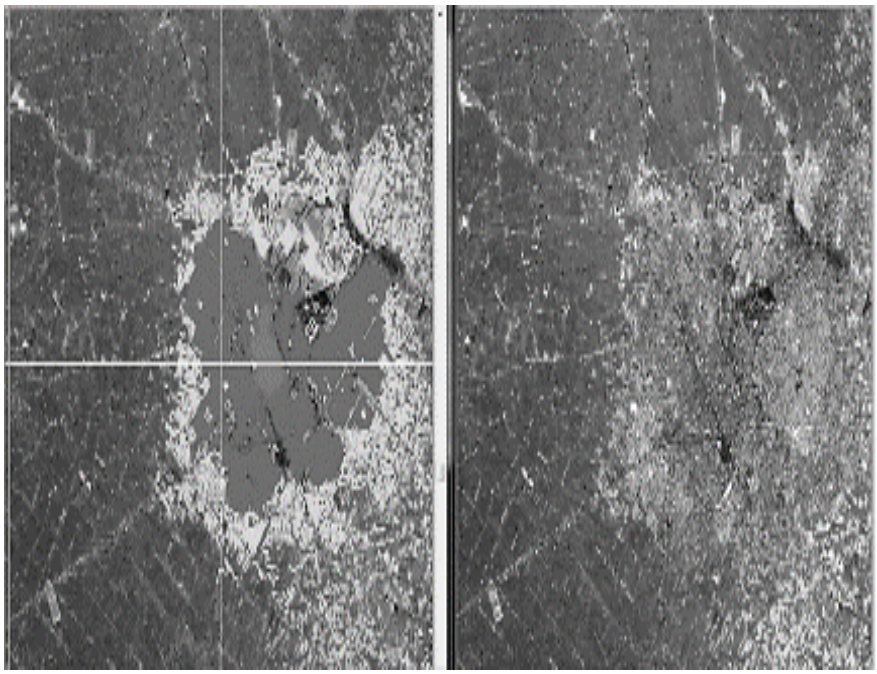

Figure 1.3. Use of Satellite Images for High Performance Applications

Satellite images, with their ability to repeatedly return to the same locations, are very helpful for analyzing the harm caused by natural catastrophes like earthquakes, floods, landslides, and cyclones which become impassable at such times. Because they provide information that is quick and accurate about the region that was impacted by the calamity, satellite photographs are particularly useful for planning rescue and relief operations. Also, for deciding where to put storm and flood shelters. The before and after images, which are shown in figures 1.4, make it clear how much damage the disastrous flood events produced.

It is imperative that agricultural resources be managed effectively to satisfy the requirements of a rising worldwide population. A crucial tool for this management is satellite imagery. The quantity of land that is suitable for agricultural use is also being

negatively impacted by the problems of deforestation and desertification. Excessive irrigation has a detrimental effect on salinization in many areas, and people who depend on rain constantly live in terror of frequent droughts.

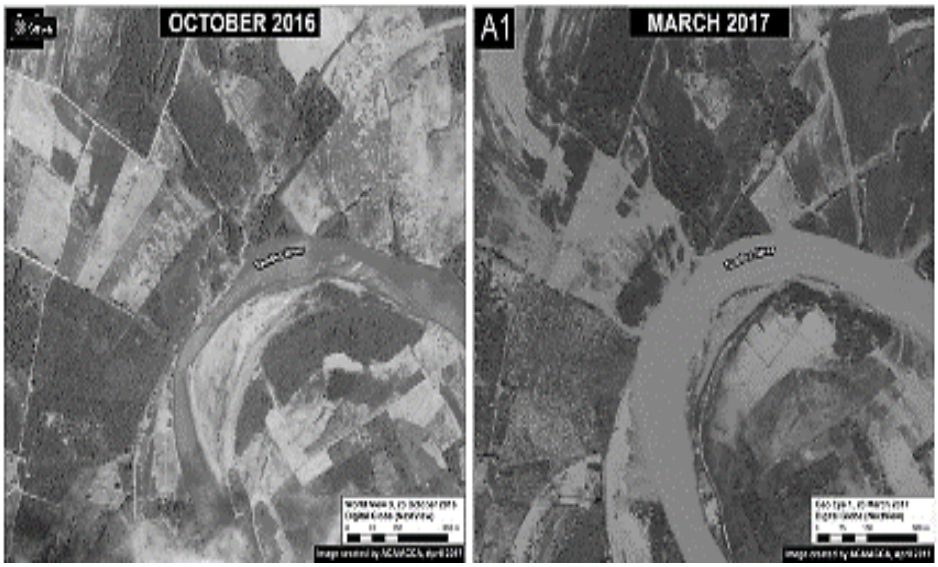

Figure 1.4. Temporal Changes in the Image Sets

Remote sensing and geographic information systems (GIS) may assist offer solutions for greater agricultural output and the correct administration of farmlands by gathering proper information on kinds and also the quality, place, and amount of these resources. By offering solutions for higher agricultural productivity, this may be achieved. Studies using remote sensing may provide accurate data on acreage, crop health monitoring, and output estimates as shown in Figure 1.5.

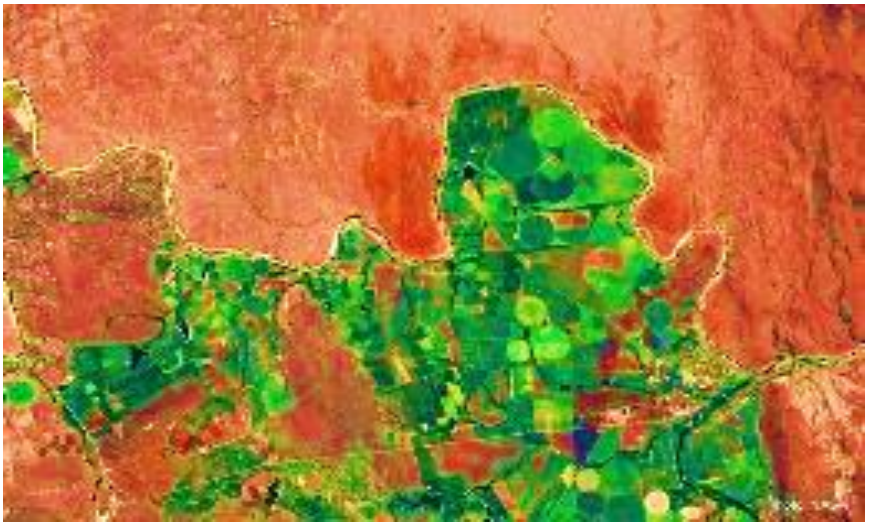

Figure 1.5. Use of Satellite Images in Land Classification Scenarios

Wide expanses of forest are under risk due to a variety of circumstances, including forest fires, illegal tree cutting for agriculture, urbanization, and infrastructure developments like roads and dams. The process of enhancing current approaches to collecting and creating maps and resource data for forestry mapping may benefit greatly from the use of satellite imagery and geographic information systems (GIS). Without the information acquired, decisions on the proper management of this crucial resource cannot be made, making its acquisition crucial. The pink areas of the figure demonstrate how mangrove jungles in the sunder ban were destroyed for agricultural use. Because of this sensitive environment of the mangroves is put in peril. Photos taken by satellites, which can be used as an "eye in the sky," which are an important source for monitoring the polar ice caps. These pictures provide powerful and incontestable proof of the huge variations taking place in the Polar Regions or the worldwide retreat of many glaciers as a consequence of increasing temperatures as shown in figure 1.6.

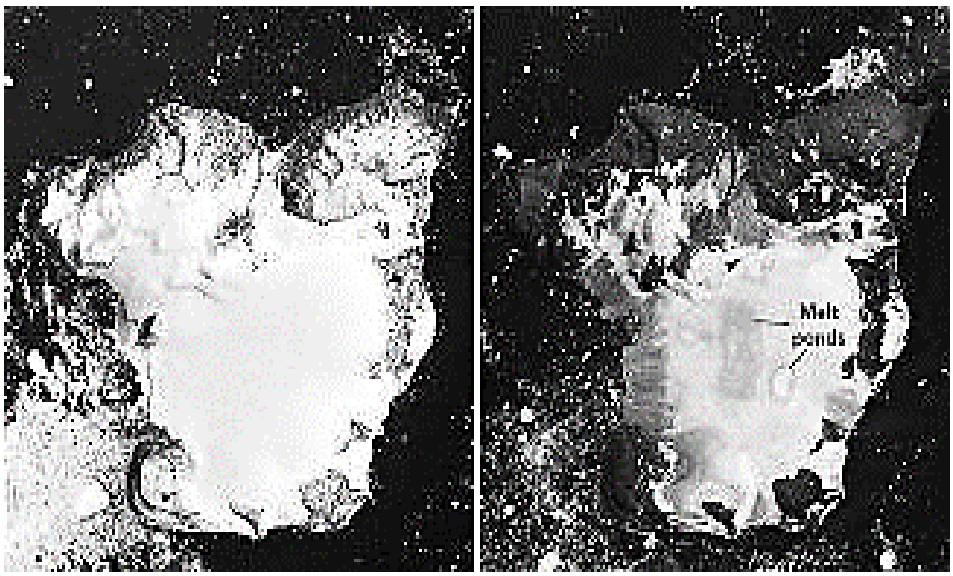

Figure 1.6. Use of Satellite Images for Polar Ice Caps.

In a manner comparable to this, satellite photographs depict the development of deserts into once uninhabited areas and massive deforestation, both of which often compel environmental groups and governments to take necessary preventative measures. There are various applications and benefits that may be gained by using satellite pictures. This is a trustworthy as well as cost effective technique of gathering essential information that can be used by researchers, planners, and decision-makers to keep an eye on the state of the world for the benefit of humankind as a whole in a variety of different

contexts. The area of remote sensing has benefited from the advancements made in the subject of machine learning (ML). We examine a model architecture that is thought to be cutting-edge in this thesis. It is known as the transformer and was first created to address Natural Language Processing (NLP) issues, while it is now often used with many other kinds of sequential data. According to the work by W. Zhang et al. they employ a modified version of this architecture to recognize agricultural areas based on a series of satellite images acquired over time. By doing this, they are able to provide results that are superior to those produced by more traditional methods (such random forests) while using less resources than recurrent networks.

1.2 Band-Based Classification Models

The rapid growth of technology has led to an increase in the prevalence of the usage of digital image processing. Satellites are used to acquire pictures for remote sensing, which has various uses beyond just monitoring images. Some of these applications include military, navigation, and others. Image size has naturally expanded throughout the course of time as a direct result of the development of increasingly advanced systems for obtaining satellite images. Because there is a restriction on the amount of storage space available, it is impossible to preserve these images for future use. The process of working through it takes a significant amount of time. Different methods for processing images reported till date, each of which has ability to improve an image in some manner, whether it is in terms of the file size or the clarity of the image. The satellite images include a significant amount of textural contrast in addition to a wide range of color variation, all of which contribute to the images' dual qualities of being attractive and somewhat perplexing. Because of this, it might potentially be challenging to apply processing algorithms to the satellite data. Because the satellite data is gathered from such a great distance, there is a possibility that it will pick up unwelcome interferences that will make the image quality worse. The quality of the final image will also suffer as a direct result of this since the subsequent processing stages will be made more challenging. The finished image is essential for both the ongoing inquiry and the process of making decisions. Before the noise-distorted satellite images can be further processed, they need to go through a step called pre-

processing. This step removes noise from the image. These days, remote sensing has shown itself to be an ever-increasing means of obtaining satellite data, and it is essential for determining the geographical and temporal changes that take place on the surface of the earth. This data comes from all across the globe, and it is compiled by scientists and government groups so that people may better understand how our planet is changing. Data obtained through remote sensing may be particularly useful in a wide variety of contexts, like estimating global climate change; detecting changes in land cover; disaster management; security; and urban and land development. These applications are just a few examples of the potential applications of this data.

The phrase "land cover" may be used to refer to everything that is situated above the ground, including vegetation, structures, bodies of water, soil, and a variety of other components. It is very necessary to recognize and categorize the land cover in order to monitor changes at the ground level. Image classification is an integral part of modern remote sensing and is used extensively for the study of patterns and visual data. A wide variety of scholars from a variety of backgrounds have come up with and implemented their own individual classification systems for images. The categorization of satellite images gives us the ability to keep a watch on a wide variety of various topics [28], including pollution, mapping of forest cover, mapping of wetland area, mapping of land cover, and more. Alexey Dosovitskiy and his fellow researchers [23] suggested using ViT as an alternative to CNN for solving image classification problems. For datasets like as ImageNet, CIFAR-100, VTAB, and others, the classification results that can be generated using ViT are better to those that can be achieved with CNN.

In the case of the Merced, AID, Optimal31, and NWPU datasets, remote sensing scene classification applications often make use of ViT [21]. When categorizing 63 distinct classes using metadata and image attributes from the IARPA fMoW dataset, work in [29] employed CNN as a set to achieve exceptional accuracy [25]. When trained on the SAT4 dataset, a pre-trained Resnet50 network showed encouraging results [27] in terms of its capacity to extract features from the data. Because of the significant amount of overlap that exists across the bands, Work in [26] made use of two convolutional neural networks (CNNs) that were trained using data from both the visible and the near-infrared (NIR). Because of this connection, conventional CNNs can only make limited use of the information. Calculating the normalized differential

vegetation index may be done using either the NIR or the red band of the spectrum. When this is utilized as input for VGG, Alexnet, or Convnet [30, 31], the training efficiency of these neural networks is improved since it delivers great accuracy while using a reduced number of parameters. The conversion of color images to grayscale is one of the most critical processes in the image processing pipeline. Work in [31] developed an image for transforming images based on singular value decomposition, which was subsequently utilized to change SIFT characteristics. In order to integrate these two approaches, structure similarity index was used. The images indicate that the accuracy of the model improves with each image transformation that is applied to it. In this investigation, we utilize ViT to compare 13-band spectral datasets to the conventional RGB dataset, the RGB & NIR dataset, as well as all other kinds of datasets.

Another important application of image processing is Change detection in past and present image for which we can implement different machine learning algorithms. To identify the changes in the satellite image the fully convolutional neural network based on Siamese Autoencoder (SA) is presented by Y. Zhou et al, as shown in Figure 1.7. This give 93% accuracy which is higher than 78% of kernel density estimation Global Algorithm, 90% of SAFC difference network (90%) and 91% of Residual Network,

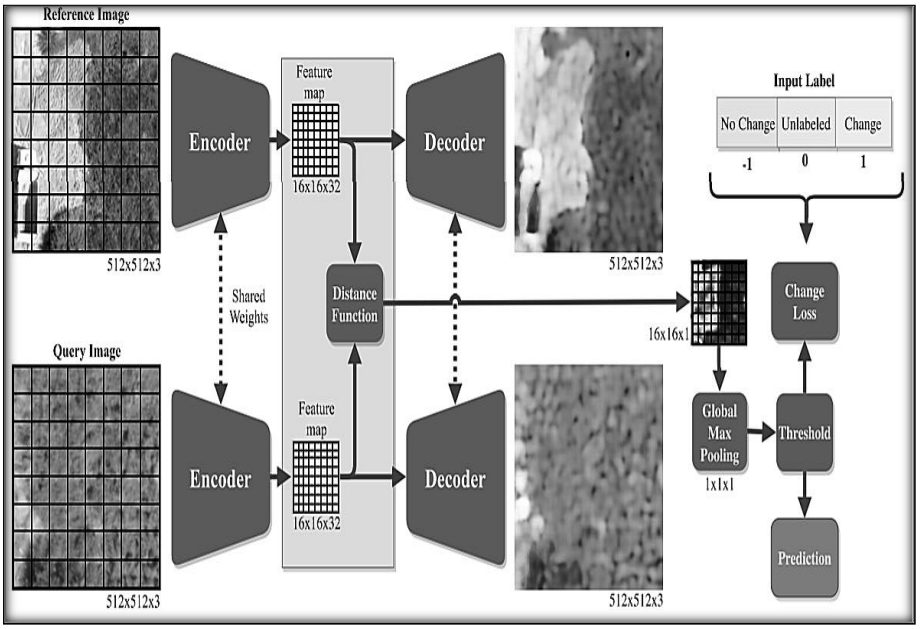

Figure 1.7. SAFCNN for change detection

1.3 Machine Learning Models

Several mathematical methods and algorithms have been created and made accessible for use in the context of satellite image processing. This page describes several satellite images processing techniques, including segmentation, enhancement, feature extraction, and feature detection. Figure 1.8 depicts a variety of satellite image processing techniques.

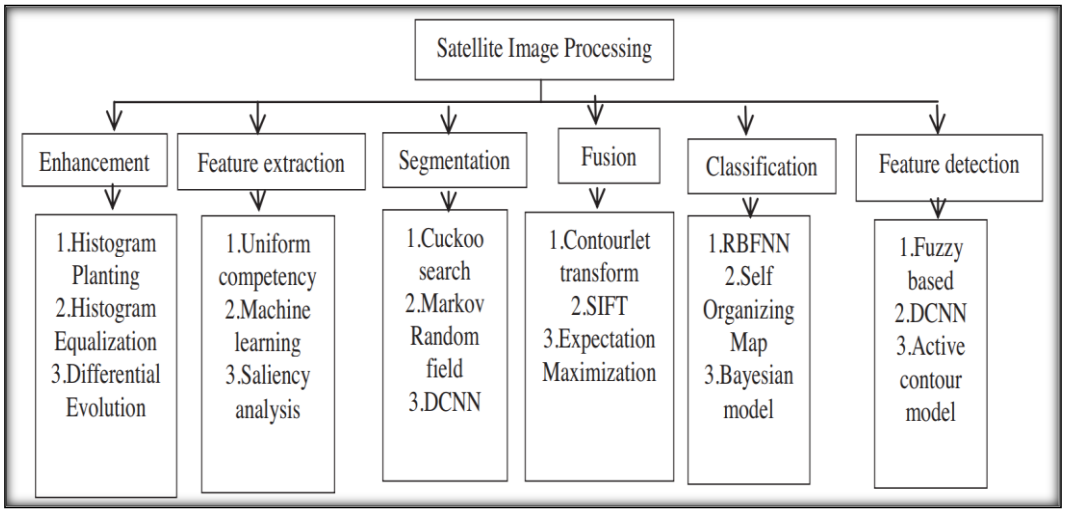

Figure 1.8. Different Models for Satellite Image Processing Scenarios

It is very uncommon for satellite images to only display a limited tonal range. Consequently, it will be necessary to enhance these images; nonetheless, it is very essential that essential particulars be preserved and that the operation result in no loss of data. There are a number distinct approaches to image enhancement, but they may generally be placed into one of two categories: spatial domain methods or frequency domain techniques. One of the most common image editing methods, known as histogram equalization, may be employed on the whole image or merely on the areas of the image that have been cropped out. It's an image that's added to a photograph to make the overall look better. In present scenario, there has been a renaissance in the utilization of algorithms that are based on metaheuristics. Image enhancement is one application that makes use of algorithms like the one known as Particle Swarm Optimization (PSO). In addition, more traditional images of evolutionary computing are used in the process of image enhancement. Utilizing a Genetic Algorithm (GA), which evaluates a person's degree of fitness, is yet another strategy that has been

suggested for improving the contrast of a satellite gray-level image. To accomplish this goal, they implemented strategy of Locating the intensity of spatial edges. It is standard procedure to make advantage of GA's alteration capabilities in order to generate a more desirable image. It seems that one positive outcome of using this technique is the enhancement of the image's quality. Both the GA and PSO procedures have a possibility of being stuck in local minima, which is one of the problems with optimization. In more recent times, there has been an uptick in the attention placed on combining a number of different optimization strategies with one another.

The Particle Swarm optimization technique and the Cuckoo Search (CS) algorithm are both components of one method that falls into this category. A "cuckoo search" is a method of doing global searches by utilizing samples from a variety of populations. The phrase "cuckoo search" refers to this method. The results that were obtained by using the CS algorithm in conjunction with the PSO algorithm were demonstrated to be a great deal nearer to the optimum solution than the results that were obtained by using either the PSO or GA algorithms on their own. Both the CS approach and the algorithm known as Modified Differential Evolution (MDE) are used often in the field of image improvement [32]. The MDE algorithm is one of the methods that has gained the greatest notoriety in recent years.

The process of developing features for the purpose of using them in data filtering and classification is referred to as feature extraction. When deciding on a method of classification, one should take into consideration the characteristics that may be utilized to differentiate the various categories. The Scale- Invariant Feature Operator and the Scale Invariant Feature Transform (SIFT) are two well-known feature extraction methods that make use of scale space theory to identify both the location and the scale of local features. These two approaches are also among the most effective (SFOP). In addition, point feature identification algorithms such as FAST are becoming more widespread. [32] employs a technique of feature-matching that was conceptualized with the help of graph theory. This strategy is flawed as a result of the non-linear character of the intensity changes that it creates. K-Means Clustering is additional method that has been utilized to separate important aspects of an image from the rest of the picture.

It is an unsupervised method in which the user chooses the threshold at which the clustering process is finished. Methods that are based on statistics, such as machine learning, are now being used. For the purpose of feature extraction, an approach that makes use of machine learning in conjunction with Euclidean distance has been used [33]. This approach takes the satellite product as its starting point and produces an image that includes features such as rivers. Finding out which of an image's feature blocks are really present inside the image is the primary objective of applying machine learning to images. In this demonstration, we make use of REPTree, a program that builds trees in an iterative fashion. There will be a selection of three of the most famous contestants. When it comes to feature extraction, another technique that is used is known as saliency analysis. The image that is described in [34] is utilized in order to generate a saliency map that takes into account information from multispectral as well as panchromatic images. In order to identify saliency maps, this technique performs an analysis on a group of images to search for similar characteristics. The most significant problem that might arise during the process of feature extraction is the chances of extremely large structures will be miscalculate as a result of certain image differences. The shadows that were present in these shots were another factor that led to various inconsistencies.

In order to segment an image, its pixels must first be grouped together into clusters based on the characteristics that they have in common. It is essential to have the ability to identify important elements within an image, such as the presence of metropolitan centers, disaster-prone regions, and forest cover. This is important in its own right and has its own weight. The team is able to incorporate a wide variety of methodologies thanks to the use of metaheuristic algorithms, which enables them to extend their study into the realm of segmentation. In recent years, new techniques for segmentation have been created. These new techniques make use of CNN features and Conditional Random Fields (CRFs). Accurate segmentation may now be achieved with the help of these techniques. In order to find a solution to the segmentation issue, one may try modeling support vector machines (SVM), which is another frequent strategy. Because of the prevalence of situations in which it is essential to differentiate buildings from the environments in which they are situated, a method that makes use of deep convolutional networks for the purpose of image segmentation has seen widespread

use. Instruction is provided via the use of a large dataset and supervised classification using this approach. It has been suggested in [35] that a Markov Random Field (MRF) [35] may be used in order to more accurately identify the data. A quantization step, a clustering step, and a computation of the probability using the fewest number of clusters that were practically possible were all included in the procedure. Y. Zheng et al., makes the recommendation that Deep Convolution Neural Networks (DCNNs) be used for the semantic segmentation of high-quality satellite images. Here, a new architecture is first built by adding boundary detection to an already existing SEGNET encoder. This is done so that the methodology may be used. Convolutional networks and encoders have been combined in this hybrid system to take use of their respective capabilities. Nevertheless, the enormous scale of the model is a significant shortcoming that has specialists on edge. The borders that are produced by this are likewise not entirely clear.

1.4 Image Fusion Models

The image of integrating many images into a single one is known as "image fusion." As a result of this, the primary objective of these fused images is to preserve as much of the information from the original source as is reasonably possible, and it is hoped that the performance of the fused image will be superior to, or at the very least, on par with, that of the images that were used as input. The overall architecture of the fusion process is shown here by a block diagram, which may be seen in Figure 1.9. Image fusion techniques may be categorized according to the level at which they operate, which might be either the decision level, the feature level, or the pixel level. The Synthetic Variable Ratio and the Bovey Transform (BT) are two of the most well-known examples of the mathematical computing approaches that are now in use (SVR). However, the technique does have a drawback, and that is that it is not very good at swiftly merging such enormous amounts of satellite data. This is the system's primary limitation. This makes the concept very difficult to implement in its current form. Recent years have seen the development of a large number of innovative methods of geometric analysis that may be used to transform-based image fusion. These types of approaches are shown by, for example, the Non-Subsampled Contourlet Transform, the Wedgelet Transform, and the Curvelet Transform (NSCT). When looking at satellite

images of the building, it is essential to carry out a geometric analysis of the structure. In the context of remote sensing image fusion, the Shift-Invariant Shearlet transform (SIST) has been suggested as a technique of achieving this objective [37]. The multispectral and panchromatic images are used as a starting point for deriving the feature vectors. Following this, fuzzy C algorithms are used in order to split the feature vectors into their respective classes (FCM). The SIST is the primary constituent of the multispectral image's first significant subcomponent.

The entropy component theory may be used to evaluate panchromatic images in order to determine which aspect of the image is more prominent. In the field of image fusion, other model-based approaches are also being used in the process. When several multi-band images are combined, one option that may be taken is to use a hierarchical Bayesian model. [38] details the presentation of a notion for image fusion that makes use of sparse representation and image decomposition. In this step, the picture that was provided to us is broken down into its cartoon and texture components. A method known as spatial fusion is used in order to bring together the dissimilar components. The sparse representation-based fusion approach is used so that all of the individual textural features may be combined into one for different use cases.

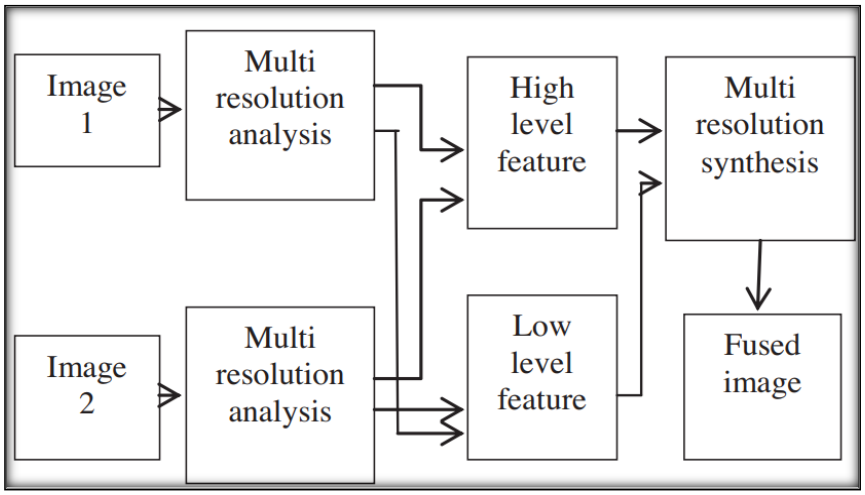

Figure 1.9. Image Fusion Process

If the spatial abnormalities in the fused images concern you, you can get past them by fusing the textural components of the images, which can be done by utilizing a dictionary learning technique. This can be done even if the spatial inconsistencies worry you. One of the most significant downsides linked with a merged image is the

possibility of noise effects, which lessen the attractive effects made by such images. An image that is optimized using a spider generates two improved images of itself, one of which has a high contrast and the other of which has a high PSNR (peak signal-to-noise ratio) [39]. In this particular examination method, agents assume the form of spiders, and the search space is modeled like a web.

The position of each individual spider in the web represents the best possible answer. When these two images are combined into a single one, a new image is produced that has a noise-to-contrast ratio that is completely unique. This method achieves a greater harmony between contrast and PSNR than other methods of image enhancement, such as Linear Contrast Stretching (LCS), Histogram Equalization (HE), and the Particle Swarm Optimization (PSO). He stands for Histogram Equalization, LCS stands for Linear Contrast Stretching, and PSO stands for Particle Swarm Optimization. One method for classifying scenes is shown in [40], and it is based on the spatial integration of global as well as local image information. The classification of images is the purpose that this approach was created for. After the image is broken up into dense parts, the next step is to apply the k-means clustering approach to the information that has been gleaned from it. In order to do multi modal feature-based fusion, it is necessary to make use of two distinct feature extractions, as stated in [41]. Deep feature extraction and shallow feature extraction are two approaches that are used to get the low-level characteristics of each pixel in an image. These two methods are distinct from one another yet are connected. This method involves the extraction of several features. After the low-level features have been collected, the next step is to produce the mid-level features using those low-level features. When training Deep Belief Networks to create high-level features, mid-level characteristics are used as a starting point in the training process (DBN). Next, a Restricted Boltzmann Machine (RBM) is used to investigate the link between the deep and shallow returned features, and ultimately, image fusion is carried out making use of the data obtained from the RBM. Researchers came to the conclusion that multi modal fusion is improved to its single modal cousin after analyzing efficiency of annotation. One of the most evident problems with the present techniques of fusion is that they are unable to capture the continuity that exists across the many forms.

When attempting to categorize the satellite images according to the elements that are visible in the images, several aspects need to be taken into consideration. When designing an effective classification system, various factors, including the spatial resolution of the image obtained through remote sensing, the requirements of the user, any additional processing methods, and the amount of time that is available, must all be taken into consideration. Each part should be able to function independently of the others, have sufficient information for analysis, and be immediately distinguishable from the others in terms of its uniqueness. Following satellite image classification, further processes such as denoising, segmentation for image extraction, augmentation, and so on may be carried out to get the further increase the quality of the picture processing. Classification of an image also takes into account the kind of satellite imagery that was utilized to acquire it. Images obtained from several satellites, each of which have their own unique sensors, might vary greatly from one another. The vast majority of the currently available techniques for image categorization make use of either expert systems, fuzzy algorithms, or artificial neural networks. [43] Radial Basis Function Neural Network, most often abbreviated as "RBFNN," is a powerful neural network that offers a broad variety of tunable parameters and is sometimes shortened to "RBFNN." The resistance to noise signals is the most important benefit.

Image tagging for video captured by UAVs is another crucial factor to take into account. Support vector machine, often known as SVM, is one of the most used methods, and it is responsible for producing a classification map. The categorization system was built on the radial basis function, which served as the basis for the construction of the system. There are certain inaccuracies in the categorization, and the SVM does not ensure that the results will be accurate. In the field of object-based categorization, the approach known as supervised methodology is now the method that sees the greatest use. However, fuzzy-based classification algorithms have inherent limitations when it comes to the task of categorizing things [44]. The Random Forest algorithm, abbreviated as RF in certain circles, is yet another well-liked classification method. Both supervised and unsupervised classification algorithms have a place in the world of machine learning. In supervised classification, the majority of the time, two different approaches are utilized: The Fitting equation will be used as the foundation for the first equation. At this point in the process, the equation is modified such that the

mean area of the given objects is input. This allows for the determination of the various categorization scales. To establish how unlike the input item is to the reference one, an additional possibility is to make use of the Euclidean distance. The approach known as rate of change (ROC) is used while carrying out the unsupervised procedure. The difference between two indices is what is used to get the best solution for this process. The use of one of the numerous possible categorization strategies might be beneficial to a variety of different industries. The RF approach is used to classify different land coverings, as well as different kinds of forests and urban land uses.

The support vector machine is used extensively in the process of determining whether regions are susceptible to landslides as well as which land uses should be classified. In forest mapping, gap analysis may be useful in identifying possible uses. The use of RF in conjunction with SVM is utilized in both the categorization of agricultural zones as well as the partitioning of natural catastrophe zones. Deep feature learning is used in [45] to provide a strategy for the categorization of high-resolution satellite images. This strategy was presented as part of the study. After the original image has been shrunk down through a number of levels, the images from those levels are used to train the DCNN. The use of a method known as spatial pyramid pooling is one that has the potential to make the training process go more quickly (SPP). Regardless of the size of the input image, SPP nets are able to maintain constant values for their weight parameter values. It's possible that tweaking the parameters of a fully connected model might make training each SPP net go more quickly. As the classification process takes place the weights are optimized by the use of multiple kernel learning. There is a possibility that the quality of the final result may be improved by combining a number of different categorization models and determining how well each model categorizes the data.

Recent advancements in deep learning have made feature identification an issue that is receiving attention by the researcher and scientist. The ability to distinguish buildings, roads, plants, and other properties within an image may be valuable in a variety of scenarios, including urban planning, environmental monitoring, disaster risk assessment, and other related areas of study. Among the many valuable applications of image processing and computer vision, edge detection is among the most significant. Many edge detection algorithms are presently in use. Preweitt, PSO, Laplacian, and the

Laplacian of Gaussian are only few of the others. When using this method, you will not be able to alter the thickness of the edge, and it will be difficult to choose an appropriate threshold. These are two potential issues that might develop as a result of using the approach. A reliable marine oil spill detection system is required by the International Maritime Organization to conduct inspections of maritime trade routes. Because of this, it is necessary to use a technique of feature selection that is based on machine learning [46]. Images captured using SAR images are often used to depict oil spills visible on the surface of the sea. It has the potential to cover a large area while yet presenting a distinct image. When trying to pinpoint the location of an oil leak, there are generally three steps that need to be taken. Dark spot segmentation is the first step that has to be taken in order to proceed with the process. This will separate the feature from the backdrop. In the second step, known as "feature extraction," the feature vectors that contain the data necessary to detect oil spills in an image are obtained via the process of extracting features. These feature vectors include the information that is necessary for an undertaking such as this one. The very last thing that has to be done is to categorize the black areas. At this point in the process, we are going to apply the criteria that separate feature areas from non-feature regions. In machine learning, one of the most important steps is called Feature Selection, and its purpose is to create a collection of features that exactly describe the detection issue that is currently being worked on. Cloud cover is one of the most significant challenges since it lowers the image quality of satellite images, making them less useful. The researcher who is seeking to learn about the landscape will find it more difficult to do so as a result of this. This indicates that the identification of clouds is an essential component of satellite image analysis. The detection of clouds using panchromatic satellite images is made more difficult by the very variable cloud distribution that is present throughout all of the various sets.may be simply interpreted in terms of the physical world for different use cases.

1.5 Motivation of Research

Crop damage is caused by irregular fertilization, natural disasters, improper handling etc. For planning and executing corrective actions an estimating of this damage is important. Both near-field images and satellite images are needed to make

this estimate with high accuracy. Near-field imagery aids in assessing damage from crop diseases while satellite imagery helps assess damage from natural disasters. The overall accuracy of damage detection is reducing because separate models were developed to process these images. As the accuracy of the presented model till date is not sufficient to use them to real time application this put limit on their use for real-world scenarios. As accurate damage detection of the crop is important for policy makers for the very important task like food security. This motivated us to pursue this research and try to attempt to developed a novel method which will overcome this lacuna. In addition, researchers propose a variety of satellite image processing models, but the accuracy and scalability of this model is limited in the real time scenarios due to variation in the dataset parameters and internal process parameters. To design a novel model capable of overcoming these problems is the main motivation of this research.

Now a days society is facing the problem of rapid urbanization, huge de-forestation in this scenario it is important to monitor the land use. At the same time separation of crop filed from other area is the challenging and under-researcher area. This drives us to undertake this research problem and come up with a method using deep learning techniques for crop filed classification to improve classification accuracy.

1.6 Gaps in Existing Models

Based on the review, following gaps are identified in the current field of research,

- Limited study of different damage detection technologies and datasets has been done under current scenarios.
- Evaluate of the best models for damage detection and classification using near field imaging, satellite imaging and statistical analysis is still under research for different deployments
- A relationship engine to identify similarity patterns between each of these damage detection and classification techniques is not designed for large-scale sets
- There is a need for an efficient machine learning algorithm to improve damage detection and classification accuracy based on the mutual relationships between different techniques

- The work is currently focused either on crop type detection, or land-type detection
- Limited research is done in the area of crop damaged areas detection using hyper spectral imagery
- Damage detection along with prediction of yield is currently under research, and needs lot of experimentation
- Effect of the integration of crop type detection with land damage detection is yet to be performed, which is our plan of research in this thesis

1.7 Quality Measures

To evaluate any system, it is always suggested that one must decide the system evaluating parameter or Quality Measures of that system first. The most common way to evaluate the machine learning experiments or the information retrieval systems or to present results for binary decision problems in machine learning are Accuracy, Precision, recall, F-measure, AOC. All these parameters are listed and defined below.

Precision

How accurately a classification model can identify the relevant data points is called as precision. It can also call positive predictive value for the classification model. Precision should take into account all positive samples that are categorized as positive, whether properly or wrongly.

Precision = T P / T P+F P

Recall

Ratio of relevant images that were found by an image classification model to total number of relevant images in the database is known as Recall value of that classification model. It can also know as sensitivity. It is concerned with appropriately categorizing all positive samples. It makes no distinction between positive and negative samples.

Recall = TP / TP+FN

Accuracy

Accuracy is the percentage of correct predictions made by our model. It is one of the parameters consider when we assist classification algorithm. Informally, accuracy is the fraction of predictions our model got right. it is defined as

Accuracy = Correct predictions/ Total number of predictions

Area Under Curve

Another of the most commonly employed measure for model assessment is Area Under Curve (AUC). AUC is a two-dimensional region that exists under the complete ROC curve. In binary classification problem it is typically applied. The greater the AUC, the better the model is thought to be in distinguishing between classes. An explanation of the ROC curve that enables a classifier to distinguish between classes is the Area Under the Curve.

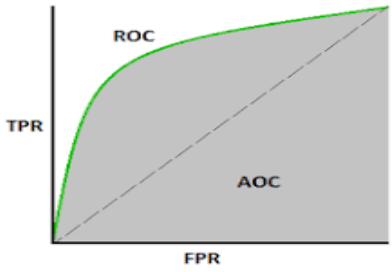

Figure 1.10. Area Under Curve

F-measure/ F-score

The F-score is frequently used to evaluate machine learning models, notably in natural language processing, as well as information retrieval systems like search engines. The F-score, which is defined as the harmonic mean of the model's precision and recall, is a technique for integrating the accuracy and recall of the model. It is employed to evaluate methods for binary classification that label samples as "positive" or "negative."

2 x [(Precision x Recall) / (Precision + Recall)].

1.8 Dataset Details

The following datasets were used in order to process satellite images,

- xView3 Dark Vessel Detection 2021 (xView3 Team, Aug 2021)
- EuroSAT (DFK, Aug 2017),
- Agricultural Crop Cover Classification Challenge (CrowdANALYTIX, Jul 2018),
- PASTIS : Panoptic Agricultural Satellite Time Series (IGN, July 2021)
- FloodNet (University of Maryland, Jun 2021),
- LPIS agricultural field boundaries Denmark, Netherlands, France

1.9 Problem Definition

Based on the studies conducted previously in this filed, it can be observed that researchers have either worked on near field images for disease identification, or satellite imaging-based crop damage identification operations. But, for a real-time crop damage detection system it is necessary that all these methods must be combined in such a way that the output of one method must be able to enhance the damage detection accuracy of other methods. Thus, our problem statement is to devise an architecture that can initially perform crop damage detection using each of the individual methods, and then combine these methods in such a manner that there is a mutual dependency between them. Learning from this mutual dependency a convolutional neural network will be trained that can observe patterns from these individual systems and perform incremental learning to improve the crop damage detection accuracy of the given field sets.

Also, we observed that separation of crop filed from other area is the challenging and under-researcher area. So, we have decided to take the benefits of the latest development happening in the field of ML and DL to address this issue and to design a method using deep learning techniques for crop classification here we have kept our focus on to improve classification accuracy so that it can be used for real-time application like land use monitoring, crop insurance settlement, etc.

1.10 Objectives

The following are the objectives of the proposed research,

1. To deeply analyze existing damage detection techniques and classification models from satellite images for remote sensing.

2. To develop a method for hyper-spectral images analysis techniques for damage detection.

3. To design a method using deep learning techniques for crop filed classification to improve classification accuracy.

4. To compare and validate the proposed model with the majority of existing models

1.11 Methodology

In this work we work on deep convolutional model which are combine with different CNN architectures, deep feature extraction model, and a transfer learning approach. This combination allows the system to produce highly efficient features, which have large inter-class variance, and minimum intra-class variance. To improve this scalability, this thesis proposes a high-efficiency temporal engine for real-time satellite image classification using augmented incremental transfer learning for crop analysis.

1.12 Flow of Thesis

This dissertation starts with a brief overview of satellite image processing before moving on to a discussion of how these pictures might be used to classify crop images. Introduction covers a comprehensive review of the related work reported in the recent past in the field of damage detection techniques and classification models from satellite images for remote sensing. The debate and the flaws in existing models are evaluated based on the discussion that has taken place here. This chapter paves the foundation for the problem statement. The chapter also lists the objectives of research undertaken. This

is followed by a description of the dataset, an explanation of the issue, and a set of goals.

Next, in Chapter 2, we'll talk about a review of existing satellite image classification models for processing crop images, which will include discussions of linear classification models, models inspired by biology, and models based on deep learning.

Chapter 3 is devoted to discussing how to create an effective ensemble learning model for detecting crop damage using deep convolutional networks, this section covers the following: an overview of the model, a survey of existing models for detecting crop damage, the design of the proposed model for detecting crop damage by utilizing an ensemble of DCN, and an analysis of the results with comparisons using enhanced incremental transfer learning for crop analysis.

Chapter 4 discusses the implementation of a high efficiency model for satellite picture categorization. This is followed by an overview of related work, an explanation of the model's motivations, a description of the proposed model and a comparison of the engine's performance to that of existing models.

Chapter 5 provides the concluding remarks on re-search by showcasing the substantial contributions of the job completed. Future instructions of the applied research work are provided towards the tail end of the chapter. The chapter concludes the thesis, by detailing briefly, the result of every one of the chapters.

Chapter 6 shows the dissemination of work done in which a list of published, accepted and communicated research work with title, year and journal name are written.

Chapter No 2

Review of Literature

Chapter No 2

Review of Literature

Outline

Here we'll talk about a review of existing satellite image classification models for processing crop images, which will include discussions of linear classification models, models inspired by biology, and models based on deep learning.

2.1 Review of Real-Time Satellite Image Classification Models

There are many methods for categorizing satellite images, and the most popular ones are designed for a specific purpose. The most well-known categories of models centre on certain types of satellite pictures. The findings in study found [4,5,6] that Multispectral and Multangle 3D CNN classification is beneficial for the impervious surface analysis, classification of urban images, and a study of multitemporal images using the MDFN. To make this model more scalable, the study presented in [7] proposes creating a CNN model that can be used in remote sensing applications.

The models suggested in [8], [9] and [10] are designed for different purposes - land cover classification by using Features Extraction and Classification Algorithms, comprehensive dominant forest species classification by using Neural-Based Hierarchical Approach, and semi-supervised adversarial deep Network (SSADN) for Segmentation of Satellite Images, but they were inspired by this technique. Researchers have proposed models that are very similar to each other. These methods seek to reduce duplication to increase classification performance, which is scalable to many applications. A few of these methods include TPTSC [12], using DL to categorize land use and land cover [11], ship detection using artificial training datasets [13], and rice paddy detection using deep learning [14]. Each of these methods is discussed in detail,

including their use cases and common pitfalls. While anyone of these algorithms can be utilised in large-scale classification applications, they must be validated further. [15, 16, 17] provides the evidence behind the use of support vector machines (SVMs), attention-based CNN (ACNN), Graph Models with deep learning and for the processing of polarimetric data. Although these models are effective in a range of different contexts, they only offer modest levels of accuracy and precision. Researchers are discussing topics such as spatial and temporal hidden Markov models [18], deep learning for automatic yield prediction [19], and CNNs for local climate zone classification [20]. They're also looking at morphology feature extraction or collaborative classification with LBP [21], which is a type of deep learning model [22]. These topics are intended to improve system performance. To predict image changes while maintaining a low error rate, these models combine various types of images and eliminate redundant features. To provide enough time for a model or two to accumulate data and get feedback, these models need a lot of delays.

Articles published in [23] and [24] propose a multiple-scale, linear iterative clustering model: the simple linear iterative clustering CNN (SLIC-CNN). This SLIC-CNN incorporates both stacked convolutional auto-encoders and deep neural networks for batter performance. The main task of the model is to reduce the delay it takes to process information while still maintaining a reasonable level of accuracy.

Table 2.1 Literature Survey Summary

Detail of the Paper	**Main findings or conclusion relevant to the proposed research work**	**Remarks**
(Ghazaryan et al. 2018)	Classifying the time series data from Landsat photographs was done by using Google Earth Engine. It's effective because it uses a process called decision fusion which combines expertise from several different classification techniques.	Winter cereals performed the most accurate categorization, but summer crops made more mistakes.
(Azar et al. 2016)	Supervised classification (EVI, NDFI, RGRI), multi-temporal data	It can be used for the complete year.
(Bagheri et al. 2018)	As classification techniques, quadratic discriminant analysis, SIMCA, linear discriminant analysis, and Mahala Nobis discriminant analysis were implemented.	

(Hao et al. 2016)	In the red, near-infrared, and blue wavebands, two vegetation indexes are derived from atmospherically corrected reflectance. i. e. EVI and NDVI	By incorporating additional data sources, one might be able to construct an analytical system for this. In the near future, one might also get more accurate training samples from the crop type.
(Kuželka and Surový 2018)	This software integrates a technique called Structure from Motion to automatically segment crops with automated classification.	The use of spectral knowledge from images or image processing techniques dependent on entities could further the development
(Hütt and Waldhoff 2018)	Multi-Data Approach (MDA). TerraSAR-X only collects one image every six days and requires cloudy conditions. The Solution: Use six TerraSAR-X multitemporal and dual-polametric strip map images to classify land cover without the need for fog or clouded skies.	As evidenced by recurring disparities with variances in the realms of training and authentication, categorization is not dependably specific for potatoes.
(Basukala et al. 2017)	Many algorithms were used in the study. These were: non-parametric machine learning algorithms, RF, SVM, and MLC. The classifier output was also evaluated and compared to either field-based or pixel-based methods of choice.	
(Melgani and Bruzzone 2004)	Band depth & Segmented Principal Component Analysis	Successional plant communities from canopy fields
(Shwetank and .J 2002)	Gini Index, Random Forest	Savanna tree species from airborne images
(Lu and Weng 2007)	Linear Discriminant Analysis VIP score	Forestry species from airborne images
(Steele 2000)	Normalized Two Sample T-test	Seagrass species field covering spectra
(Gislason and Benediktsson, J. An., Sveinsson 2006)	Analysis of Variance (Tukey HSD), Classification, and Regression Tree 98%	Rice genotypes from covering spectra

(Ham et al. 2005)	Resampled 1st derivative Stepwise Discriminant Analysis	Eucalypt forest species from lab spectra
(M. Chi, Benediktsson, and Feng 2009)	Continuum Removed Stepwise Discriminant Analysis	Himalayan forest species from satellite images
(Rodriguez, Kuncheva, and C. J. Alonso 2006)	Mann Whitney U Test	Tropical wetland species from field leaf spectra
(D. Chen and Stow 2002)	Principal Component Analysis, Lambda-Lambda R-Squared, Stepwise Discriminant Analysis, Derivative Greenness Vegetation Indices	Crops and grassland cover types from field covering spectra
(Zhang 2010)	Analysis of Variance, Linear Discriminant Analysis	Mangrove classes from lab leaf spectra

Table 2.1 summarizes our research and findings so far. Form table 2.1 we can say that these models use different types of features to produce super-features, which are then used for classification purposes after refinement. Despite these disadvantages, researchers have created various models to help with classification. Majority of these models are either not applicable in broad range of situations or are application-specific. For this reason, research has shown that there is still a need for classification algorithms to reach the level of performance needed for real-time applications.

2.2 Review of Application Specific Classification Models

Researchers have come up with a number of different approaches in order to produce crop damage detection systems that are very precise. In this section, we will investigate the ways in which a variety of techniques are similar to one another as well as the ways in which they vary. The reason we do this is so that we can evaluate how well the various strategies stack up against the one that we have proposed. These tactics, for the most part, are dependent on deep learning in order to accomplish their goals; for instance, the study presented in [26] advises complementing with a region CNN model.

Before using CNN's feature classification approach, this model first segments a portion of the image with the purpose of achieving the most accurate classifications possible. The model has a potential accuracy of 91.04% over a wide variety of various kinds of pests, and it has the potential to be applied to additional categorization jobs in order to enhance its utility.

A process that is quite similar to this one is described in [27], in which low-quality images that were taken by unmanned aerial vehicles (UAVs) are used to train convolutional neural images. The generation of heat maps from the recorded images allowed this model to attain an accuracy of 95.1% over a wide variety of image sets. The heat map is also used to study the amount of damage present in the near-field images, which is another way that it helps with the overall process of estimating the amount of damage that has occurred across the board. Comparisons with the results of other CNN models, such as those presented in [28], which offers explanations of models such as rapid CNN and spiking CNN, are possible with this one. Other CNN models include: Using a DCNN (Deep Convolutional Neural Network), as suggested in [29], which is where the LodgedNet architecture is constructed, is one way that the efficiency of such architecture may be enhanced. This is also one strategy that may be used to increase the accuracy of other models. By combining a grey-level co-occurrence matrix (GLCM) with the conventional VGGNet-16 architecture, classification and local binary pattern estimation this model achieves an accuracy of 97.6% for various forms of crop damage. With the aid of the work done in [30] and [31], high-precision models that are capable of evaluating bird and predator patterns, both of which have direct effects on crop damages, may be implemented.

Methods of deep learning very similar to those illustrated in [32], [33], and [34] are presented there. The CNN models that are used in these studies make use of a variety of methodologies, such as 9-fold cross-validation, parallel convolutions, and area proposal networks established by Zeiler and Fergus. The accuracy of these models may range from 90% all the way up to 98.0%, depending on factors such as the dataset, the number of layers, and the CNN architecture that was used. According to the information presented in [35], which details broad residual networks, when trained particularly for a purpose, these networks, which are spinoffs of CNN, have the potential to attain almost flawless accuracy. Another model of this sort can be found in [36], and it makes

use of DCNN in conjunction with transfer learning to enhance the efficiency with which banana farms are categorized.

It has been noticed that this model can be modified to accommodate a wider variety of crop kinds, and that the accuracy of its damage detection can reach up to 99.7 percent. Both of these observations have been noted. It is possible to use the model to estimate the damage done to crops with an accuracy of ninety percent or higher, making it a feasible option for categorization. Other uses of these networks are explored in [37], in which it is said that they are employed to the development and protection of plants. It's possible that applications based on nanotechnology may employ deep learning models in order to classify data more effectively. Other applications for deep learning models are currently being developed as well. These applications include an improvement in the processing of insurance claims [38], the identification of previously undiagnosed illnesses [39], the recognition of rice yield damage [40], and recognition of insect pests in greenhouses [41]. Using CNN models and architectures, these applications have the potential to attain an accuracy level ranging from 91% to 99%, with the exact range depending on the number of layers used in the classifier's design. Changing the CNN models might potentially lead us to these levels of accuracy.

Deep learning and transfer learning models are being put to use in a variety of specialized applications, including the detection of damage caused by brown planthoppers [42], damage detection for general purposes [43], and high-resolution image-based damage identification [44]. These are just a few examples of the niche applications currently being explored. With the use of these models, one may be able to acquire more precise findings. ANNs[45], SVMs[46], ANNs[47], AlexNets, VGGNets[48], GoogLeNets, and InceptionNets[49] are some of the machine learning architectures that are specified by researcher. Other machine learning architectures include GoogLeNets and InceptionNets. The Disaster Vegetation Damage Index (DVDI) and The Geographic Information Systems are also topics that are suggested by several publications. These architectures deliver comparable levels of efficiency and are suitable to use in applications involving the detection of crop damage in real time. Animal attacks, geological changes, and other variables that could harm crops are investigated in [50], and their affects can be used to influence the construction of machine learning models for damage detection. [50] Animal attacks, geological shifts,

and other factors that can destroy crops are researched. [50] See [51], which explains the background of the work that was discussed earlier, if you want further information about how proximal sensors may be utilized to improve damage categorization. In addition, as described in references [52] and [53], it is possible to simulate floods and the loss of crop water in order to anticipate any potential changes that may take place in the future in relation to the crop. In the research presented in [54], [55], and [56], the models are applied to the task of developing extremely accurate deep learning algorithms for crop damage detection and categorization sets. Table 2.2 summarizes each method, its performance.

Table 2.2. Analysis of Various Existing Models

Application	Acc (%)	Method
C	98.56	PSO [5]
C	87.80	MLC [5]
C	98.00	ACO [5]
C	83.00	BF [6]
C	77.50	NB [6]
C	83.50	J48 Graft [6]
C	83.59	BTree [6]
C	87.75	RF [6]
C	90.00	Multiple VI with thresholding [8]
C	79.20	PLSR UAV [10]
C	78.70	PLSR Satellite [10]
C	85.20	PLSR Hybrid [10]
C	85.60	SVM UAV [10]
C	76.30	SVM Satellite [10]
C	89.80	SVM Hybrid [10]
C	87.00	RFR UAV [10]
C	80.50	RFR Satellite [10]
C	92.30	RFR Hybrid [10]

C	99.09	SSU, GRU, CNN [12]
C	92.85	SSU & RF [12]
C	94.11	SSU, SVM-RBF [12]
C	96.69	CNN-GRU [12]
C	86.67	RefNet, SSTM, SSMB [16]
C	55.00	Fast CNN [16]
C	62.00	YoLo [16]
C	85.30	SSMB [16]
C	86.10	RefNet& SSMB [16]
C	96.42	DARNN& DA [18]
C	95.92	DARNN & SSCLM [18]
C	95.45	DARNN & CLM [18]
C	94.91	FCRNN & PLM [18]
C	90.50	GDC-SAR [26]
C	76.30	GMMC [26]
C	92.40	Ensemble CNN [27]
C	91.60	DenseNet [27]
C	89.24	ResNet [27]
C	87.15	LSTM [27]
C	83.30	TH VI [29]
CD	85.00	DVDI with thresholding [7]
CD	93.00	SAFCNN [20]
CD	90.00	SAFC DiffNet [20]
CD	91.00	SAFC ConcNet [20]
CD	91.00	ResNet [20]
CD	78.00	KDEGA [20]
CD	80.00	LAI Thresholding [21]
CD	86.90	MODIS with Thresholding [22]

CD	96.00	RTC-UNet [23]
CD	96.00	RTC-FCNN [23]
CD	84.10	CART [24]
CD	86.27	SVM [24]
CD	86.46	RF [24]
CD	88.56	SVM+ RF+ CART [24]
DC	96.00	Hough transform with multi-level thresholding [9]
DC	98.60	Red Band with Thresholding [17]
DC	96.20	GPC [17]
DC	95.00	TL [31]
YP	85.00	LAI with Thresholding [14]
YP	81.00	MODIS&SMAP with Gaussian [15]
YP	90.30	LNL-VI [30]
YP	87.00	RF [33]
YP	83.00	GPR [35]
YP	79.00	DT [35]
YP	85.00	BPNN [35]
YP	69.50	KNN [36]
YP	85.30	NDVI with thresholding [39]
YP	79.00	GNDVI [41]

C = Classification
CD = Change Detection
DC = Detection & Counting
YP = Yield Prediction

2.3 Review of Crop Specific Classification Models

Here, various approaches proposed by researchers to detect crop damage and the nuances of each approach are explained in this thesis. One approach is illustrated by the work in [57]. It proposes the use of region-CNN model with an augmentation. Here they segment an image into different regions and uses CNN on those regions to

make very accurate classifications decision. An accuracy of 91.04% is reported by this model and can be utilized for different classification application. On the same line model that utilizes UAVs for taking an image, and implemented low-resolution images for CNN training can be seen in [58]. Because heatmap generation from captured images is used for evaluation this model can achieve 95.1% accuracy across multiple image sets. This aids in estimating damage extent in near-field photographs and hence aids in estimating damage extent for the remainder of the field. As described by models in [59], neural networks like spiking CNN and fast CNN have been shown to produce higher accuracy. The use of the deep convolutional neural network (DCNN) can also improve the performance of these neural networks, as demonstrated by LodgedNet architecture, which is defined in [60]. This model got a 97.7% accuracy by usesing a VGGNet-16 architecture with local binary pattern estimation and GLCM (gray-level co-occurrence matrix). This can be used with work by [61] & [62] to create models for bird patterns and predator patterns. And this could help farmers improve the accuracy of their estimates for damage types, leading to reduced losses.

Many DL architecture can be seen from [63], [64], and [65]; in these various examples like Zeiler & Fergus with region proposal network and 9-fold cross-validation and CNN are used respectively. These models are typically 90-98% accurate, depending on the type of CNN architecture is use and dataset used. Research in [66] suggested variety of applications of these models, such as wide residual networks (WRN). Networks like CNN extend the reach and accuracy of CNN by being designed for specific applications. The study in [67] employs a DCNN with transfer learning to improve banana plantation classification efficiency. This model can be applied to another crop type and can detect problems accurately. This model can also detect the extent of the damage, with an accuracy of 90%. The makes this model a perfect option for classification.

Another use of these system is from [68], which include descriptions of plant growth and protection. Other applications for deep learning models include improving the efficiency of insurance claims [69], detection of unreported damage pathogens [70], rice crop damage detection [71], and greenhouse insect pest detection [72]. Deep learning models are used in applications such as brown planthopper damage detection [73], crop damage detection [74], and damage identification [75]. These deep learning

models and the architectures of CNNs can be modified to improve their accuracy levels, which range from 91% to 99% depending on the number of layers used. According to [76], [77], [78], and [79] (along with other sources, including [80], [81] and the "Global Land Cover Remote Sensing Data Sets at 30 m resolution"), machine learning architectures like those used in AlexNet, ANNs, VGGNet, SVMs, InceptionNet, GoogLeNet, and other GIS systems are discussed. Finally, the DVDI is also defined in this source.

The research in [82] elaborate the effect of factor like geological changes, animal attacks and crop damage. This study can be extended at [83], where it mentions the use of proximal sensors for improving the accuracy of damage classification. The research in [84] and [85] presented the model that predict any future changes to a crop like water loss. In this paper, models in [86], [87], and [88] were used for designing efficient DL algorithms for the classification and detection of crop damages. Combining transfer learning approaches with deep learning can enhance detection of crop damage. Based on this analysis, deep convolutional networks are described below. We will also compare its performance with other models.

Table 2.2 shows the comparison between some Existing Techniques based on their qualities. It can be noticed that each Technique provides certain pros and cons. Different techniques can be efficient in different cases, which is why there's not just one best way to detect damage. For example, checking for chlorine can be accurate in most cases, but it's not dependable. It might not matter much if you have fruit trees, so this analysis would not apply to you. That can be seen from table 2.3, where each of the reviewed methods of detecting a damaged crop and their accuracy is tabulated.

Table 2.3 Comparative Analysis of Different Models

Crop	Method	Input Data	Acc.
Wheat	ANN [64]	Image	86
Apple	ComNet [83]	Image	97
Apple	CNN [88]	Image	95

Cotton	Random forest [58]	Rainfall data and Satellite images	85
Guava	CNN [84]	Image	80
Maize	NN [69]	Drone images	85
Tomato	MobileNetv2 YOLO3 [76]	Image data	93
Coffee and Citrus	SVM [64]	Image	85
Corn & Soya-bean	Neural network [63]	Nitrogen profile	80
Corn and Soya Bean	Neural network with incremental learning [59]	Image data	90
Grape, Peach	CNN [88]	Image	91
Straw-berry, Rice	SVM [64]	Image	91
Various	CNN [61]	Image	90
Various	RNN with LSTM [62]	Image	95
Various	NN [67]	Image	91
Various	DCEN [79]	Image	86
Various	PCA, WO CNN [85]	Image	93
Various	Two-tier CNN [86]	Image	77
Various	DBN [87]	Image	86
Various	CNN [88]	Image	93
Various	DNN [68]	Image	93
Various	Modified CNN [72]	Image and weather data	97
Various	Random forest [65]	Image and weather data	85
Various	DRQN [66]	Image and weather data	94

Various	NN [70]	SAT with SDS	85
Various	CNN [78]	Molecular phenotypes and physio-logical crop models	91
Various	NN with a Recomm-ender system [71]	Weather specific data	93

2.4 Deep Learning-Based Classification Models

The number of datasets that may be used for remote sensing or hyperspectral image characterization is limited; the tables that include the datasets that are used are shown in Table 2.4. There are also additional informative indexes; however, some of the characteristics associated with them are still unclear; hence, we have substituted the phrase "not certain" for the ambiguous features that are included follow.

Table 2.4. Datasets used for assessment

Type	Range	Number of Bands	Kinds of objects	Image Size	Spatial resolution
Indian Pines	0.4-2.5um	224	16	144*144	20 m
University of Pavia	0.43~0.86p m	115	9	610*340	3.7 m
Salinas	not-sure	220	16	512*217	1.3 m
Radarsat-2	0.43-0.9u m	not-sure	19	4952065	5.2-7.6 m
UC Merced	not-sure	not-sure	21	256*256	0.3 m
KSC	0.4-0.25um	224	13	512*614	18 m

The work described in [112] describes the background research that typifies the application of deep learning computations to the classification of hyperspectral images. Scientists Jie Zhang, have proposed using DCNN to classify photographs taken along the shore of the Huanghe (Yellow) River Estuary. [113] contains the results of the study. These pictures were taken in one long burst, and then the best ones—both spectral and textural—were chosen to be arranged. Several categories were chosen, some of which are included in [113]: reed, tamarisk, water, spartina, tidal level, OCA and farmland. The accuracy of the straight SVM, sigmoid SVM models, RBF SVM,

polynomial SVM, and, as well as the recommended DCNN model, were all taken into account. Applications that need ongoing hyperspectral characterization may benefit from the proposed DCNN calculation, which was demonstrated to outperform prior calculations by more than 8% in terms of center accuracy. The kappa coefficient, a measure of the precision of a calculation, is also calculated, and the results demonstrate that the recommended DCNN is at least 10% more precise than the other networks. Research by [114] uses SVM in combination with a directed channel to improve grouping execution, despite widespread agreement that DCNN is better. The more accurate representation of visuals is achieved in part by the guided channel's role as a computation for improving elements. Ultimately, this makes the computation more feasible. The results of their study [115] were compared to those obtained by using SVM, Co-SVM, Co-SVM-EPF, and SVM-EPF models, as well as the GF-SVM model and the proposed GF-SVM-EPF model. After doing many calculations, they found that the recommended GF-SVM-EPF was at least 6% more effective than the others. There hasn't been any study on integrating GF-SVM-EPF with DCNN, but any reader of this should keep it in mind as a promising avenue for investigation. According to the work of Dan Yao et al., basic tiny CNNs may be used to simulate the spatial order of multi and hyperdimensional images, making DCNNs a kind of CNN. Deep convolutional neural network abbreviates to DCNN.

They have proposed using a minimal bit of level engineering to arrange these pictures. Using this method, the images have been divided into several sections, each of which may do a certain task. Example: using gaussian channels for image pre-processing in the selected main area. This part of the process roes the work and uses the channel to ensure that all the pictures are processed properly. The same may be said for the several divisions responsible for the little but essential task of hyperspectral organization. After looking through six distinct CNN models, they concluded that their proposed design offers the highest accuracy. A combination of this proposed CNN with other, more extensive CNNs may improve the findings' precision. CNN, SVM, and deep CNN are all examples of classes that qualify as profound learning. Several alternative calculations for a deep learning-based hyperspectral order are proposed in the study reported in [116]. In particular, they looked at EMP, SVM, JSR, 3D CNN models to see which one provides the most precise computation. They looked into many

other options and found that the DFFN, also called a deep feed-forward system, may work for a hyperspectral business. Their investigation spans over 10 distinct areas; as such, it might provide any specialist with a great jumping-off place for further investigation and analysis.

Cascaded Recurrent Neural Networks, similar to DFFN, were utilized in the work described in [117] to classify hyperspectral images. As a means of maintaining order, they use the idea of combining many independent systems into one. Using a loss task and an aggregate administrator, they found that a total of ten iterative neural networks yielded 90% to 95% accuracy. They concluded that the recommended SSC as RNN [118] technique is exceptional in its capacity to carry out order tasks by comparing the accuracy rates of SSC as RNN, CasRNN-O, CasRNN, and CasRNN-F. If you compare its center precision to that of other calculations, you'll find that it's over 15% more precise. Support vector machines (SVMs) are nonparametrically validated theories for addressing issues associated with a tendency to veer off course and regress. In the same vein, no presumptions are made about the hidden information's spread. You can find the mathematical justification for the SVMs in [119], [120], and [121].

The SVM preparation calculation anticipates choosing a hyperplane that splits the training data into a defined number of classes in a predictable manner with respect to the planning axes when the strategy is given a set of data tests in the original design of SVMs [122]. The decision furthest reaches that limit the amount of misclassification that may be accomplished during the organizing stage is referred to as the "ideal detaching hyperplane." The learning advice is to set a perfect choice breaking point to divide the planning models, and then to disengage test data in line with a comparison strategy [123]. Keep an eye on [124, 125] for a well-organized description of the SVM computation as a tool for example affirmation. For any piece-based method, SVMs included, it is crucial to have a segment task that accurately represents the closeness between tests. The same holds true for any tactic that relies on individual elements. Certain support vector machines and other segment-based classifiers that satisfy Mercer's condition [126] are built using common pieces such as the straight piece, polynomial piece, extended reason work (RBF) bit, and sigmoid piece.

Thanks to their superior performance, 3D CNNs have revolutionized hyperspectral characterization. Since the authors of [127] were able to effectively use CNN's 3D model for the assignment of characterization, this work represents a significant step forward in the analysis of hyperspectral grouping. As so, this is a significant development in the study. Also, they have employed exchange-based learning technologies to further increase overall system performance. The proposed framework has been shown to achieve an amazing 98% accuracy or higher. Also, there are no bottlenecks in the calculation, therefore it may be utilized for continuous applications. In [128], we see another CNN design, this one presenting the concept of fully programmed characterization. They've fused 1D and 3D convolutional neural networks to reap the advantages of both architectures' highlight management and data organizing capabilities. The resulting framework consistently achieves a precision of 95% or higher on a wide range of datasets. The findings have been compared to many other models, including L-SVM, RF-200, MLP, RNN, RBF-SVM, 1D DCNN and 1D CNN. In terms of mean accuracy values, the proposed model exceeds the alternatives by at least 5%. Article [129] describes the use of discriminative compact representation for characterizing hyperspectral images and learning highlights. The outcomes show that honing focus on highlights may help the order framework be more precise; as a result, improving belongs to a group of estimations or methods that can help weak students become good ones. At the end of the day, the fragile understudy could be seen as a superior model to the arbitrary theory. There are fewer problems with the fragile understudy than with the arbitrary theory. On the other hand, if the student does a good job, the result is almost as precise as it might be. The word "boosting" is used to describe a wide range of techniques that may be used to enhance the efficiency of any kind of educational endeavor. In [130], the author proposes a strategy for improving students' performance based on the assumption that even the weakest among them may be made into a strong one. The essential premise of this structure is that even the weakest learner can be improved. Boosting is a progressive content show [131] that uses the whole curriculum as its building blocks. The purpose of this method is to provide an incredibly precise leading set of computations [19], and it does so by combining the results acquired from many classifiers.

In the last decade, the irregular forest has been one of the leading gathering classifiers because of the increased focus on academics. Using a random selection of planning data and components, this information-gathering technique controls the outcomes of probable alternate decision trees [132]. Due to its amazing request accuracy, the Arbitrary Forest method has swiftly gained traction as a viable choice in the field of remote recognition for the representation of images. Results from a wide range of use cases [133,134] demonstrated the reliability of Arbitrary Forest [135]. For clear motivation, researchers developed the RF classifier as a Classification and Regression Tree application [136]. Trucks are packed and delivered according to a blueprint of the relevant planning data. This indicates that the same getting ready test may be used again, whereas other models may be completely ignored. Seventy percent of the models used to evaluate the trees' readiness are brought-in-pack tests, while the remaining models are out-of-the-sack tests for each and every odd model. These out-of-the-bag tests are performed to determine how well the resulting RF sounds when using an internal cross-endorsement strategy. An "out-of-the-box" mistake is how this blunder is being described. The client is responsible for selecting two values, Number of tree and Maximum number of tries, which are necessary for this method to work (number of features). The function of each node in the tree's center is identified by means of the Maximum number of tries parameter.

RF designed the trees to have a steep slope and a wide range of variations [137]. Class task probabilities are managed by each individual tree in the forest, and [138] discusses how these probabilities are collected independently and averaged. The accuracy of the portrayal is less dependent on the parameter Ntree when it is offered in a manner distinct from the succeeding parameter Mtry, as specified by the customer [139]. In terms of computational power, RF is widely acknowledged to be an effective classifier. A large body of research indicates that 500 is an appropriate value for the estimate of parameter Ntree since this is where errors tend to settle [140]. Different experts have implemented the RF classifier with different values of Ntree (e.g., 5000 [141], 1000 [142], and 100 [143]). Physical copies of these efforts are still available. However, some specialists have shown that the above-mentioned motivation for immediate application and remarkable portrayal conclusion may obscure the significance of the estimation of the Ntree parameter. Based on the notion that

increasing the number of trees (Parameter Ntree = 70) yields a remarkable request result, the study provided in [144] employs RF to organize the SAR data. However, Mtry is seen as the square root of the number of information components [145], therefore it is a useful parameter. Using the estimate of Mtry as a proxy for the estimate of all variables does nothing except increase the computational complexity of the figure in one study [146]. Testing against other popular classifiers such as artificial neural networks, linear discriminant analysis, binary hierarchical classifiers, and decision trees showed that the RF classifier was much superior in terms of accuracy and precision [147]. Bolster Vector Machine, a classifier that uses an AI-based technique produced unfathomably high levels of accuracy across a wide range of use cases. Several studies have shown that the RF classifier performs as well as the SVM [148], and RF yields particularly impressive outcomes when applied to hyperspectral data (high dimensional data). Multi-scale question image inquiry (MOBIA) using EO satellite imagery was conducted using an RF classifier, as described in [150]. The result was imaged with very detailed metadata. Elhadim Adam examined the use of SVM and RF classifiers on Rapid Eye pictures, and he distinguished between the various Rapid Eye satellite data sets in terms of relevance. But studies in object-based image analysis have shown that SVM is the clear winner (OBIA). Baoxun Xu released a new version of the RF classifier, ensuring that it provides superior performance to state-of-the-art RF methods.

The first algorithms applied were SVM, RF, and ANN which are considered effective in classifying the damage detected in plants and distinguishing the category of this damage. These algorithms relied heavily on the extraction of features and their subsequent selection to allow the classification task to be carried out efficiently. Most predictive modelling methods have a range of accuracies. But our CNN-based data had an average of 90% accuracy for both damage detection and classification.

1. Deep learning algorithms can automatically learn and extract features from raw data. Traditional machine learning often requires handcrafted feature extraction, which can be complex and time-consuming.

2 Deep learning algorithms tend to perform better with large volumes of data. They can handle big datasets more efficiently and often achieve higher accuracy as the volume of data increases.

3. Deep learning models can adapt and improve their performance over time as they are exposed to more data, making them more flexible and capable of continuous learning.

2.5 Statistical Evaluation

Each method is compared in terms of implementation difficulty, applicability and accuracy for statistical analysis. It is clear that the majority of research has focused on, yield prediction, categorization, detection and counting of plant kinds and change detection. The effectiveness of various change detection techniques is shown in Figure 2.1.

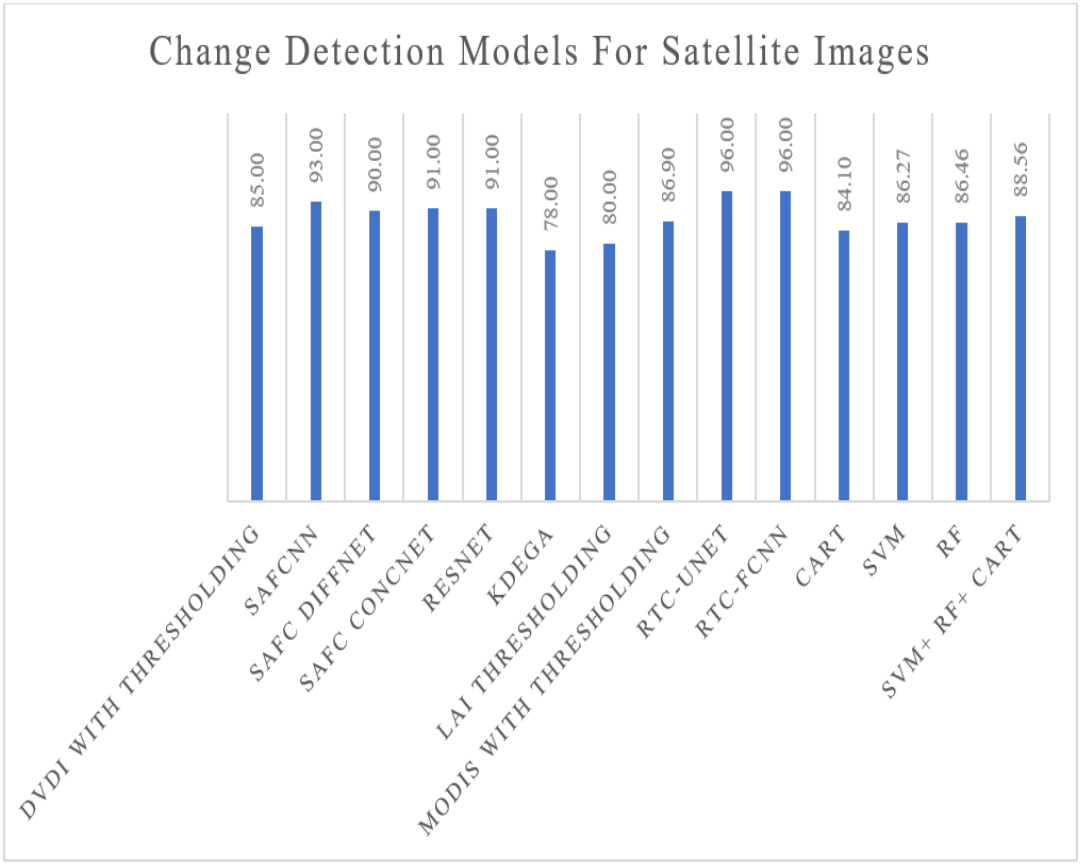

Figure 2.1. Change Detection Models

The comparative analysis of yield prediction algorithm is shown in figure 2.2 base on accuracy of model.

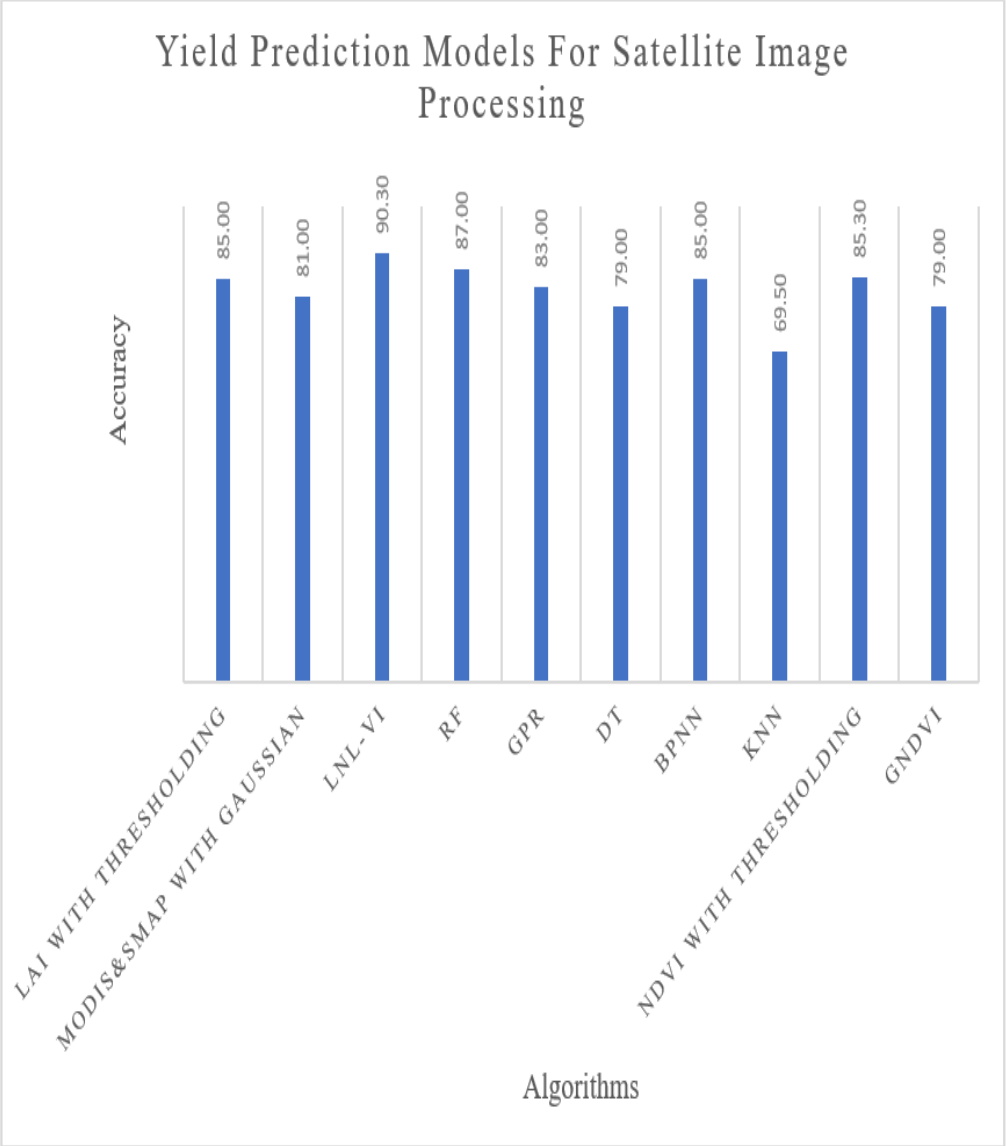

Figure 2.2. Yield Prediction Models

Figure 2.3, which contains both disease detection and crop type classification, shows how effectively these classification techniques work

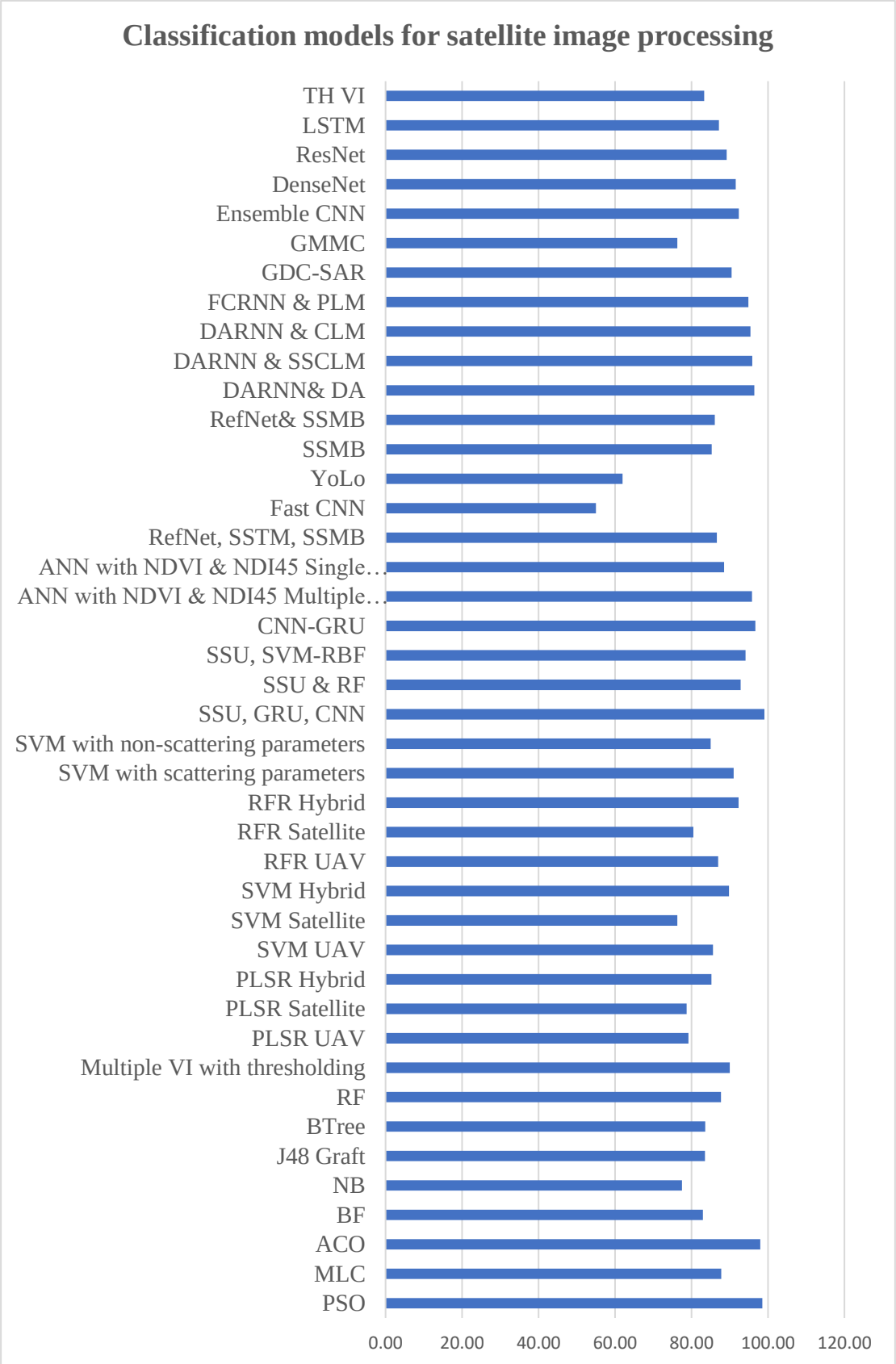

Figure 2.3. Classification Models

2.5 Conclusions

The first algorithms applied were SVM, RF, and ANN which are considered effective in classifying the damage detected in plants and distinguishing the category of this damage. These algorithms relied heavily on the extraction of features and their subsequent selection to allow the classification task to be carried out efficiently. Most predictive modelling methods have a range of accuracies. But our CNN-based data had an average of 90% accuracy for both damage detection and classification. Precision can be increased by accumulating input sources, such as image data, in addition to environmental information, nitrogen profile, weather data, and so forth.

Chapter No 3

Ensemble Learning Model for Damage Detection Using Deep Convolutional Networks

Chapter No 3

Ensemble Learning Model for Damage Detection Using Deep Convolutional Networks

Outline

This section covers an overview of the model, a survey of existing models for detecting crop damage, the design of the proposed model for detecting crop damage deep convolutional networks, also an analysis of the results with comparisons using enhanced incremental transfer learning for crop analysis,

3.1 Introduction

Natural calamities, improper treatment, and irregular irrigation are some of the reasons for crop damage. Near-field image and satellite images are essential input to accurately estimate the damage mention above for planning and executing corrective actions against it. Satellite imagery helps assess damage from natural disasters, while near-field imagery estimates damage from crop disease. Separate architecture is designed to handle these images, limiting the correlation between them and reducing overall recognition accuracy. In the comparison of the individual models the architecture suggested in this thesis perform better correlation between near-field and far-field images to predict crop damage more efficiently. When compared with some of the most advanced models, our proposed correlation-based model delivers a 10% improvement in accuracy and 8an % improvement in precision. Plus, you'll get 5% more accurate results with less effort. In order to validate the model, it was evaluated on different datasets and crop in multiple ways. This thesis also discusses upcoming research

instructions which can be consider so that the prediction model can perform more effectively.

Crop damage prediction and detection is a complex process that involves many different components. This task ranges from the design of image pre-processing to variant feature selection, fusion, and post-processing. For instance, when creating a noise filter for images, we need to design something like an adaptive median filter (AMF), Gaussian filter (GF), or Weiner filter (WF). Noisy images are very common in satellite imagery. When noise filters are applied, the image quality is improved and salt and pepper noise, speckle noise, etc., may be removed. Once these filters have been applied, image fusion modules are activated in order to improve overall image quality. These modules combine images taken from different sensor, like multiband panchromatic, and multispectral images. Combining these images gives you a final image that has aggregate information, like shape information, colour levels, edge information, crop contours, and more. In extraction process, a projector block, extract the features. These features can include a wide range of things such as local binary patterns, histogram features, colour maps, and edge maps.

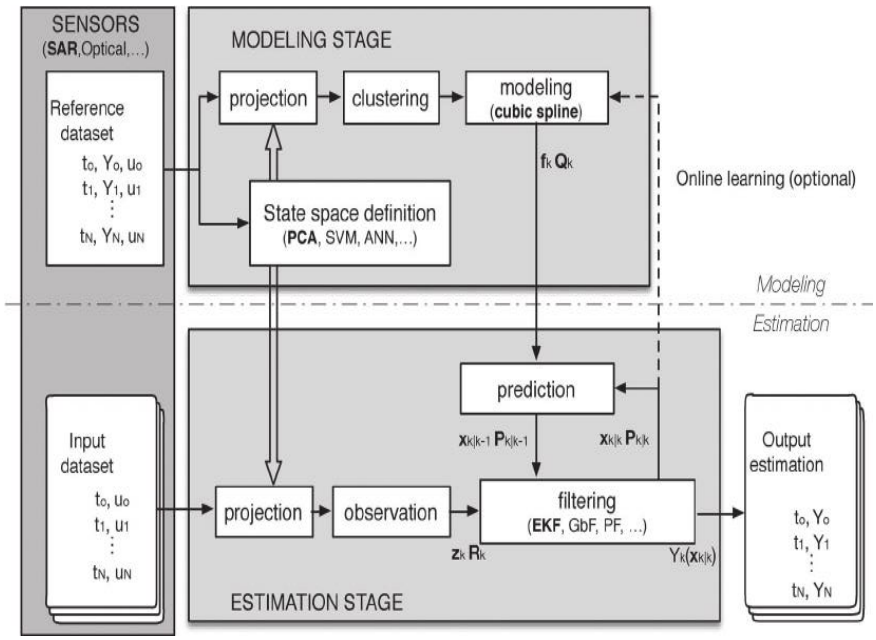

Figure 3.1. Crop Damage Detection System Model

Due to the large number of extracted features, the probability of feature redundancy increases. This redundancy reduces classification accuracy & increases processing delay. In order to avoid feature redundancy various feature selection models are implemented. Machine learning models are a great way to improve classification by analyzing the features of images. These factures should be varied widely for different types of photos and must be similar for images with similar content image. Classification engine is use to produce the crop damage system. Algorithms like SVM, NN, convolutional neural networks, and others are implemented in our model to classify the ‘non-damage' and 'damage' categories as seen in figure 3.1. When the images get classified, they are sent to a post-processing block. From there, we do an estimation of the extent of the image. The algorithm like random forest, Naïve Bayes and neural networks are used for pattern recognition models. To divides the images into several categories of damage the proposed architecture makes use of the damaged image's temporal categorization data. The enormous variety of crop damage detection system models that have been proposed by researchers over the years will be examined in the next part, and their effectiveness will be discussed in this thesis. We first fabricated a model with the proposed system structure, and then we evaluated its performance using precision, accuracy, recall, delay and F-measure. To verify the effectiveness of the recommended system, the performance of several state-of-the-art models that are currently employed for crop damage detection is compared with the suggested model. At last observations were made about the suggested system and recommended approaches to improve it.

3.2 Proposed Method

From the literature review, it can be observed that a wide variety of machine learning and deep learning models are available for satellite image classification. These models are applied to context-specific applications, which limits their scalability. To improve this scalability, a novel high-efficiency temporal engine for real-time satellite image classification using augmented incremental transfer learning for crop analysis is proposed in this section. The proposed TRSAITL model uses a combination of CNN with incremental learning to continuously improve classification accuracy using Adaptive thresholding layer with parameter tuning.

Transfer learning, several CNN architectures like VGGNet 16 network, and a deep feature extraction approach is combines in the proposed architecture. It generates extremely efficient features with significant interclass variation and low intraclass variance. Satellite crop datasets of Amravati District (India) which is generated after different disaster conditions such as floods and hailstorms in the year 2018 and 2019 is use to train the model. The model can be batter understood from following three steps:

- Multiple CNN architectures for Classification.
- Transfer learning block.
- VGGNet 16 network for Deep feature extraction.

This design has a few steps. The simplified version of it can be observed in Figure 3.2. The feature extraction model is directly provided with input images taken from our dataset. We got the result in form of tow class i.e., "non-damaged" or "damaged" by using the CNN classification model. This further aids in hyperparameter tuning of the proposed system via the transfer learning network. In order to fit the internal ImageNet model, input images are scaled to 224x224 and then features are extracted using a pre-trained VGGNet-16 architecture. Figure 3.3 illustrates the features that may be seen at 4096.

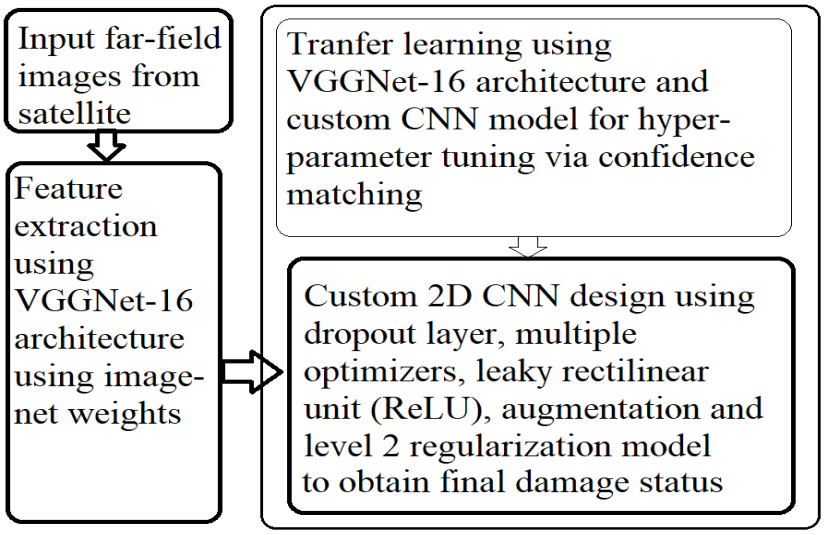

Figure 3.2. Damage Evaluation Models

To processes the images with a 64x64 window a 3x3 convolutional layer is used. 150K feature values are extracted from the image and then given to another 3x3 convolutional

layer with 64-by-64-windows for more filtering features. It's often hard to find a certain filter when you're looking for multiple filters, but thankfully this equation will tell you which one would work for your needs. The first thing that it does is reduce feature variance for any similar features, and then it will increase the variance for images that are in different classes.

$$MP_{out} = Max\left(\frac{1}{X_k} * \sum_{i=1}^{X_k} x_i\right)^{1/l_r} \quad \dots (1)$$

Here, MP_{out} is the output of the maximum pooling layer, and X_k is the input of the layer with "k=224" various feature vectors. Learning rate is represented by l_r of the pooling layer (set between 0 and 1). Following convolutional layers with sizes of 128x128, 256x256, and 512x512 are applied to the layer once more to extract 800,000, 400,000, and 200000 features, respectively. In essence, these traits were turned into 1.5 million distinct features. The same max pooling, rectilinear unit (ReLU) procedure and a fully connected neural network are then used to retrieve a total of 25,088 features. The 150K different pixels of one image is converted into 25K different features. This feature set has low variance with same class feature sets and huge variance with feature sets of different class. Extracted characteristics are provided to an ensemble CNN classification model for the purpose of identifying crops with damage. An ensemble 2D CNN model made up of leaky rectilinear units (ReLUs), multiple optimizers, level 2 regularisation, and data augmentation receives the extracted features. This neural network model's architecture is shown in Figure 3.3. Encoder and decoder layers are among the specified layers. Prior to using the neural network, a data augmentation layer receives the output from the VGGNet 16 model. Every set of input features undergoes specialised calculations in this layer,

- Using equation 2, data rotation up to 40 degrees is implemented.

$$d_{out_i} = \frac{d_{in_i} * \sin\ (\emptyset_i) + d_{in_i} * \cos\ (\emptyset_i)}{2} \dots (2)$$

Where $\emptyset_i$ indicates the angle and ranges from 40 to 0 degrees in steps of 1 degree, and, d_{out_i} and subscript are d_{in_i} are output, and input data for the specified angle.

• A typical autoregressive integrated moving average (ARIMA) model is used to enhance the samples when the width shifts between 0 and 0.2, as shown in equation 3.

$$d_{out_i} = R + \emptyset_1 * d_{in_i} + \emptyset_2 * d_{in_{i-1}} + \emptyset_3 * d_{in_{i-3}} \ldots + \emptyset_p * d_{in_{i-p+1}} \ldots . (3)$$

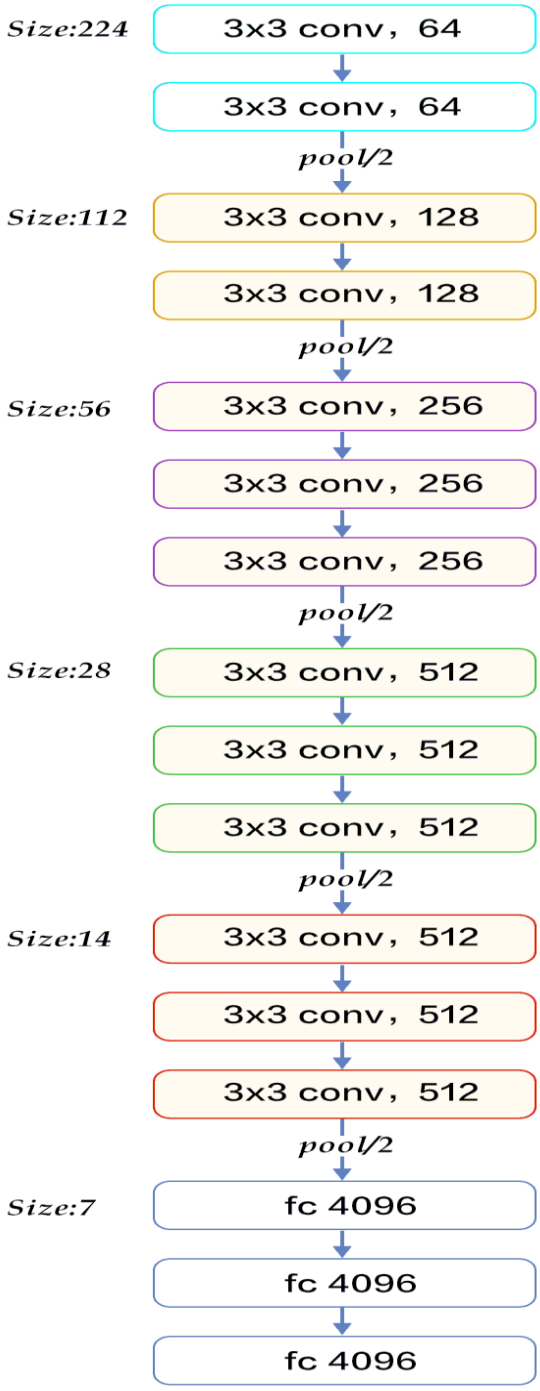

Figure 3.3. The VGG16 ImageNet Model

Where, 'R' stands for ARIMA constant, the i^{th} value of angle for width shifting is denoted by $\emptyset_i$. and *'p'* stands for the width shifting from 0 to 20 (20%).

Cropping with a range of 0 to 0.2 is used to enhance samples using the shearing operation as seen in equation 4. This operation is used to determine the feature's shearing stress value using statistical moment values.

$$d_{out} = {d_{in} * M_{in}}/{M_n * b} \ldots (4)$$

Where '*b*' denotes the shearing range and M_{in} denote the moments that are evaluated using mean values and M_n denote the moments that are evaluated using around the neutral axis.

- When the supplied features are zoomed in between 0 and 0.2, equation 5's detection of the zooming operator is used to enhance the given features. This operator enables the use of several values for the same feature vector, assisting in the assessment of enhanced variant features.

$$d_{out} = \frac{d_{in}}{2 * \tan\left(\frac{Z_f}{2}\right)} \ldots (5)$$

In this case, Z_f is the zoom factor that is utilised to estimate the zooming values. The super feature vector may be created by combining all of these characteristics, which is then supplied to the ensemble CNN design. In order to create a deep, 21-layered network, this design syndicates many CNN models; separately, these layers are specified as follows:

Layer No.	**Design**	**Purpose**
I.	2D Convolutional layer with 32x32 size and 3x3 kernel size	For maximum pooling, the window is shifted via a 3x3 window, which aids in the extraction of extended features. This layer is responsible for extracting 1024 features per line from extracted feature sets.

II.	Leaky ReLU layer with alpha=0.1	The output of the preceding layer is sent to the leaky ReLU layer at this stage for feature variance optimization. The output of this stage, which is controlled by the equation below, is displayed in the results once feature variance has been verified. $$x_{out} = alpha * x_{in},$$ $$when$$ $$var(x_{in}) > 0, else,$$ $$x_{out} = 0 \dots \dots (6)$$
III.	Maximum pooling layer with a pool size of 2x2	The features that are retrieved for a particular data point will have the highest value in relation to the feature variance. There will only be 512 features each stride if we lower the amount of features by a factor of 2x2.
IV.	Drop-out layer with a dropout rate of 0.25	During the optimization phase, around 25% of the characteristics are deleted to guarantee that only the most relevant features are chosen.
V.	2D Convolutional layer with 64x64 size and 3x3 kernel size	The extracted features are treated via a max-pooling layer that elongates it and extracts more from the 4096 features per stride to generate an extended feature set. The window is 3x3 in size, which assists in the extraction.
VI.	Leaky ReLU layer with alpha=0.1	This leaky ReLU layer optimizes variance by assigning features extracted from the previous layer. The output of this ReLU is governed by equation 6, which checks for variance.

VII.	Maximum pooling layer with a pool size of 2x2	The retrieved characteristics are decreased to a factor of 2x2 in order to get the greatest value. As a consequence, each stride has 1024 characteristics.
VIII.	Drop-out layer with a dropout rate of 0.25	For customer satisfaction, we remove about 25% of the features from a product.
IX.	2D Convolutional layer with 128x128 size and 3x3 kernel size	A stride is used to go from one layer to the next via a 3x3 window in order to create more features from the retrieved sets. This aids in giving extraction a wider context.
X.	Leaky ReLU layer with alpha=0.1	The preceding layer's features, if any, are passed on to the layer of a leaky neuron for feature variance optimization. This layer's output is dictated by equation 6, which outputs the variance-optimized features.
XI.	Maximum pooling layer with a pool size of 2x2	Feature reducers are used when there are too many features. They extract the maximum value from all of the extracted features and then reduce them by a factor of 2x2. That means that there are 2048 features per stride.
XII.	Drop-out layer with a dropout rate of 0.25	To optimise the selecting process, we have deleted about 25% of the features.
XIII.	2D Convolutional layer with 128x128 size and 3x3 kernel size	This method attaches a 3x3 window to the extracted feature sets and utilizes this pre-selected window to extract 16384 features per stride. Max pooling is then implemented.
XIV.	Leaky ReLU layer with alpha=0.1	Features are taken from the preceding layer and delivered to a leaky ReLU layer. After running the result via equation 6,

		this layer assesses the variance in each characteristic.
XV.	Maximum pooling layer with a pool size of 2x2	This procedure takes the most variability from the retrieved features and decreases them by a factor of 2x2, resulting in a halving of the number of features. As a result, it has 1024 features per stride.
XVI.	Drop-out layer with a dropout rate of 0.25	For an optimized experience and better performance, we will remove approximately 25% of the features.
XVII.	Drop-out layer with a dropout rate of 0.5	To optimise the selecting process, we have deleted about 50% of the features.
XVIII.	Dense layer with 512x1 size and Leaky ReLU activation	Using a dense layer that reduces the number of features with each stride. The 512 features will be combined to form one feature value. LeakyReLU is used for activation, as described by equation 6.
XIX.	Dense layer with 512x1 size and Leaky ReLU activation	The input features are integrated in thick layers, with 512 features combining to generate a single feature value in each layer.
XX.	Dense layer with 2x1 size and Sigmoid activation & Stochastic Gradient Descent optimizer.	This layer looks for and analyzes the crops: whether they're damaged or undamaged.
XXI.	Dense layer with 2x1 size and Sigmoid activation & root mean squared property (RMSProp) optimizer using a learning rate of 0.0001 for better classification.	This is a completely linked layer for classifying crops into one of two categories: damaged crops and undamaged crops. It employs many optimization strategies to achieve the best possible outcome.

XXII.	Dense layer with 2x1 size and Sigmoid activation & room Adam optimizer.	This layer is used to categories different agricultural damage kinds into one of two classes: undamaged and damaged crop.

Table 3.1. The Ensemble CNN Design

Performance indicators including precision, recall, F-measure, and accuracy are obtained from this network by combining the outputs of all dense layers using a mode operation to get the final output class. By studying a pretrained architecture like VGGNet, the proposed architecture's hyper-parameters are optimised. The operation of this system is explained as follows:

Table 3.1 now has an additional layer. The pre-trained VGGNet-16 model is trained with fewer layers than a fully convolutional network and makes use of the ImageNet architecture.

- This model is used to classify images that have already been classified. Statistical analysis is then performed to compare the classification results with the original classification.
- Leaky ReLU activation units are swapped out for regular ReLU activations in Table 1.
- Hyper-parameters are adjusted in accordance with the outputs of these models, i.e., the outputs of transfer learning ($C_{out_{TL}}$), leaky ReLU ($C_{out_{LR}}$), and normal ReLU ($C_{out_{NR}}$),
    - If, $C_{out_{TL}}$=$C_{out_{LR}}$ and $C_{out_{TL}}$=$C_{out_{NR}}$, then no hyperparameter tuning needed.
    - If $C_{out_{TL}}$=$C_{out_{LR}}$ and $C_{out_{TL}} \neq C_{out_{NR}}$, then adapt layer sizes to match the VGGNet-16 architecture. If not, we must adjust the hyper-parameters such that they gradually match the transfer learning model.
    - Else if $C_{out_{TL}} \neq C_{out_{LR}}$ and $C_{out_{TL}} = C_{out_{NR}}$, Change alpha in the hyper-parameters to match the non-leaky ReLU model since out-of-process computation time and in-process computation time are not equivalent. Alpha should be adjusted by a factor of 0.01 either up or down until it is equal to the value of a non-leaking ReLU architecture.

- Otherwise, change the hyper-parameters to gradually match the non-leaky ReLU model if $C_{out_{LR}} = C_{out_{NR}}$. A 0.01 factor is used to enhance or reduce alpha. To match the layer sizes of VGGNet-16, layer sizes are also raised or lowered by a factor of 8.

Hyper-parameters are tuned continuously after every classification. In the next section results of these iterative tuning procedures can be observed.

3.3 Results & Comparisons

To understand the work batter, we have divided the result on two sections visual analysis and quantitative analysis.

3.3.1 Visual Analysis

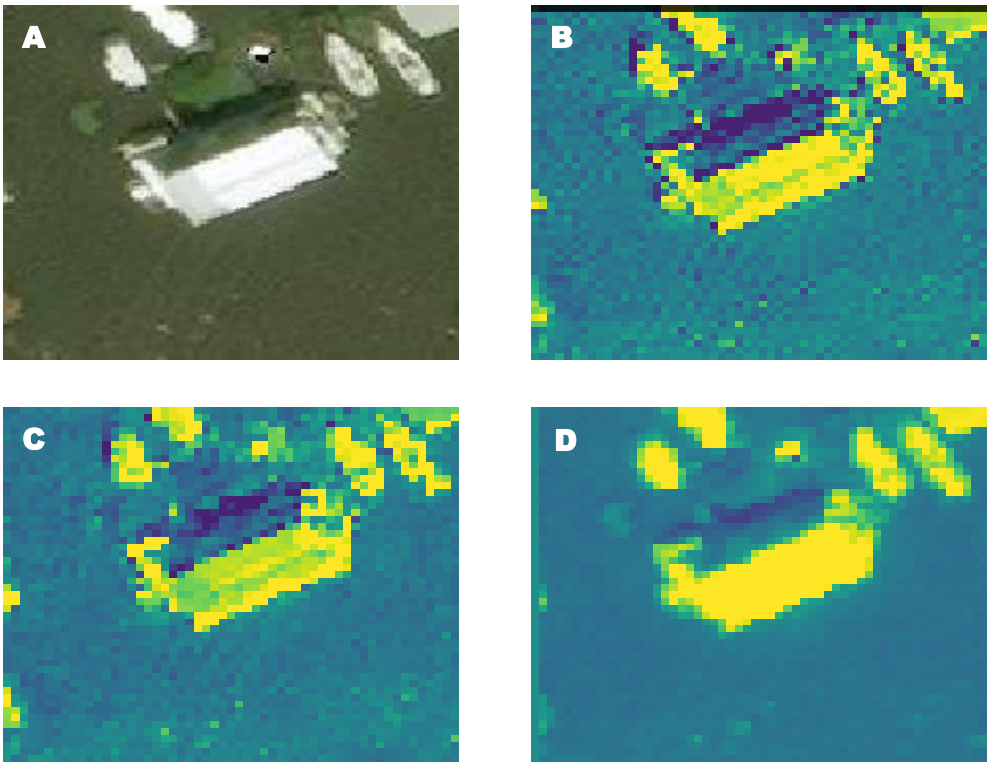

Figure 3.4 Experimental Results

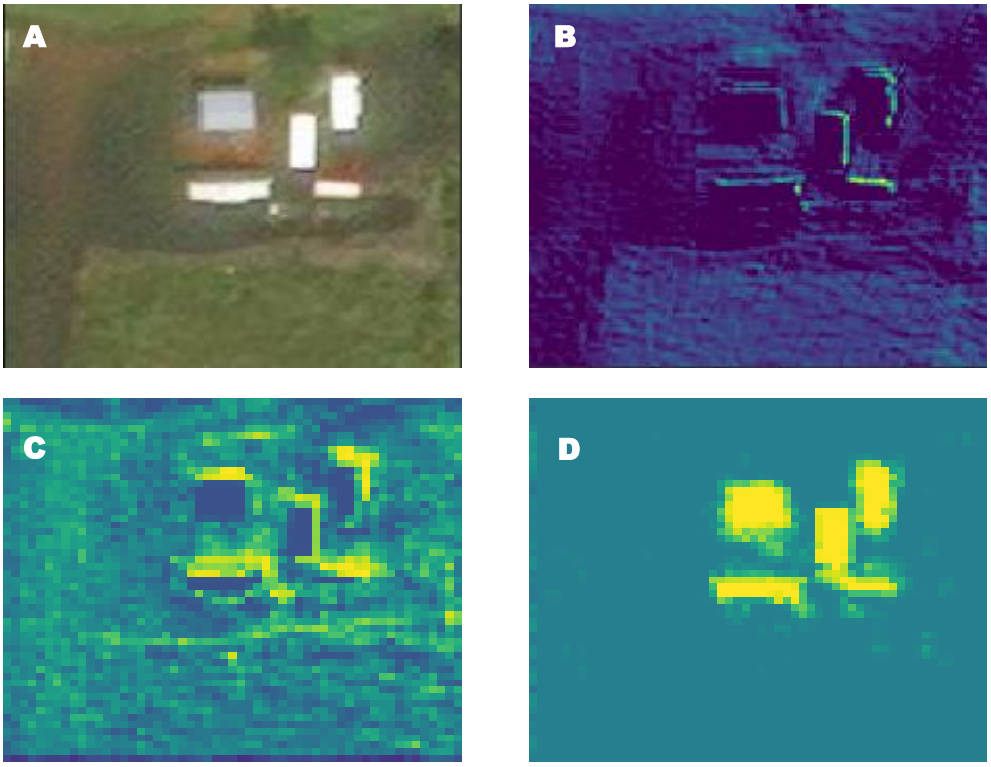

Figure 3.5: Experimental Results

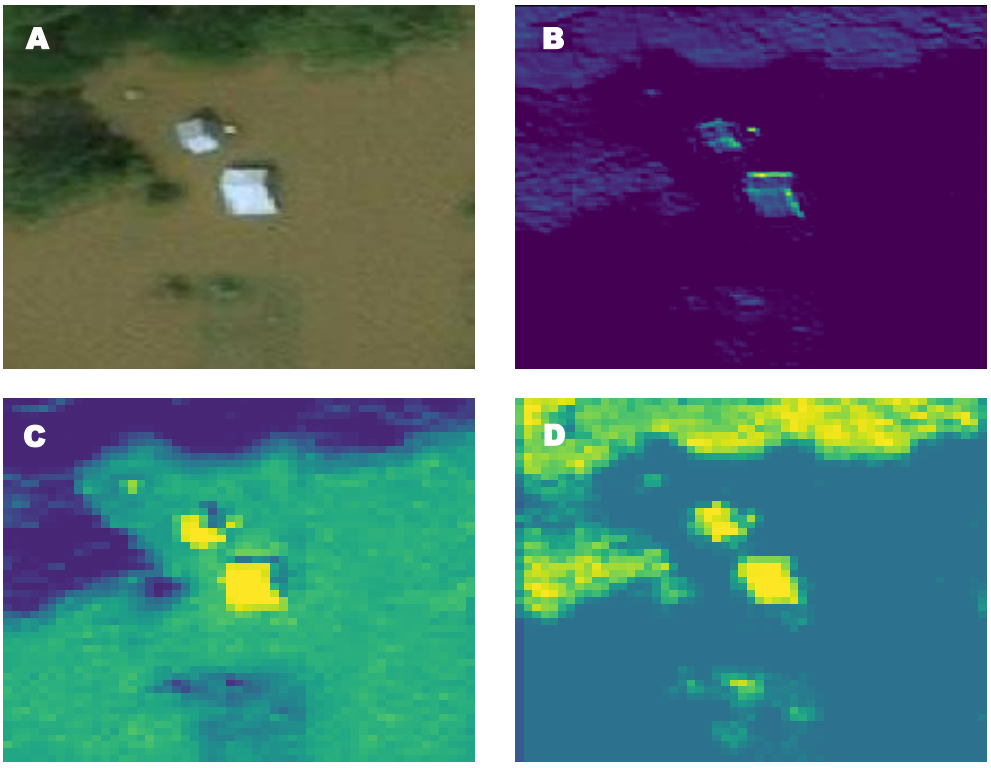

Figure 3.6: Experimental Results

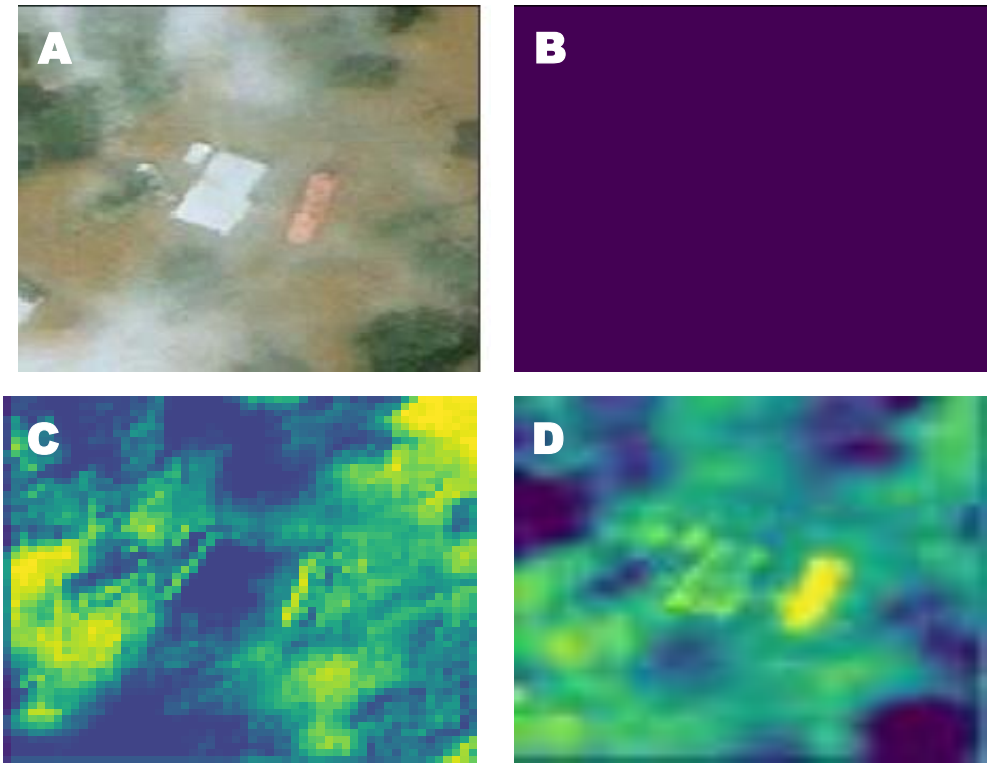

Figure 3.7: Experimental Results

(A) Input Image (B) DCNN (C) VGG Net (D) Proposed Model

As demonstrated by figure 3.4, 3.5 3.6 and 3.7 (a) Input Image and figure 3.4, 3.5, 3.6 and 3.7 (B) DCNN [103] output, 3.4, 3.5, 3.6 and 3.7 (C) VGG Net [116] output, 3.4, 3.5, 3.6 and 3.7 (D) output of proposed model, which shows the batter results as compare to DCNN [103], VGG Net [116], CNN [123].

3.4.2 Quantitative Analysis

Because scientists can access LANDSAT images, collecting satellite data for different time periods has become easy. Here in this architecture, the data of Amravati District (India) from hailstorms during February 2018 and floods during March 2018 is evaluated. In this dataset, the selection of a region's farming population is important. Performance was evaluated for publications in [103], and [123], by putting the precision score from the literature so that we can compared the proposed model concerning the recall, precision, accuracy and F-measure values. The results concerning the evaluation of different testing images as shown in Tables 3.2, 3.3, 3.4, and 3.5.

Number of input images	Precision Values of VGG Net [116]	Precision Values of DCNN [103]	Precision Values of CNN [123]	Precision Values of Proposed Model
90	0.79	0.79	0.8	0.889
190	0.79	0.79	0.8	0.897
390	0.80	0.80	0.81	0.905
490	0.80	0.80	0.81	0.907
590	0.81	0.81	0.82	0.912
690	0.81	0.81	0.82	0.916
790	0.82	0.82	0.83	0.919
890	0.82	0.82	0.83	0.923
990	0.82	0.82	0.83	0.927
1090	0.82	0.82	0.83	0.931
1190	0.83	0.83	0.84	0.934
1290	0.83	0.83	0.84	0.938
1390	0.84	0.84	0.85	0.942
1490	0.84	0.84	0.85	0.946
1590	0.84	0.84	0.85	0.95
1690	0.85	0.85	0.86	0.953
1790	0.85	0.85	0.86	0.957
1890	0.85	0.85	0.86	0.961
1940	0.86	0.86	0.87	0.967
1990	0.87	0.87	0.88	0.972

Table 3.2. Precision Scores of Various Algorithms

By using of multiple CNN architecture for classification, it gives 10% improvement. Table 3.3 below show evaluating recall values,

Number of input images	Recall Values for VGG Net [116]	Recall Values for DCNN [103]	Recall Values for CNN [123]	Recall Values for Proposed Model
90	0.640	0.618	0.650	0.709
190	0.650	0.624	0.660	0.715
390	0.650	0.632	0.660	0.721
490	0.650	0.632	0.660	0.723
590	0.660	0.636	0.670	0.727
690	0.660	0.639	0.670	0.730
790	0.660	0.641	0.670	0.732
890	0.670	0.643	0.680	0.735
990	0.670	0.646	0.680	0.738
1090	0.670	0.649	0.680	0.741
1190	0.670	0.651	0.680	0.744
1290	0.680	0.654	0.690	0.747
1390	0.680	0.657	0.690	0.750
1490	0.680	0.659	0.690	0.753
1590	0.680	0.662	0.690	0.757
1690	0.690	0.665	0.700	0.760
1790	0.690	0.667	0.700	0.763
1890	0.690	0.670	0.700	0.766
1940	0.700	0.673	0.710	0.774
1990	0.710	0.678	0.720	0.785

Table 3.3. Recall Scores of Various Algorithms

The comparison of multiple reference models allowed us to find that incremental gains were seen in terms of recall performance (7%). The fMeasure provides true accuracy rates for the given set of architecture. It can be seen below in table 3.4

Number of input images	F1 Values for VGG Net [116]	F1 Values for DCNN [103]	F1 Values for CNN [123]	F1 Values for Proposed Model
90	0.710	0.694	0.720	0.789
190	0.710	0.701	0.720	0.796
390	0.720	0.711	0.730	0.803
490	0.720	0.710	0.730	0.805
590	0.730	0.714	0.740	0.809
690	0.730	0.718	0.740	0.812
790	0.730	0.721	0.740	0.815
890	0.730	0.723	0.740	0.819
990	0.740	0.726	0.750	0.822
1090	0.740	0.729	0.750	0.825
1190	0.740	0.732	0.750	0.829
1290	0.750	0.735	0.760	0.832
1390	0.750	0.738	0.760	0.835
1490	0.750	0.741	0.760	0.839
1590	0.760	0.744	0.770	0.842
1690	0.760	0.747	0.770	0.846
1790	0.760	0.750	0.770	0.849
1890	0.770	0.753	0.780	0.853
1940	0.770	0.757	0.780	0.860
1990	0.780	0.761	0.790	0.868

Table 3.4 fmeasure Scores of Various Algorithms

Our proposed models achieve appreciable improvements in fMeasure values. This is indicative of our model performing well and being appropriate for real-time crop damage detection. The comparison of accuracy of different model is shown in table 3.5.

Number of input images	Accuracy Values for VGG Net [116]	Accuracy Values for DCNN [103]	Accuracy Values for CNN [123]	Accuracy Values for Proposed Model
90	0.86	0.84	0.87	0.89
190	0.86	0.85	0.87	0.89
390	0.87	0.87	0.88	0.90
490	0.87	0.86	0.88	0.90
590	0.88	0.87	0.89	0.91
690	0.88	0.87	0.89	0.91
790	0.89	0.88	0.90	0.92
890	0.89	0.88	0.90	0.92
990	0.89	0.88	0.90	0.92
1090	0.90	0.89	0.91	0.93
1190	0.90	0.89	0.91	0.93
1290	0.90	0.89	0.91	0.93
1390	0.91	0.90	0.92	0.94
1490	0.91	0.90	0.92	0.94
1590	0.92	0.90	0.93	0.95
1690	0.92	0.91	0.93	0.95
1790	0.92	0.91	0.93	0.95
1890	0.93	0.92	0.94	0.96
1940	0.93	0.92	0.94	0.96
1990	0.95	0.92	0.96	0.97

Table 3.5 Accuracy Scores of Various Algorithms

Figure 3.8, which shows the effect of flood, and Figure 3.9, which highlights the effect of hail storms.

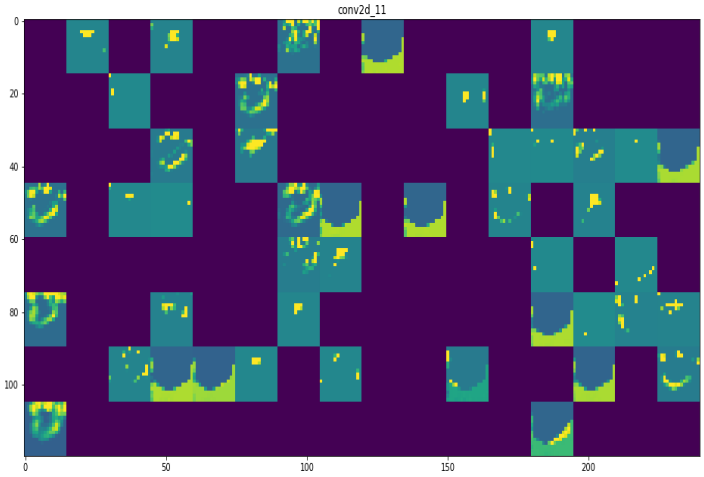

Figure 3.8 Flood-Affected Areas Identified

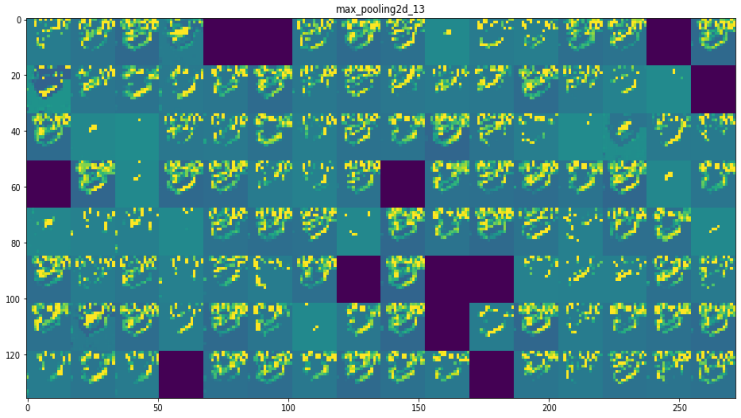

Figure 3.9 Hailstorm-Affected Areas Identified

Figure 3.10 and 3.11 show the results of different drone-based spot damage detection percentages.

Figure 3.10 Drone Images with 20% Damage Detected

Figure 3.11 Drone Images with 40% Damage Detected

This data can be used to observe the accuracy or inaccuracy of drone-based damage findings across varying levels of damage. An accuracy improvement of 5% when compared with [103] , and 1.5%, when compared with [123] , is observed. This improvement assists the model to be applied for high efficiency & large-scale applications that are accuracy aware like monitoring of remote areas. Thus, the proposed model can be applied to a wide variety of crop damage detection systems with high performance.

3.4 Conclusions

CNN models help improve the performance of classification of existing as well as new systems. High-efficiency convolutional, ReLU, dropout layers and max pooling, are used for faster feature extraction, which is what helps make CNN models so effective. Each of these layers consists of a different neural network to extract features with more accuracy. In the suggested architecture combine several learning rate optimizers such as RMSProp, SGD, and Adam so that the accuracy performance of the dense layer may be enhanced. The transfer learning model and ensemble CNN classifier are used to improve accuracy, precision, recall, and F-measure automatically by iterative updating of its hyper-parameters. We can see that this is true in Tables 3.2, 3.3, 3.4, and 3.5. This thesis' suggested model outperforms existing deep learning models and can be implemented for high-efficiency applications like satellite-based crop

damage detection. LSTM and GRU models may also improve performance. GANs (generative adversarial networks) are another option to investigate since they can increase the output of both near-field and satellite images when assessing damage in already classed damaged images.

Chapter No 4

Satellite Image Classification for Real-Time Using Augmented Incremental Transfer Learning

Chapter No 4

Satellite Image Classification for Real-Time Using Augmented Incremental Transfer Learning

Outline

This chapter describes an overview of related work, an explanation of the model's motivations, a description of the proposed architecture for satellite image classification for real-time by means of transfer learning with augmentation for crop condition examination, and a comparison of engine's performance to that of existing models.

4.1 Introduction

In satellite image processing multidomain are involves like image capturing, segmentation, denoising, feature reduction, feature extraction, post-processing tasks, and classification. Researchers propose a variety of satellite image processing architecture, each with diverse process and data necessities. For example, the image acquisition module may receive images in the form of layered, while the feature extraction module may require data in 3D or 2D form. In addition, accuracy and scalability of this model is limited in the real time scenarios due to variation in the dataset parameters and internal process parameters. The motivation behind this research is to develop a novel method which will be able to overcome these issues. A new architecture is recommended and analyzed in this thesis to overcome the restrictions and limitations of existing work. This model uses backscatter coefficient analysis to create a transfer learning-based CNN architecture for analysing real-time satellite images obtained from Google's Earth Engine. As an output of this we get the average

intensity value of PRI (precision image intensity) of coefficient at the time we analyzed it for many targets. The presented architecture characterizes crop images in HV (Horizontal Tx, Vertical Rx) and VV (Vertical Tx, Vertical Rx) modes, as an outcome of using backscattering coefficients. After this the data set is divided into three class i.e., VV, VH and Original which largely help the CNN architecture to extract different features sets from given satellite data. To visual identification of affected areas an incremental learning layer is activated which processed already classified images. The final outcome of all this block (like Convolutional Neural Network, Incremental learning) the implemented architecture come up with 97.8% average accuracy for detecting damage severity and crop type. The consistent results were seen when we tested this new architecture for different regions around our local area. Hence the proposed new architecture is highly recommended as model was found to have a 7.9% better recall value, 5.6% improvement in accuracy and 4.6% better precision when compared with various state-of-the-art approaches reported till date. Additionally, the PSNR of the recommended model is up to 29.6 dB for various data set.

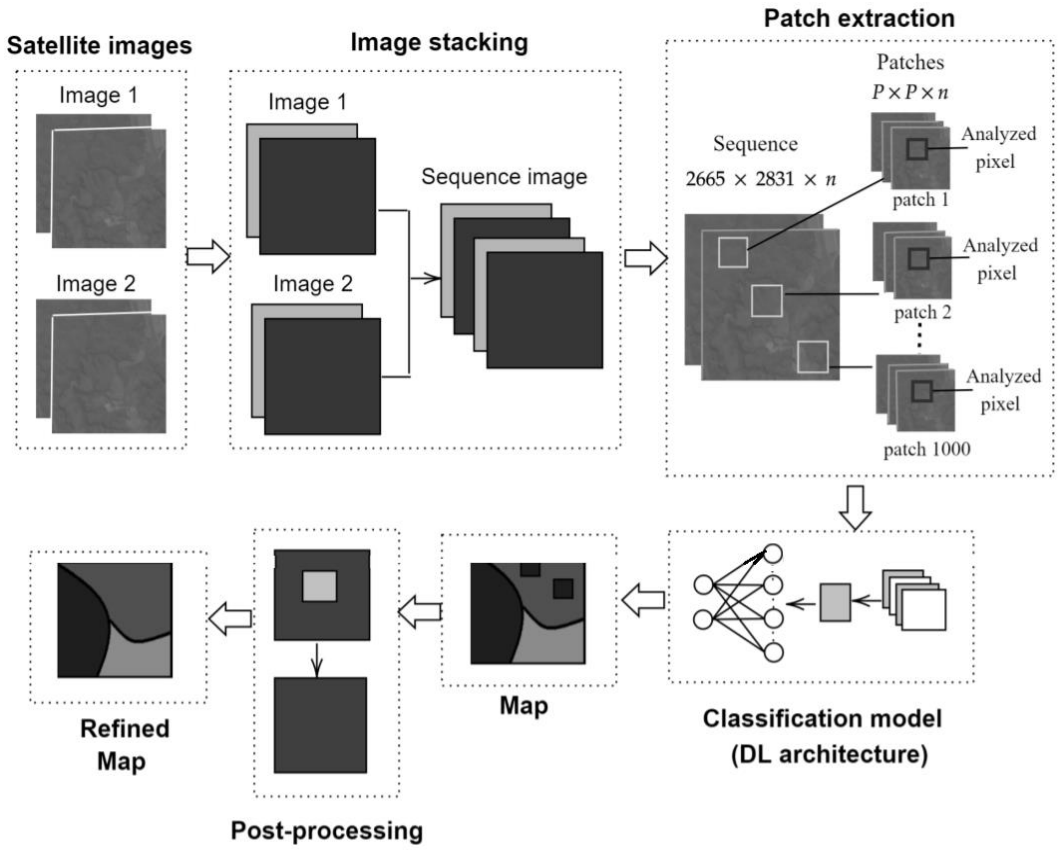

Figure 4.1 A Typical Satellite Image Processing Model

Multiple image processing jobs that should be able to function with various bands of image data must be designed in order to classify satellite images. These include feature extraction, feature selection, classification, band-based, band fusion, pre-processing, post processing, segmentation, and feature-based pre-processing. Figure 4.1 show the typical satellite image processing model.

This involves stacking and sequencing images from several bands in order to extract patches and estimate sequences. In order to extract a large number of features, the extracted patches are sent to a windowing layer, which separates them into smaller components. This sets feature is categorised using a deep learning (DL) model that creates the first clustered map by combining several convolutional neural networks (CNNs). A post-processing layer receives this initial map and helps create a refined map that can help identify the various components of the region being tested. These elements may include urban cover, crop type, crop cover, water cover, and land cover.

Numerous classification methods and architectures are suggested by researchers [1, 2, 3], each with a unique applicability, accuracy, classification delay, complexity, and other characteristics. We have proposed the concept of far-filed image classification for real-time application employing enhanced incremental transfer learning for crop in order to increase this performance. This model's performance is assessed in terms of latency, precision, area under the curve (AUC), recall, and accuracy and it is contrasted with other recent advanced techniques. At the conclusion, we discussed the findings about our model and offered similar suggestions for enhancing performance.

4.2 Proposed Model

It is very clear from the literature review that the model reported till date are very much application specific with their specific data set requirement and algorithm. Also, the model developed can provide a specific and accurate result for a specific condition but will give tremendous bad result for different data set. This put limit on their use for general purpose application at the same time a single model cannot be implemented for all scenario. In this thesis we have suggested a satellite image classification model to overcome this limitation of existing model. The suggested model use augmented

incremental transfer learning which make the model more efficient and applicable for real-time problem.

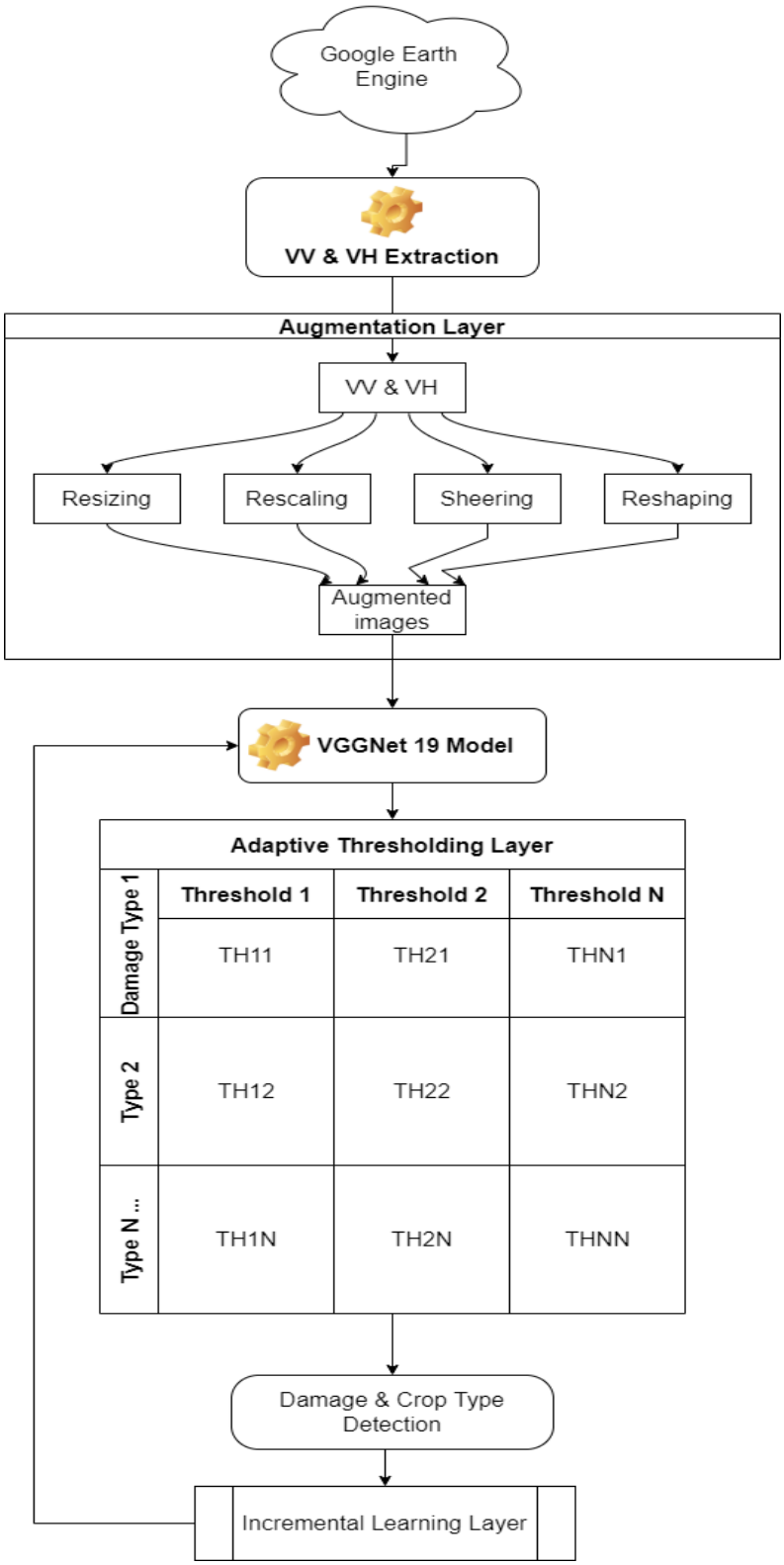

Figure 4.2. Flow of the Proposed Model

As we have implemented the CNN architecture with incremental learning it helps in continuously improving classification accuracy. Figure 4.2 show the Overall flow of the proposed model. In the suggested model images are downloaded from Google Earth Engine from which the VV & VH components are extracted and then augmented via reshaping, resizing, rescaling, and sheering operations. After that VGGNet-19 architecture is implemented for crop image classification. The input to the crop damage detection model is images which are tag with crop type. the main function of the block is to detect the damage severity by using adaptive threshold engine. A block of the incremental learning layer is used to confirm the threshold engine's results. The correlation-based matching & hyperparameter tuning methods, aid in fine-tuning the VGGNet model.

The data was collected in and around the Amravati area (77.7523, 20.9320) from 2015 to 2021, and analysed using the suggested model. Google Earth engine is the best tool in the hand of researcher now a days which will help in accessing the real-time satellite images with different Temple zone, we have collected the images from this engine for our work. These sources were interpolated via multiple location-based data access, wherein current area was segregated into different sub-regions, and each region was processed via different transmitter receiver polarization.

Following process is adopted to extract the region from Google Earth engine longitude and latitude

- Provide the targeted area in the form of $Lat_{target}, Long_{target}$
- Download the Extract COPERNICUS surface temperature collections and MODIS land cover collection images for this target.
- Fine out the VH and VV component via equations 1 and 2 as follows,

$$VV_i = \frac{\sum_{i=1}^{NBands} B_i - B_{RGB}}{\sum_{i=1}^{NBands} B_i + B_{RGB}} \dots (1)$$

$$HV_i = \frac{\sum_{i=1}^{NBands} G_i - G_{RGB}}{\sum_{i=1}^{NBands} G_i + G_{RGB}} \dots (2)$$

Where, G & B represents their green & blue components, G_{RGB} & B_{RGB} represents green & blue components of RGB band, and $NBands$ represents number of bands extracted from Google Earth Engine.

- VV and HV images are formed for current location after these values are extracted for each pixel.
- To extract a greater number of images from the current location the current latitude and longitude are modified via equation 3,,

$$New_{lat} = Lat_{target} \pm 0.1, New_{long} = Long_{target} \pm 0.1 \dots (3)$$

- VV and VH images are extracted to form the initial training set for each of these latitude and longitude positions.

Different crop kinds and damage percentages are recorded with each image in the training set, which is manually annotated. For the purpose of developing training sets accurately, this data was taken from the Indian Meteorological Dataset (https://mausam.imd.gov.in/), and it may be scaled to any global geographic region. There aren't enough images in the gathered dataset to allow for effective CNN training. An augmentation layer is activated to fix this problem by resizing, resizing, sheering, and reshaping each of the input images. Equation 4 carries out the rescaling procedure.

$$I_{scale} = \frac{I_{orig} - \min(I_{orig})}{\max(I_{orig}) - \min(I_{orig})} * S_F \dots (4)$$

Here, SF is the scaling factor, which is changed from 1 to 128 in steps of 2 to produce 64 distinct images for each input image. Where I orig, I scale stand for the original and scaled images, respectively. Resizing procedures are used to further enhance the input image and are carried out using equation 5 as follows:

$$I_{resize} = \bigcup_{i=1}^{N} \left| I_{orig_i} \right|_{i=i+r} \dots (5)$$

In above equation r stands for the resizing factor and is adjusted in steps of 0.1 from 0.1 to 10. By using resizing operation 100 different images are obtained from one input image. Equation 6, in the same way governed the reshaping operating as noted below.

$$I_{reshape} = \bigvee_{r=1}^{R} \bigvee_{c=1}^{C} |I_{r+s_1,c+s_2}| \ \ldots (6)$$

Where C and R stands for the number of columns and rows in the given image, and S_1, and S_2 stands for reshaping constants that are adjusted between 2 and 8 to produce 64 alternative images from the original image. Equation 7 governed the process of sheering as noted below.

$$I_{sheer} = Q * \frac{I_{orig}}{C_{sheer}} \ldots (7)$$

In this case, C sheer stands for the constant of sheering and Q stands for the quality factor, 64 distinct images for each input image produce by adjusting them from 1 to 8.

For each input image, these augmented images are merged to produce 292 images, which are then provided to the VGGNet19 model. The retrieved images are scaled down to 128x128 for the initial convolution operations that help with the extraction of enhanced features. Multiple layers of convolution with various stride sizes, padding sizes and window sizes, are employed to aid in large-scale feature extraction. The extraction of over 1 million features from each augmented image set is made possible by the use of stride sizes from 3x3 to 5x5, padding sizes from 3x3 to 5x5 and window sizes ranging from 8x8 to 512x512. The convolutional processes are managed by an activation layer, which selects essential features. A leaky rectilinear unit (LReLU) is employed for VGGNet-19, allowing for variance-based feature extraction for improved accuracy performance. Equation 8 controls the output features that convolutional layers extract as shown below.

$$F_{out} = Leaky_{ReLU}\left(\frac{r}{2} + a, \frac{c}{2} + b\right) * \sum_{a=0}^{\frac{r}{2}} \sum_{b=0}^{\frac{c}{2}} I_{aug}(i - a, j - b) \ldots (8)$$

Where a, b are the sizes of the strides which range from 3 by 3 to 5 by 5 for each layer, m, n are the convolutional window sizes for the particular convolution layer, and I_{aug} is an enhanced satellite image for the present layer. The leaky RELU utilised in this scenario eliminates 5% of all low variance features and aids in the initial feature selection phase. Equation 9 controls the Leaky ReLU as follows:

$$LReLU(x, y) = 0.05 * (x, y), when\ x < 0\ or\ y < 0$$
$$else, 1, when\ x \geq 0\ and\ y \geq 0 \ldots (9)$$

This variance assessment makes it feasible to extract several features and reduce them depending on variance. Equation 10 estimates the total number of features that this model has retrieved and chosen as follows:

$$f_{conv} = \frac{2 * p - k + f_{prev}}{s} + 1 \ldots (10)$$

Where k is the leaky ReLU kernel size for convolutions, s is the size of the stride, f_{prev} represents the total number of features extracted by previous convolutional layer, f_{conv} represents the total number of convolutional features extracted by current convolutional layer, and p represents the padding size of the leaky ReLU based convolutions. However, the Leaky ReLU has the drawback of estimating variance based on a fixed threshold, which is inefficient for large datasets. A layer called MaxPooling (maximum variance pooling) is utilised to improve feature selection capabilities. By computing a variance-based threshold for each extracted feature set, this layer selects features according to this variance threshold. If a feature's intensity exceeds this cutoff, it will be advanced to the following level; otherwise, it will be discarded at the current level alone. Equation 11 assesses this variance threshold.

$$f_{th} = \sqrt[p_k]{\left(X_k^{-1} \sum_{x \in X_k} x^{p_k} \right)} \ldots (11)$$

Where p k specifies the amount of features to be pooled at each layer and reflects the probability of pooling, and X k represents the input image. Hyperparameter optimization is used to change the pooling probability in order to optimise feature selection. To estimate a large number of features from the provided satellite images, this procedure is repeated for various step sizes and windows. As shown in Figure 4.3, these operations are made available to an FCNN (Fully Connected Neural Network) model for image classification into damage severity kinds and crop types.

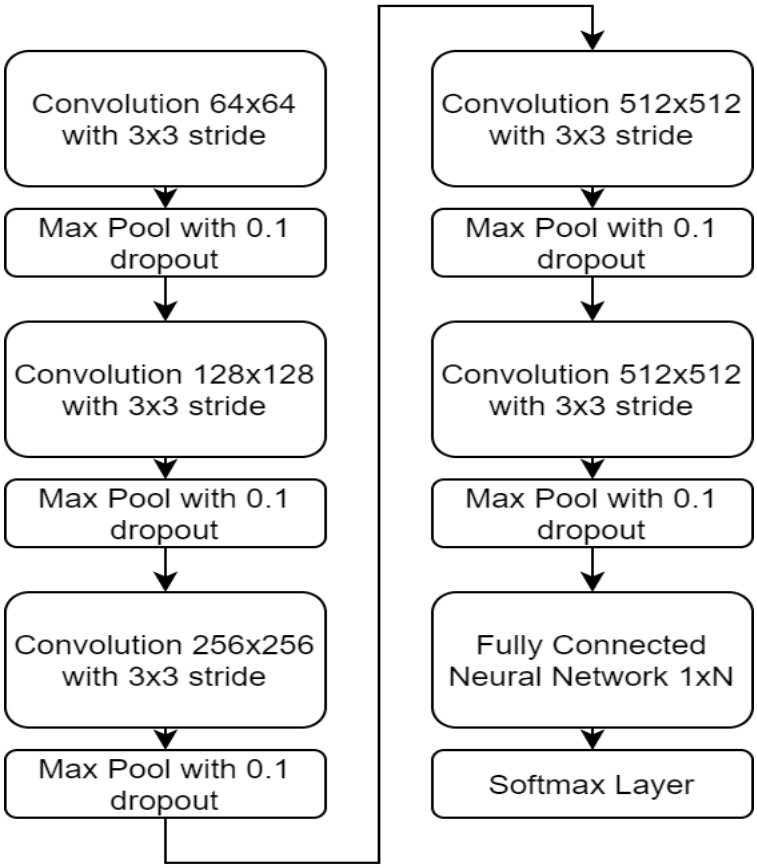

Figure 4.3. CNN Model Used for Classification

The classification layer employs a Soft Max Activation Model to estimate the final class probability, which aids in classifying the severity of the crop damage. The Soft Max Activation Model includes the ability to backpropagate, which helps with ongoing accuracy improvement. Equation 12 provides the probabilities for each kind of output.

$$c_{out} = SoftMax\left(\sum_{i=1}^{N_f} b + f_i * w_i\right) \ldots (12)$$

Where N f is the total number of features extracted using a mixture of multiple convolutional layers, Fi is the number of features extracted by all previous convolutional and Max Pooling layers, Wi is a tailored weight value for the given class, and b is bias value. For adaptive threshold evaluation with parameter adjusting procedures, these classes are employed.

Before activating an adaptive thresholding layer for final processing and ongoing accuracy improvement the CNN Model measures crop type and damage severity. Depending on the season in which the image was taken, the layer employs various thresholds for the R, G, and B components to evaluate various damage kinds. The following thresholds are listed in table 4.1:

Season -> Damage Type	**Winter**	**Summer**	**Rainy**	**Autumn**
Low Damage	$\frac{G}{R} > 0.6$ & $\frac{G}{B} > 0.5$	$\frac{G}{R} > 0.5$ & $\frac{G}{B} > 0.65$	$\frac{G}{R} > 0.6$ & $\frac{G}{B} > 0.6$	$\frac{G}{R} > 0.55$ & $\frac{G}{B} > 0.65$
Moderate Damage	$\frac{B}{R} > 0.2$ & $B > 0.5 * G$	$\frac{B}{R} > 0.6$ & $B > 0.6 * G$	$\frac{B}{R} > 0.8$ & $B > 0.85 * G$	$\frac{B}{R} > 0.75$ & $B > 0.85 * G$
High Damage	$R > 0.3 * B$ & $R > 0.35 * G$	$R > 0.45 * B$ & $R > 0.55 * G$	$R > 0.35 * B$ & $R > 0.65 * G$	$R > 0.75 * B$ & $R > 0.8 * G$

Table 4.1. Adaptive Threshold Evaluation for Damage Severity Detection

After the damage categories are determined for the images, equation 13 is used to determine whether there is a correlation between the testing dataset and the corresponding ground truth:

$$C_{train,test} = \frac{\sum I_{test} - I_{train}}{\sqrt{(\sum (I_{test} - I_{train})^2)}} \ldots (13)$$

When the test set image closely resembles one of the training set images, the correlation value is over 0.999. In certain situations, the test set image is discarded and not used for parameter adjustment. In such situation, we had to upload new images to the CNN architecture in order to retrain it. Because of this, the model is constantly updated, and its accuracy gradually increases. The examination of accuracy performance was covered in the text after along with numerous other performance indicators.

4.3 Analysis of Result & Comparisons

We have divided the result on two sections visual analysis and quantitative analysis.

4.3.1 Visual Analysis

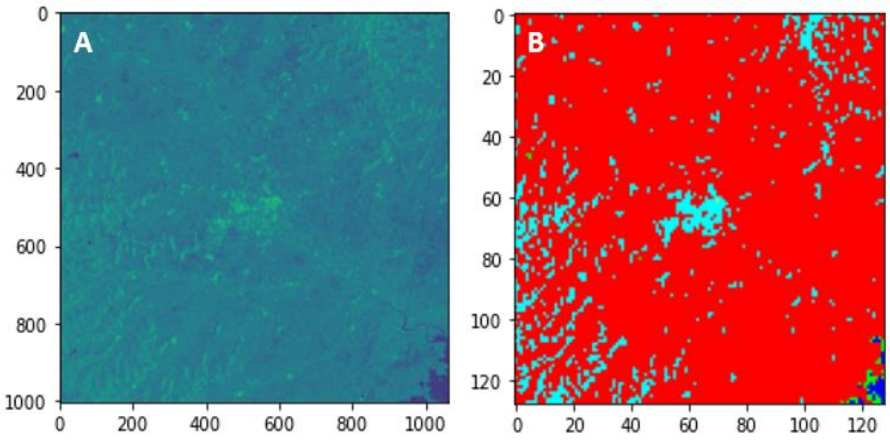

Figure 4.4: Experimental Results

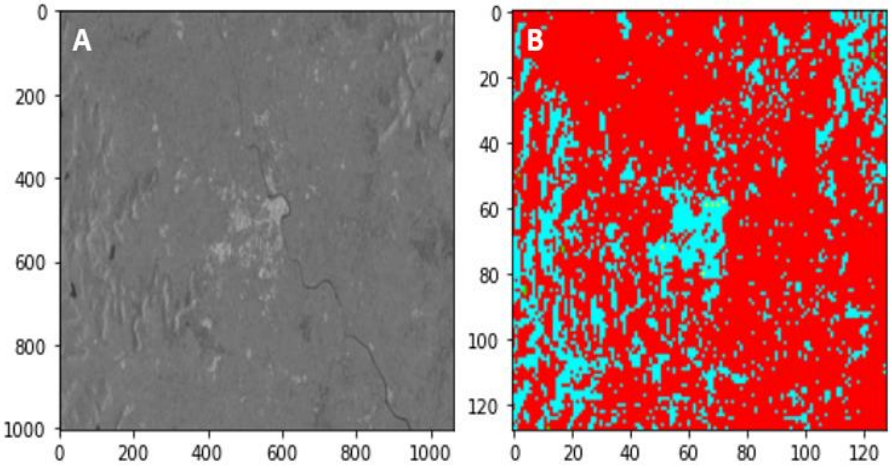

Figure 4.5: Experimental Results

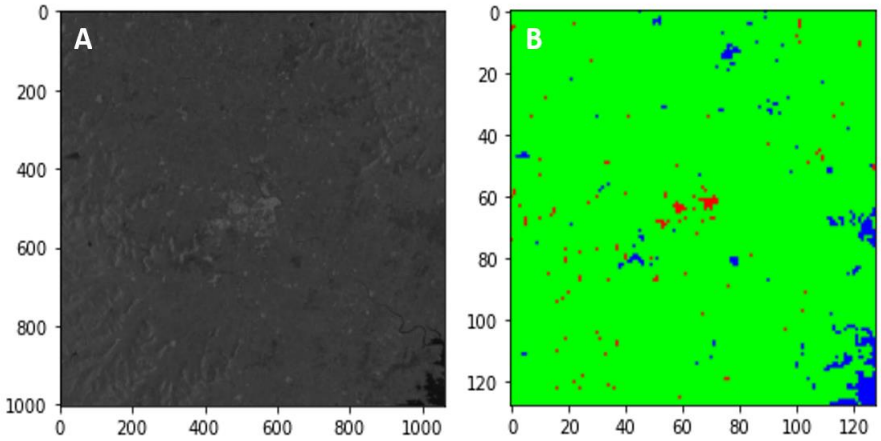

Figure 4.6: Experimental Results

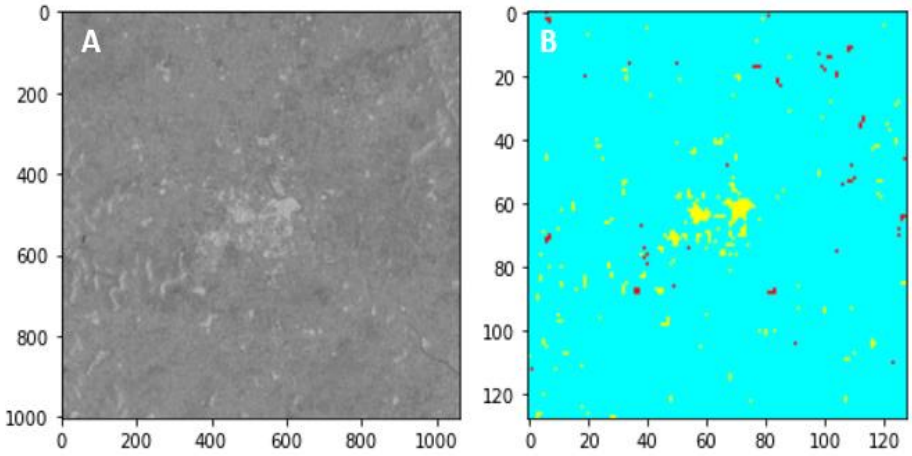

Figure 4.7: Experimental Results

As demonstrated by figure 4.4, 4.5. 4.6 and 4.7 (A) are the input images and figure 4.4, 4.5. 4.6 and 4.7 (B) shows results for the proposed model.

4.3.2 Quantitative Analysis

The data was collected in and around the Amravati area (77.7523, 20.9320) from 2015 to 2021, and analysed using the suggested model. The recommended model employs Google Earth Engine for collecting of a wide variety of datasets from MODIS satellite data collections. Also, USGS SRTMGL1 ground elevations and the COPERNICUS

subset were utilised for dataset collection. The Rice, Bajra, Cotton, and Wheat crop images were retrieved for this model data set in 3 distinct severity categories. The data set have 2000 images in total which are classified in the following ratios: 70:15:15 for training, testing, and validation.

Performance was evaluated for publications in [128], [136], and [138], by putting the precision score from the literature so that we can compared the proposed model concerning the recall, precision, accuracy, delay and F-measure values. The results concerning the evaluation of different testing images as shown in Tables 4.2, 4.3, 4.4, 4.5 and 4.6.

By combining CNN with incremental learning, with several high-performance classification and adaptive thresholding level we were able to obtain decreased error rates. Table 4.2 show the comparison of precision (P) values with different models

Table 4.2. Precision Scores of Various Algorithms

Number of input images	Precision Values for MSRPS [136]	Precision Values for HCNN [128]	Precision Values for CNN TSS [138]	Precision Values for Proposed Model
120	71.02	80.41	84.02	85.43
250	71.66	81.14	84.8	85.91
390	71.81	81.31	84.98	86.17
520	72.11	81.65	85.33	86.43
650	72.26	81.82	85.51	86.57
790	72.34	81.91	85.6	86.61
920	72.34	81.91	85.6	86.62
1050	72.35	81.91	85.6	86.64
1190	72.35	81.92	85.61	86.64
1290	72.35	81.92	85.61	86.64
1490	72.37	81.92	85.61	86.64
1590	72.37	81.92	85.61	86.64
1720	72.37	81.92	85.61	86.65
1850	72.37	81.94	85.63	86.65
1990	72.37	81.94	85.63	86.83

the proposed architecture is 14.2% more precise and has a higher recall than MSRPS, 5% more accurate and has a higher recall than H. Convolutional Neural Network, and 1.5% more precise and has a higher recall than Convolutional Neural Network TSS. Because of this the proposed architecture is adaptable to a wide range of high-precision real-time applications. Based on this dataset collection, accuracy was examined by equation 14

$$A = \frac{N_C}{N_T} * 100 \ldots (14)$$

Where, N_T & N_C represents total number of images used for classification and number of correctly classified images. The model is compared with the state-of-the-art methods like HCNN, CNN TSS, MSRPS. The table 4.3 show the comparison of this methods with respect to number of images used for evaluation (NI).

Table 4.3. Accuracy Scores of Various Algorithms

Number of input images	Accuracy Values for MSRPS [136]	Accuracy Values for HCNN [128]	Accuracy Values for CNN TSS [138]	Accuracy Values for Proposed Model
120	65.55	73.22	83.93	96.66
250	66.16	73.89	84.71	97.21
390	66.29	74.05	84.89	97.51
520	66.57	74.36	85.24	97.8
650	66.70	74.50	85.41	97.96
790	66.77	74.59	85.5	98.01
920	66.77	74.59	85.5	98.02
1050	66.78	74.60	85.51	98.03
1190	66.79	74.60	85.52	98.03
1290	66.79	74.60	85.52	98.04
1490	66.79	74.61	85.53	98.04
1590	66.79	74.61	85.53	98.04
1720	66.79	74.61	85.53	98.05
1850	66.80	74.62	85.54	98.05
1990	66.80	74.62	85.54	98.05

The output of suggested model 15% better than HCNN & MSRPS and at least 12.5% improvement when compare to the Convolutional Neural Network TSS, in terms of multiple domain accuracy performance. Also, the comparison is done on the basics of AUC. The following table 4.4 show observations for area under the curve (AUC) values.

Table 4.4. Area Under the Curve (AUC) Scores of Various Algorithms

Number of input images	AUC Values for MSRPS [136]	AUC Values for HCNN [128]	AUC Values for CNN TSS [138]	AUC Values for Proposed Model
120	63.44	70.87	81.23	93.56
250	64.03	71.52	81.99	94.08
390	64.16	71.67	82.16	94.37
520	64.43	71.96	82.5	94.66
650	64.55	72.11	82.66	94.81
790	64.63	72.19	82.75	94.86
920	64.63	72.19	82.75	94.87
1050	64.63	72.19	82.76	94.88
1190	64.64	72.20	82.77	94.88
1290	64.64	72.20	82.77	94.89
1490	64.64	72.21	82.77	94.89
1590	64.64	72.21	82.77	94.89
1720	64.64	72.21	82.77	94.9
1850	64.65	72.22	82.78	94.9
1990	64.65	72.22	82.78	95.61

When evaluated against various types of satellite image data sets, the suggested model has 28.6% higher AUC than MSRPS, 22.5% higher AUC than HCNN, and 12.4%

higher AUC than CNN TSS. Because of which, the implemented model is capable of being used for large variety of low-error applications. The recall is one of the most important parameters to test the model applicability in real world hence we have compared the model with different algorithms. Table 4.5 show the observations are made for recall (R) values,

Table 4.5. Recall Scores of Various Algorithms

Number of input images	Recall Values for MSRPS [136]	Recall Values for HCNN [128]	Recall Values for CNN TSS [138]	Recall Values for Proposed Model
120	70.13	79.40	82.99	90.85
250	70.78	80.14	83.75	91.37
390	70.93	80.30	83.92	91.65
520	71.21	80.63	84.26	91.93
650	71.36	80.78	84.43	92.07
790	71.44	80.87	84.53	92.11
920	71.44	80.87	84.53	92.12
1050	71.45	80.89	84.53	92.14
1190	71.45	80.89	84.55	92.14
1290	71.45	80.89	84.55	92.14
1490	71.47	80.90	84.55	92.14
1590	71.47	80.90	84.55	92.14
1720	71.47	80.90	84.55	92.15
1850	71.47	80.92	84.56	92.15
1990	71.47	80.92	84.56	92.35

The proposed model is observed to be 20.5% efficient than MSRPS, 10.2% efficient than HCNN and 5.9% efficient than CNN TSS.

In digital image prosecting and machine learning delay in the out put can affect the applicability of the model in real world. Hence, it is very important and significant to evaluate the suggested model on the basics of their speed. Table 4.6 show the similar observations are made for delay (D) values,

Table 4.6. Average Delay (D) Scores of Various Algorithms

Number of input images	Delay Values for MSRPS [136]	Delay Values for HCNN [128]	Delay Values for CNN TSS [138]	Delay Values for Proposed Model
120	10.62	9.38	8.97	6.82
250	10.52	9.29	8.89	6.76
390	10.50	9.27	8.87	6.75
520	10.46	9.23	8.83	6.72
650	10.43	9.21	8.82	6.7
790	10.42	9.21	8.81	6.71
920	10.42	9.21	8.81	6.92
1050	10.42	9.21	8.81	6.86
1190	10.42	9.21	8.81	7.12
1290	10.42	9.21	8.81	7.14
1490	10.42	9.21	8.81	7.16
1590	10.42	9.21	8.81	7.24
1720	10.42	9.21	8.81	7.26
1850	10.42	9.21	8.81	7.27
1990	10.42	9.21	8.81	7.28

Effective feature extraction using incremental learning leads to better feature selection. It enhances classification efficiency across a range of satellite image classification applications and improve the speed of classification. As a result, it is appropriate for real-time applications.

4.4 Conclusions

To increase overall precision, accuracy, recall, and AUC, the proposed architecture combines DL (Deep Learning) with augmented dataset acquisition and incremental learning. Because of these features, the proposed model achieved precision of 85.60%, accuracy of 98.06%, AUC of 95.6% and 92.05% recall for various image types. For different satellite image data set, the suggested model is found to be 14.2% more precise than MSRPS, 1.5% more precise than CNN TSS. and 4.9% more precise than HCNN. Furthermore, the model is 3.4% faster than CNN TSS, 5.9% faster than MSRPS, and 4.1% faster than HCNN for various types of satellite images. In terms of multiple domain accuracy performance, the developed model outperformed CNN TSS by 12.5% and MSRPS by at least 15%. Across diverse image types, the implemented model had a low latency of 6.85 ms. As a result, this type is excellent for a variety of high-speed applications.

To find out the gap in the suggested model researchers can also verify the suggested version's overall performance on various datasets. The researchers can use Q-Learning and ensemble classification models to enhance accuracy and precision.

Chapter No 5

Conclusions

Chapter No 5

Conclusions

5.1 Conclusions

Early uses of SVM, RF, and ANN included the precise classification of plant diseases and the prediction of agricultural yields. These algorithms have to engage in complex procedures for the extraction of features and the selection of characteristics in order for them to be effective in the job that they do. The immediate effect of this was to make some architectural designs function exceptionally effectively, while other architectural designs were unable to reach the necessary degree of accuracy. In order for CNN-based systems to be regarded reliable, the accuracy criteria for yield prediction and illness detection must, however, be at least 90%. As a consequence of this, the ideas that are covered in this article are used significantly in the majority of real-time systems. By drawing on information from a wide variety of sources, these systems have the potential to provide illness and production forecasts that are very accurate. These input sources might be anything from picture data to environmental data to a nitrogen profile to meteorological data and more.

There are many more possible input sources as well. Additionally, they might be any mix of the aforementioned things. Models that are based on convolutional neural networks (CNN) are employed in order to enhance the categorization skills of both freshly constructed systems and those that are already in place. This is done by improving the accuracy of the CNN. The enhanced performance which was reported by this thesis is the outcome of using combination of max-pooling, ReLU, high-efficiency convolutional, and dropout layers. Because every one of these layers makes a contribution of some kind to the process of feature extraction, it is feasible to achieve

a higher level of performance overall. The execution of an ensemble of these layers is a component of the model that has been proposed. The objective of this component is to enhance the efficiency with which the method for feature extraction is carried out. In order to accomplish the goal of achieving an even higher level of performance in terms of the dense layer's accuracy, this ensemble architecture makes use of a number of distinct learning rate optimizers, such as SGD, RMSProp, and Adam. This architecture's overall goal is to achieve an even higher level of performance. This ensemble CNN classifier experiences significant increases in its accuracy, precision, recall, and fMeasure scores when it is combined with a transfer learning model for the purpose of hyper-parameter tuning. These types of advancements occur in a piecemeal fashion throughout time. It is plainly evident that this is the case thanks to the comparison with a large number of other high-efficiency models, which is supplied in Table 3.1, and the analysis of the parameters, which is provided in Tables 3.2, 3.3, 3.4, and 3.5, respectively. From the output we can see that the implemented architecture is batter then the most existing and cutting-edge deep learning models in terms of the parametric performance, and it has a great deal of potential for utilization in crop damage detection applications that depend on satellite photos. It is possible to make use of LSTM and GRU models in order to carry out more research about the model's near-field imaging performance (Gated Recurrent Unit). It is feasible that combining two independent models might increase the overall performance of the model even more. Researchers have the option of using Generative Adversarial Networks (GANs) to get a batter accuracy when determining the level of damage present in images that have already been labelled as damaged. This helps the researchers get a better understanding of the extent to which the images have been affected (GANs).

The technique that has been presented is made up of several different components, the most important of which are deep learning, enhanced dataset collecting, and incremental learning. These four factors, when considered collectively, have a beneficial effect not just on the area under the curve, but also on recall, accuracy, and precision (AUC). As a direct consequence of the existence of these qualities, the model that was provided was in a position to successfully deliver the following findings over a broad spectrum of various kinds of photographs: The area under the curve was 95.6%, the recall was 92.05%, the precision was 85.6%, and the accuracy was 98.06%.

In the proposed model, an incremental learning layer has been introduced so that it may make the most of the variance in the features and, as a consequence, continuously increase its accuracy. This was done in order for the model to be able to: These findings demonstrated that the suggested model was capable of obtaining a low latency across a wide range of picture types, which suited it to be used in the process of implementing a wide variety of high-speed applications since it was suitable for doing so.

- Attaining an accuracy level that was at least 15% greater than that attained by CNN TSS [138], HCNN [128], and MSRPS [136] over a broad range of application domains was one of the goals that the proposed technique set out to accomplish.
- Furthermore, the proposed architecture is 14.2% more precise and has a higher recall than MSRPS, 5% more accurate and has a higher recall than Heterogeneous Convolutional Neural Network, and 1.5% more precise and has a higher recall than Convolutional Neural Network TSS.
- All of these findings are documented in [4, 136, and 138]. These discoveries were derived from observations made using a variety of different satellite images.
- In addition, the proposed model outperforms HCNN [128], MSRPS [136], and CNN TSS [138] when applied to the analysis of a variety of satellite images by 4.1, 5.9, and 3.4 percentage points, respectively.

5.2 Future Scopes

- In the future, researchers could make the decision to utilize ensemble classification models and Q-Learning to additional improve precision and accuracy performance.
- Putting the suggested model through its paces on a variety of different data sets and looking for any possible problems that may be present is one way to verify that the work done by the researchers is accurate. This may be done by searching for any potential problems that may be there.
- Depending on the kind of application being used, these issues could be solved by using augmentation and deep learning classification models that are more suitable for the setting under different use cases.

Chapter No 6

Dissemination of Work

Chapter No 6

Dissemination of Work

6.1 Published

[1] Dhande, A., Malik, R. “Design of a highly efficient crop damage detection ensemble learning model using deep convolutional networks”. *Journal of Ambient Intelligence and Humanized Computing* (2022). https://doi.org/10.1007/s12652-022-04352-4. (SCI Index Journal)

[2] Dhande, A., Malik, R. “Empirical Study of Far-Field Crop Quality Examination Models: A Numerical Outlook”. In: Das, B., Patgiri, R., Bandyopadhyay, S., Balas, V.E. (eds) Modeling, Simulation and Optimization. *Smart Innovation, Systems and Technologies*, vol 292. Springer, Singapore (2022). https://doi.org/10.1007/978-981-19-0836-1_1 (Scopus Index Journal)

[3] Dhande, A., Malik, R. “Hyper Spectral Remote Sensing for Damage Detection and Classification Models in Agriculture - A Review” *Journal of Information Technology in Industry* (2021). https://doi.org/10.17762/itii.v9i1.142 (ESCI Index Journal)

[4] Dhande A. and Malik R., "Empirical Study of Crop-disease Detection and Cropyield Analysis Systems: A Statistical View," 2022 International Conference on Emerging Smart Computing and Informatics, 2022, pp. 1-4, https://doi.org/10.1109/ESCI53509.2022.9758284 (Scopus Index Journal)

[5] Dhande A. and Malik R., “Experimental investigation of crop-disease detection and crop-yield analysis systems: A numerical outlook”. International Conference on Materials for Emerging Technologies (ICMET-21) At Lovely Professional University, Punjab. (Scopus Index Journal)

6.2 Accepted for Publication

[1] Dhande A. and Malik R., “Design of a high-efficiency temporal engine for real-time satellite image classification using augmented incremental transfer learning for crop analysis” *Journal of Algebraic Statistics* (2022)

6.3 Patent

[1] Dhande A. and Malik R., "Computational Approaches for The Analysis of Crop Monitoring Using Satellite Image" in Official Journal of the Patent Office, December 2021.

The Patent Office Journal No. 16/2022 Dated 22/04/2022 *Page No. 24880*

Link:- http://tiny.cc/uxthvz

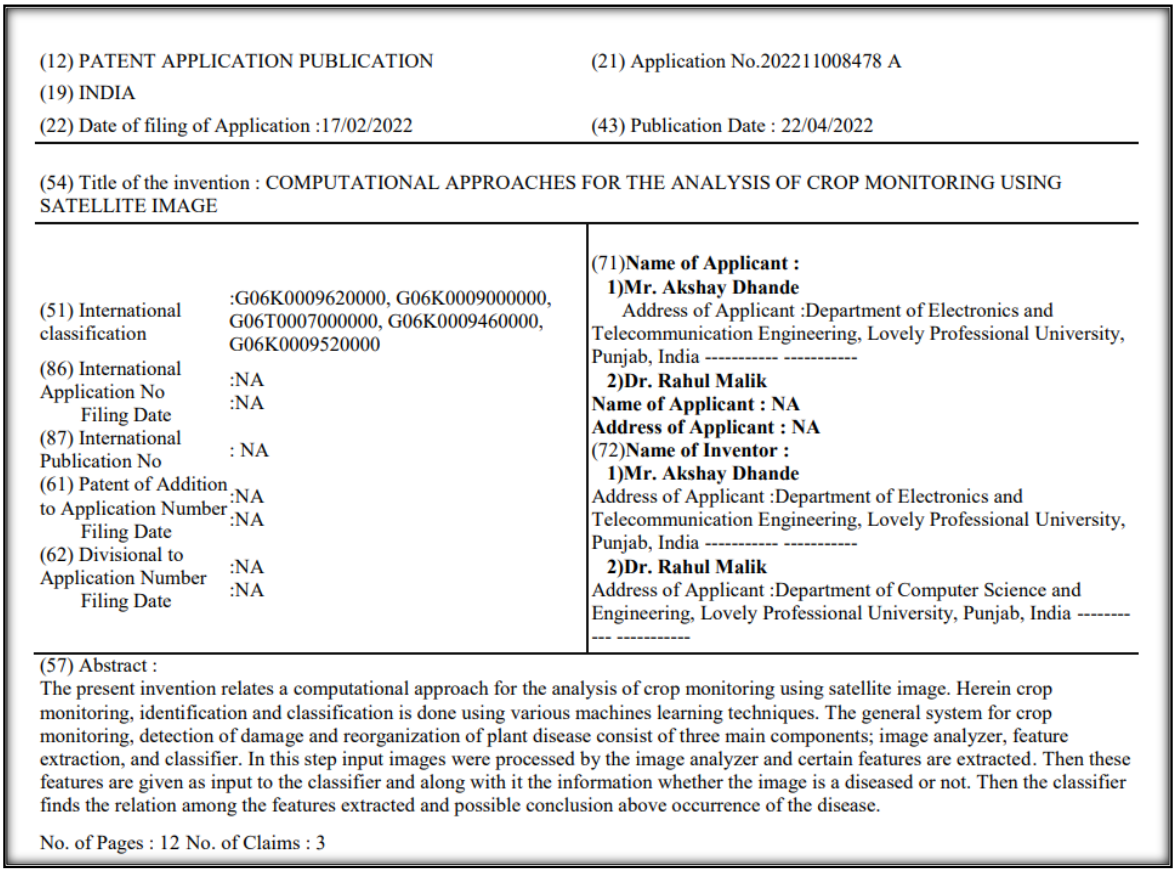

(12) PATENT APPLICATION PUBLICATION
(19) INDIA
(22) Date of filing of Application :17/02/2022

(21) Application No.202211008478 A
(43) Publication Date : 22/04/2022

(54) Title of the invention : COMPUTATIONAL APPROACHES FOR THE ANALYSIS OF CROP MONITORING USING SATELLITE IMAGE

(51) International classification :G06K0009620000, G06K0009000000, G06T0007000000, G06K0009460000, G06K0009520000
(86) International Application No :NA
Filing Date :NA
(87) International Publication No : NA
(61) Patent of Addition to Application Number :NA
Filing Date :NA
(62) Divisional to Application Number :NA
Filing Date :NA

(71)**Name of Applicant :**
1)Mr. Akshay Dhande
Address of Applicant :Department of Electronics and Telecommunication Engineering, Lovely Professional University, Punjab, India ---------- ----------
2)Dr. Rahul Malik
Name of Applicant : NA
Address of Applicant : NA
(72)**Name of Inventor :**
1)Mr. Akshay Dhande
Address of Applicant :Department of Electronics and Telecommunication Engineering, Lovely Professional University, Punjab, India ---------- ----------
2)Dr. Rahul Malik
Address of Applicant :Department of Computer Science and Engineering, Lovely Professional University, Punjab, India ---------- ----------

(57) Abstract :
The present invention relates a computational approach for the analysis of crop monitoring using satellite image. Herein crop monitoring, identification and classification is done using various machines learning techniques. The general system for crop monitoring, detection of damage and reorganization of plant disease consist of three main components; image analyzer, feature extraction, and classifier. In this step input images were processed by the image analyzer and certain features are extracted. Then these features are given as input to the classifier and along with it the information whether the image is a diseased or not. Then the classifier finds the relation among the features extracted and possible conclusion above occurrence of the disease.

No. of Pages : 12 No. of Claims : 3

6.4 Copyright

[1] Dhande A. and Malik R., "Computational Approaches for The Analysis of Crop Monitoring Using Satellite Image" in Copyright Office, New Delhi. 2022.

ROC No: L-119677/2022 Dated on 19/12/2022

Link:- http://tiny.cc/exthvz

[2] Dhande A. and Malik R., "Augmented Visual Toolkit Design for Crop Malignancy Analysis" in Copyright Office, New Delhi. 2022.

ROC No. L-126510/2023 Dated on 19/06/2023

Link:- http://tiny.cc/pxthvz

References

References

[1] W. Zhang et al., "An Improved Feature Set for Hyperspectral Image Classification: Harmonic Analysis Optimized by Multiscale Guided Filter," in IEEE Journal of Selected Topics in Applied Earth Observations and Remote Sensing, vol. 13, pp. 3903-3916, 2020, doi: 10.1109/JSTARS.2020.3006772.

[2] Y. Shen, J. Chen, L. Xiao and D. Pan, "A Bilevel Contextual MRF Model for Supervised Classification of High Spatial Resolution Remote Sensing Images," in IEEE Journal of Selected Topics in Applied Earth Observations and Remote Sensing, vol. 12, no. 12, pp. 5360-5372, Dec. 2019, doi: 10.1109/JSTARS.2019.2950946.

[3] C. -J. Zhang, X. -J. Wang, L. -M. Ma and X. -Q. Lu, "Tropical Cyclone Intensity Classification and Estimation Using Infrared Satellite Images With Deep Learning," in IEEE Journal of Selected Topics in Applied Earth Observations and Remote Sensing, vol. 14, pp. 2070-2086, 2021, doi: 10.1109/JSTARS.2021.3050767.

[4] X. Huang et al., "A Multispectral and Multiangle 3-D Convolutional Neural Network for the Classification of ZY-3 Satellite Images Over Urban Areas," in IEEE Transactions on Geoscience and Remote Sensing, vol. 59, no. 12, pp. 10266-10285, Dec. 2021, doi: 10.1109/TGRS.2020.3037211.

[5] Z. Miao et al., "Integration of Satellite Images and Open Data for Impervious Surface Classification," in IEEE Journal of Selected Topics in Applied Earth Observations and Remote Sensing, vol. 12, no. 4, pp. 1120-1133, April 2019, doi: 10.1109/JSTARS.2019.2903585.

[6] Y. Zheng, S. Liu, Q. Du, H. Zhao, X. Tong and M. Dalponte, "A Novel Multitemporal Deep Fusion Network (MDFN) for Short-Term Multitemporal HR Images Classification," in IEEE Journal of Selected Topics in Applied Earth Observations and Remote Sensing, vol. 14, pp. 10691-10704, 2021, doi: 10.1109/JSTARS.2021.3119942.

[7] Y. Zi, F. Xie, N. Zhang, Z. Jiang, W. Zhu and H. Zhang, "Thin Cloud Removal for Multispectral Remote Sensing Images Using Convolutional Neural Networks Combined With an Imaging Model," in IEEE Journal of Selected Topics in Applied Earth Observations and Remote Sensing, vol. 14, pp. 3811-3823, 2021, doi: 10.1109/JSTARS.2021.3068166.

[8] R. Ratajczak, C. F. Crispim-Junior, E. Faure, B. Fervers and L. Tougne, "Automatic Land Cover Reconstruction From Historical Aerial Images: An Evaluation of Features Extraction and Classification Algorithms," in IEEE Transactions on Image Processing, vol. 28, no. 7, pp. 3357-3371, July 2019, doi: 10.1109/TIP.2019.2896492.

[9] S. Illarionova, A. Trekin, V. Ignatiev and I. Oseledets, "Neural-Based Hierarchical Approach for Detailed Dominant Forest Species Classification by Multispectral Satellite Imagery," in IEEE Journal of Selected Topics in Applied Earth Observations and Remote Sensing, vol. 14, pp. 1810-1820, 2021, doi: 10.1109/JSTARS.2020.3048372.

[10] M. Barthakur, K. K. Sarma and N. Mastorakis, "Modified Semi-Supervised Adversarial Deep Network and Classifier Combination for Segmentation of Satellite Images," in IEEE Access, vol. 8, pp. 117972-117985, 2020, doi: 10.1109/ACCESS.2020.3005085.

[11] P. Helber, B. Bischke, A. Dengel and D. Borth, "EuroSAT: A Novel Dataset and Deep Learning Benchmark for Land Use and Land Cover Classification," in IEEE Journal of Selected Topics in Applied Earth Observations and Remote Sensing, vol. 12, no. 7, pp. 2217-2226, July 2019, doi: 10.1109/JSTARS.2019.2918242.

[12] Y. Yuan and L. Lin, "Self-Supervised Pretraining of Transformers for Satellite Image Time Series Classification," in IEEE Journal of Selected Topics in Applied Earth Observations and Remote Sensing, vol. 14, pp. 474-487, 2021, doi: 10.1109/JSTARS.2020.3036602.

[13] S. -J. Lee and K. -J. Lee, "Efficient Generation of Artificial Training DB for Ship Detection Using Satellite SAR Images," in IEEE Journal of Selected Topics in Applied Earth Observations and Remote Sensing, vol. 14, pp. 11764-11774, 2021, doi: 10.1109/JSTARS.2021.3128184.

[14] H. -W. Jo et al., "Deep Learning Applications on Multitemporal SAR (Sentinel-1) Image Classification Using Confined Labeled Data: The Case of Detecting Rice Paddy in South Korea," in IEEE Transactions on Geoscience and Remote Sensing, vol. 58, no. 11, pp. 7589-7601, Nov. 2020, doi: 10.1109/TGRS.2020.2981671.

[15] E. Kalinicheva, D. Ienco, J. Sublime and M. Trocan, "Unsupervised Change Detection Analysis in Satellite Image Time Series Using Deep Learning Combined

With Graph-Based Approaches," in IEEE Journal of Selected Topics in Applied Earth Observations and Remote Sensing, vol. 13, pp. 1450-1466, 2020, doi: 10.1109/JSTARS.2020.2982631.

[16] D. Ienco, Y. J. E. Gbodjo, R. Gaetano and R. Interdonato, "Weakly Supervised Learning for Land Cover Mapping of Satellite Image Time Series via Attention-Based CNN," in IEEE Access, vol. 8, pp. 179547-179560, 2020, doi: 10.1109/ACCESS.2020.3024133.

[17] M. Ghanbari, D. A. Clausi, L. Xu and M. Jiang, "Contextual Classification of Sea-Ice Types Using Compact Polarimetric SAR Data," in IEEE Transactions on Geoscience and Remote Sensing, vol. 57, no. 10, pp. 7476-7491, Oct. 2019, doi: 10.1109/TGRS.2019.2913796.

[18] C. Liu, W. Song, C. Lu and J. Xia, "Spatial-Temporal Hidden Markov Model for Land Cover Classification Using Multitemporal Satellite Images," in IEEE Access, vol. 9, pp. 76493-76502, 2021, doi: 10.1109/ACCESS.2021.3080926.

[19] R. Luciani, G. Laneve and M. JahJah, "Agricultural Monitoring, an Automatic Procedure for Crop Mapping and Yield Estimation: The Great Rift Valley of Kenya Case," in IEEE Journal of Selected Topics in Applied Earth Observations and Remote Sensing, vol. 12, no. 7, pp. 2196-2208, July 2019, doi: 10.1109/JSTARS.2019.2921437.

[20] Y. Zhou, T. Wei, X. Zhu and M. Collin, "A Parcel-Based Deep-Learning Classification to Map Local Climate Zones From Sentinel-2 Images," in IEEE Journal of Selected Topics in Applied Earth Observations and Remote Sensing, vol. 14, pp. 4194-4204, 2021, doi: 10.1109/JSTARS.2021.3071577.

[21] D. Cao, M. Zhang, W. Li and Q. Ran, "Hyperspectral and Infrared Image Collaborative Classification Based on Morphology Feature Extraction," in IEEE Journal of Selected Topics in Applied Earth Observations and Remote Sensing, vol. 14, pp. 4405-4416, 2021, doi: 10.1109/JSTARS.2021.3072843.

[22] Y. Wang, C. Wang, C. Shi and B. Xiao, "A Selection Criterion for the Optimal Resolution of Ground-Based Remote Sensing Cloud Images for Cloud Classification," in IEEE Transactions on Geoscience and Remote Sensing, vol. 57, no. 3, pp. 1358-1367, March 2019, doi: 10.1109/TGRS.2018.2866206.

[23] F. Oriani, M. F. McCabe and G. Mariethoz, "Downscaling Multispectral Satellite Images Without Colocated High-Resolution Data: A Stochastic Approach Based on Training Images," in IEEE Transactions on Geoscience and Remote Sensing, vol. 59, no. 4, pp. 3209-3225, April 2021, doi: 10.1109/TGRS.2020.3008015.

[24] R. Jing, Z. Gong and H. Guan, "Land Cover Change Detection With VHR Satellite Imagery Based on Multi-Scale SLIC-CNN and SCAE Features," in IEEE Access, vol. 8, pp. 228070-228087, 2020, doi: 10.1109/ACCESS.2020.3045740.

[25] R. Jing, Z. Gong and H. Guan, "Land Cover Change Detection With VHR Satellite Imagery Based on Multi-Scale SLIC-CNN and SCAE Features," in IEEE Access, vol. 8, pp. 228070-228087, 2020, doi: 10.1109/ACCESS.2020.3045740.

[26] L. Yao et al., "Design and Testing of an Active Light Source Apparatus for Crop Growth Monitoring and Diagnosis," in IEEE Access, vol. 8, pp. 206474-206490, 2020, doi: 10.1109/ACCESS.2020.3037966.

[27] Y. Alebele et al., "Estimation of Crop Yield From Combined Optical and SAR Imagery Using Gaussian Kernel Regression," in IEEE Journal of Selected Topics in Applied Earth Observations and Remote Sensing, vol. 14, pp. 10520-10534, 2021, doi: 10.1109/JSTARS.2021.3118707.

[28] J. Jiang et al., "HISTIF: A New Spatiotemporal Image Fusion Method for High-Resolution Monitoring of Crops at the Subfield Level," in IEEE Journal of Selected Topics in Applied Earth Observations and Remote Sensing, vol. 13, pp. 4607-4626, 2020, doi: 10.1109/JSTARS.2020.3016135.

[29] W. Wang et al., "AAVI: A Novel Approach to Estimating Leaf Nitrogen Concentration in Rice From Unmanned Aerial Vehicle Multispectral Imagery at Early and Middle Growth Stages," in IEEE Journal of Selected Topics in Applied Earth Observations and Remote Sensing, vol. 14, pp. 6716-6728, 2021, doi: 10.1109/JSTARS.2021.3086580.

[30] Y. Wang et al., "Monitoring Crop Growth During the Period of the Rapid Spread of COVID-19 in China by Remote Sensing," in IEEE Journal of Selected Topics in Applied Earth Observations and Remote Sensing, vol. 13, pp. 6195-6205, 2020, doi: 10.1109/JSTARS.2020.3029434.

[31] C. -H. Huang, B. -W. Chen, Y. -J. Lin and J. -X. Zheng, "Smart Crop Growth Monitoring Based on System Adaptivity and Edge AI," in IEEE Access, vol. 10, pp. 64114-64125, 2022, doi: 10.1109/ACCESS.2022.3183277.

[32] V. Grimblatt, C. Jégo, G. Ferré and F. Rivet, "How to Feed a Growing Population—An IoT Approach to Crop Health and Growth," in IEEE Journal on Emerging and Selected Topics in Circuits and Systems, vol. 11, no. 3, pp. 435-448, Sept. 2021, doi: 10.1109/JETCAS.2021.3099778.

[33] G. Fontanelli, F. Montomoli, R. Azar, G. Macelloni and P. Villa, "Assessing Interactions Between Crop Biophysical Parameters and X-Band Backscattering Using Empirical Data and Model Sensitivity Analysis," in IEEE Transactions on Geoscience and Remote Sensing, vol. 60, pp. 1-12, 2022, Art no. 4405612, doi: 10.1109/TGRS.2021.3119146.

[34] C. Silva-Perez, A. Marino, J. M. Lopez-Sanchez and I. Cameron, "Multitemporal Polarimetric SAR Change Detection for Crop Monitoring and Crop Type Classification," in IEEE Journal of Selected Topics in Applied Earth Observations and Remote Sensing, vol. 14, pp. 12361-12374, 2021, doi: 10.1109/JSTARS.2021.3130186.

[35] G. Nagasubramanian, R. K. Sakthivel, R. Patan, M. Sankayya, M. Daneshmand and A. H. Gandomi, "Ensemble Classification and IoT-Based Pattern Recognition for Crop Disease Monitoring System," in IEEE Internet of Things Journal, vol. 8, no. 16, pp. 12847-12854, 15 Aug.15, 2021, doi: 10.1109/JIOT.2021.3072908.

[36] Y. Du, J. Jiang, Z. Liu and Y. Pan, "Combining a Crop Growth Model With CNN for Underground Natural Gas Leakage Detection Using Hyperspectral Imagery," in IEEE Journal of Selected Topics in Applied Earth Observations and Remote Sensing, vol. 15, pp. 1846-1856, 2022, doi: 10.1109/JSTARS.2022.3150089.

[37] S. Yang et al., "Integration of Crop Growth Model and Random Forest for Winter Wheat Yield Estimation From UAV Hyperspectral Imagery," in IEEE Journal of Selected Topics in Applied Earth Observations and Remote Sensing, vol. 14, pp. 6253-6269, 2021, doi: 10.1109/JSTARS.2021.3089203.

[38] B. Zhao, M. Liu, J. Wu, X. Liu, M. Liu and L. Wu, "Parallel Computing for Obtaining Regional Scale Rice Growth Conditions Based on WOFOST and Satellite

Images," in IEEE Access, vol. 8, pp. 223675-223685, 2020, doi: 10.1109/ACCESS.2020.3043003.

[39] D. Mandal et al., "A Radar Vegetation Index for Crop Monitoring Using Compact Polarimetric SAR Data," in IEEE Transactions on Geoscience and Remote Sensing, vol. 58, no. 9, pp. 6321-6335, Sept. 2020, doi: 10.1109/TGRS.2020.2976661.

[40] Y. Yuan, Z. Xu and G. Lu, "SPEDCCNN: Spatial Pyramid-Oriented Encoder-Decoder Cascade Convolution Neural Network for Crop Disease Leaf Segmentation," in IEEE Access, vol. 9, pp. 14849-14866, 2021, doi: 10.1109/ACCESS.2021.3052769.

[41] S. P. Raja, B. Sawicka, Z. Stamenkovic and G. Mariammal, "Crop Prediction Based on Characteristics of the Agricultural Environment Using Various Feature Selection Techniques and Classifiers," in IEEE Access, vol. 10, pp. 23625-23641, 2022, doi: 10.1109/ACCESS.2022.3154350.

[42] J. F. Elfferich, D. Dodou and C. D. Santina, "Soft Robotic Grippers for Crop Handling or Harvesting: A Review," in IEEE Access, vol. 10, pp. 75428-75443, 2022, doi: 10.1109/ACCESS.2022.3190863.

[43] Z. Li, J. Liu, Y. Xiang, X. Zhang and Y. Chai, "Agricultural load modeling based on crop evapotranspiration and light integration for economic operation of greenhouse power systems," in CSEE Journal of Power and Energy Systems, vol. 7, no. 5, pp. 1113-1121, Sept. 2021, doi: 10.17775/CSEEJPES.2019.00750.

[44] S. Wu, J. Ren, Z. Chen, P. Yang, H. Li and J. Liu, "Evaluation of Winter Wheat Yield Simulation Based on Assimilating LAI Retrieved From Networked Optical and SAR Remotely Sensed Images Into the WOFOST Model," in IEEE Transactions on Geoscience and Remote Sensing, vol. 59, no. 11, pp. 9071-9085, Nov. 2021, doi: 10.1109/TGRS.2020.3038205.

[45] M. H. Asad and A. Bais, "Crop and Weed Leaf Area Index Mapping Using Multi-Source Remote and Proximal Sensing," in IEEE Access, vol. 8, pp. 138179-138190, 2020, doi: 10.1109/ACCESS.2020.3012125.

[46] G. Zhao, W. Cai, Z. Wang, H. Wu, Y. Peng and L. Cheng, "Phenotypic Parameters Estimation of Plants Using Deep Learning-Based 3-D Reconstruction From Single RGB Image," in IEEE Geoscience and Remote Sensing Letters, vol. 19, pp. 1-5, 2022, Art no. 2506705, doi: 10.1109/LGRS.2022.3198850.

[47] M. Qiao et al., "Exploiting Hierarchical Features for Crop Yield Prediction Based on 3-D Convolutional Neural Networks and Multikernel Gaussian Process," in IEEE Journal of Selected Topics in Applied Earth Observations and Remote Sensing, vol. 14, pp. 4476-4489, 2021, doi: 10.1109/JSTARS.2021.3073149.

[48] M. M. G. de Macedo, A. B. Mattos and D. A. B. Oliveira, "Generalization of Convolutional LSTM Models for Crop Area Estimation," in IEEE Journal of Selected Topics in Applied Earth Observations and Remote Sensing, vol. 13, pp. 1134-1142, 2020, doi: 10.1109/JSTARS.2020.2973602.

[49] F. Ji, J. Meng, Z. Cheng, H. Fang and Y. Wang, "Crop Yield Estimation at Field Scales by Assimilating Time Series of Sentinel-2 Data Into a Modified CASA-WOFOST Coupled Model," in IEEE Transactions on Geoscience and Remote Sensing, vol. 60, pp. 1-14, 2022, Art no. 4400914, doi: 10.1109/TGRS.2020.3047102.

[50] J. Yu et al., "A Deep Learning Approach for Multi-Depth Soil Water Content Prediction in Summer Maize Growth Period," in IEEE Access, vol. 8, pp. 199097-199110, 2020, doi: 10.1109/ACCESS.2020.3034984.

[51] T. Kim, S. -H. Lee and J. -O. Kim, "A Novel Shape Based Plant Growth Prediction Algorithm Using Deep Learning and Spatial Transformation," in IEEE Access, vol. 10, pp. 37731-37742, 2022, doi: 10.1109/ACCESS.2022.3165211.

[52] R. Priya, D. Ramesh and V. Udutalapally, "NSGA-2 Optimized Fuzzy Inference System for Crop Plantation Correctness Index Identification," in IEEE Transactions on Sustainable Computing, vol. 7, no. 1, pp. 172-188, 1 Jan.-March 2022, doi: 10.1109/TSUSC.2021.3064417.

[53] S. K. Roy, S. Misra, N. S. Raghuwanshi and S. K. Das, "AgriSens: IoT-Based Dynamic Irrigation Scheduling System for Water Management of Irrigated Crops," in IEEE Internet of Things Journal, vol. 8, no. 6, pp. 5023-5030, 15 March15, 2021, doi: 10.1109/JIOT.2020.3036126.

[54] W. Khan et al., "On the Performance of Temporal Stacking and Vegetation Indices for Detection and Estimation of Tobacco Crop," in IEEE Access, vol. 8, pp. 103020-103033, 2020, doi: 10.1109/ACCESS.2020.2998079.

[55] Hu, Y., Zhang, J., Ma, Y. et al. Profound learning characterization of waterfront wetland hyperspectral image consolidated spectra and surface highlights: A contextual

investigation of Huanghe (Yellow) River Estuary wetland. Acta Oceanol. Sin. 38, 142–150 (2019).

[56] Guo, Y., Yin, X., Zhao, X. et al. Hyperspectral image characterization with SVM and guided channel. J Wireless Com Network 2019, 56 (2019). https://doi.org/10.1186/s13638-019-1346-z

[57] Gao, H., Yang, Y., Li, C. et al. Convolutional neural system for ghastly spatial grouping of hyperspectral images. Neural Comput and Applic 31, 8997–9012 (2019). https://doi.org/10.1007/s00521-019-04371-x

[58] S. Li, W. Tune, L. Tooth, Y. Chen, P. Ghamisi and J. A. Benediktsson, "Profound Learning for Hyperspectral Image Classification: An Overview," in IEEE Transactions on Geoscience and Remote Sensing, vol. 57, no. 9, pp. 6690-6709, Sept. 2019.

[59] R. Hang, Q. Liu, D. Hong and P. Ghamisi, "Fell Recurrent Neural Networks for Hyperspectral Image Classification," in IEEE Transactions on Geoscience and Remote Sensing, vol. 57, no. 8, pp. 5384-5394, Aug. 2019.

[60] Melgani, Farid and Bruzzone, Lorenzo. (2004). Characterization of Hyperspectral Remote Sensing Images with Support Vector Machines. Geoscience and Remote Sensing, IEEE Transactions on. 42. 1778 - 1790. 10.1109/TGRS.2004.831865.

[61] J. Xia et al., "Hyperspectral Identification and Classification of Oilseed Waterlogging Stress Levels Using Parallel Computing," in IEEE Access, vol. 6, pp. 57663-57675, 2018.

[62] B. Liu, X. Yu, P. Zhang, A. Yu, Q. Fu and X. Wei, "Regulated Deep Feature Extraction for Hyperspectral Image Classification," in IEEE Transactions on Geoscience and Remote Sensing, vol. 56, no. 4, pp. 1909-1921, April 2018.

[63] G. Cheng, Z. Li, J. Han, X. Yao and L. Guo, "Investigating Hierarchical Convolutional Features for Hyperspectral Image Classification," in IEEE Transactions on Geoscience and Remote Sensing, vol. 56, no. 11, pp. 6712-6722, Nov. 2018.

[64] Hayder Hasan and Helmi Z.M. Shafri and Mohammed Habshi; A Comparison Between Support Vector Machine ({SVM}) and Convolutional Neural Network ({CNN}) Models For Hyperspectral Image Classification; {IOP} Conference Series: Earth and Environmental Science

[65] Wang, Yi and Duan, Hexiang; Classification of Hyperspectral Images by SVM Using a Composite Kernel by Employing Spectral, Spatial and Hierarchical Structure Information; Remote Sensing

[66] K. S. Ettabaa, M. A. Hamdi and R. Ben Salem, "SVM for hyperspectral images characterization dependent on 3D otherworldly signature," 2014 first International Conference on Advanced Technologies for Signal and Image Processing (ATSIP), Sousse, 2014, pp. 42-47.

[67] P. Hsieh, C. Li and B. Kuo, "A nonlinear component choice technique dependent on part distinctness measure for hyperspectral image grouping," 2015 IEEE International Geoscience and Remote Sensing Symposium (IGARSS), Milan, 2015, pp. 461-464.

[68] X. Yang, Y. Ye, X. Li, R. Y. K. Lau, X. Zhang and X. Huang, "Hyperspectral Image Classification With Deep Learning Models," in IEEE Transactions on Geoscience and Remote Sensing, vol. 56, no. 9, pp. 5408-5423, Sept. 2018.

[69] M. Zhang, W. Li and Q. Du, "Assorted Region-Based CNN for Hyperspectral Image Classification," in IEEE Transactions on Image Processing, vol. 27, no. 6, pp. 2623-2634, June 2018.

[70] Z. Tian, J. Ji, S. Mei, J. Hou, S. Wan and Q. Du, "Hyperspectral Classification Via Spatial Context Exploration with Multi-Scale CNN," IGARSS 2018 - 2018 IEEE International Geoscience and Remote Sensing Symposium, Valencia, 2018, pp. 2563-2566.

[71] Y. Chen, Y. Wang, Y. Gu, X. He, P. Ghamisi and X. Jia, "Profound Learning Ensemble for Hyperspectral Image Classification," in IEEE Journal of Selected Topics in Applied Earth Observations and Remote Sensing, vol. 12, no. 6, pp. 1882-1897, June 2019.

[72] S. Kalita and M. Biswas, "Hyperspectral Image Classification Using Modified Convolutional Neural Network," 2018 Second International Conference on Intelligent Computing and Control Systems (ICICCS), Madurai, India, 2018, pp. 1884-1889.

[73] L. Mou and X. X. Zhu, "Figuring out how to Pay Attention on Spectral Domain: A Spectral Attention Module-Based Convolutional Network for Hyperspectral Image

Classification," in IEEE Transactions on Geoscience and Remote Sensing, vol. 58, no. 1, pp. 110-122, Jan. 2020.

[74] S. Wang, A. Dou, X. Yuan and X. Zhang, "The airborne hyperspectral image grouping dependent on the irregular timberland calculation," 2016 IEEE International Geoscience and Remote Sensing Symposium (IGARSS), Beijing, 2016, pp. 2280-2283.

[75] V. Jain and A. Phophalia, "Exponential Weighted Random Forest for Hyperspectral Image Classification," IGARSS 2019 - 2019 IEEE International Geoscience and Remote Sensing Symposium, Yokohama, Japan, 2019, pp. 3297-3300.

[76] W. Feng et al., "Gathering Margin Based Semi-Supervised Random Forest for the Classification of Hyperspectral Image with Limited Training Data," IGARSS 2019 - 2019 IEEE International Geoscience and Remote Sensing Symposium, Yokohama, Japan, 2019, pp. 971-974.

[77] J. Xia, N. Falco, J. A. Benediktsson, P. Du and J. Chanussot, "Hyperspectral Image Classification With Rotation Random Forest Via KPCA," in IEEE Journal of Selected Topics in Applied Earth Observations and Remote Sensing, vol. 10, no. 4, pp. 1601-1609, April 2017.

[78] Y. Zhang, G. Cao, X. Li and B. Wang, "Fell Random Forest for Hyperspectral Image Classification," in IEEE Journal of Selected Topics in Applied Earth Observations and Remote Sensing, vol. 11, no. 4, pp. 1082-1094, April 2018.

[79] J. Ham, Yangchi Chen, M. M. Crawford and J. Ghosh, "Examination of the arbitrary backwoods system for characterization of hyperspectral information," in IEEE Transactions on Geoscience and Remote Sensing, vol. 43, no. 3, pp. 492-501, March 2005.

[80] J. Aravinth, A. Bharadwaj, K. Harikrishna and N. Vignajeeth, "Order of Urban Objects from HSR-HTIR information utilizing CNN and Random backwoods Classifier," 2018 third International Conference on Communication and Electronics Systems (ICCES), Coimbatore, India, 2018, pp. 388-391.

[81] Mengmeng Sun,1 Chunyang Wang ,1,2 Shuangting Wang,1,2 Zongze Zhao,1,2 and Xiao Li1, A New Semisupervised-Entropy Framework of Hyperspectral Image

Classification Based on Random Forest, Recent Machine Learning Progress in Image Analysis and Understanding

[82] J. Xia, N. Falco, J. A. Benediktsson, P. Du and J. Chanussot, "Hyperspectral Image Classification With Rotation Random Forest Via KPCA," in IEEE Journal of Selected Topics in Applied Earth Observations and Remote Sensing, vol. 10, no. 4, pp. 1601-1609, April 2017.

[83] A. Hernández, H. Fabelo, S. Ortega, A. Báez, G. M. Callicó and R. Sarmiento, "Arbitrary backwoods preparing stage speeding up utilizing illustrations handling units," 2017 32nd Conference on Design of Circuits and Integrated Systems (DCIS), Barcelona, 2017, pp. 1-6.

[84] S. Amini, S. Homayouni and A. Safari, "Semi-managed characterization of hyperspectral image utilizing irregular backwoods calculation," 2014 IEEE Geoscience and Remote Sensing Symposium, Quebec City, QC, 2014, pp. 2866-2869.

[85] J. Xia, N. Yokoya and A. Iwasaki, "Hyperspectral Image Classification With Canonical Correlation Forests," in IEEE Transactions on Geoscience and Remote Sensing, vol. 55, no. 1, pp. 421-431, Jan. 2017.

[86] Chunhui Zhao, Xiaoqing Wan, Genping Zhao, Bing Cui, Wu Liu and Bin Qi (2017) Spectral-Spatial Classification of Hyperspectral Imagery Based on Stacked Sparse Autoencoder and Random Forest, European Journal of Remote Sensing, 50:1, 47-63,

[87] Saeid Amini, Saeid Homayouni, Abdolreza Safari and Ali A. Darvishsefat (2018) Object-based characterization of hyperspectral information utilizing Random Forest calculation, Geo-spatial Information Science, 21:2, 127-138,

[88] J. Aravinth, A. Bharadwaj, K. Harikrishna and N. Vignajeeth, "Order of Urban Objects from HSR-HTIR information utilizing CNN and Random backwoods Classifier," 2018 third International Conference on Communication and Electronics Systems (ICCES), Coimbatore, India, 2018, pp. 388-391.

[89] B. Xu, Y. Ye and L. Nie, "An improved arbitrary backwoods classifier for image characterization," 2012 IEEE International Conference on Information and Automation, Shenyang, 2012, pp. 795-800.

[90] Aili Wang, Ying Wang and Yushi Chen (2019) Hyperspectral image order dependent on convolutional neural system and irregular backwoods, Remote Sensing Letters, 10:11, 1086-1094,

[91] Y. Zhang, D. Wang and Q. Zhou, "Advances in crop fine arrangement dependent on Hyperspectral Remote Sensing," 2019 eighth International Conference on Agro-Geoinformatics (Agro-Geoinformatics), Istanbul, Turkey, 2019, pp. 1-6.

[92] L. Mou, P. Ghamisi and X. X. Zhu, "Profound Recurrent Neural Networks for Hyperspectral Image Classification," in IEEE Transactions on Geoscience and Remote Sensing, vol. 55, no. 7, pp. 3639-3655, July 2017.

[93] Dennis C. Duro, Steven E. Franklin and Monique G. Dubé (2012) Multi-scale object-based image examination and highlight choice of multi-sensor earth perception imagery utilizing arbitrary timberlands, International Journal of Remote Sensing, 33:14, 4502-4526

[94] Wu, H., Wiesner-Hanks, T., Stewart, E.L., DeChant, C., Kaczmar, N., Gore, M.A., Nelson, R.J. and Lipson, H. (2019), Autonomous Detection of Plant Disease Symptoms Directly from Aerial Imagery. Plant Phenome J., 2: 1-9 190006. https://doi.org/10.2135/tppj2019.03.0006

[95] Patel, Deven & Bhatt, Nirav. (2021). Improved accuracy of pest detection using augmentation approach with Faster R-CNN. IOP Conference Series: Materials Science and Engineering. 1042. 012020. 10.1088/1757-899X/1042/1/012020.

[96] Sharma, Parul & Berwal, Yash & Ghai, Wiqas. (2019). Performance Analysis of Deep Learning CNN Models for Disease Detection in Plants using Image Segmentation. Information Processing in Agriculture. 7. 10.1016/j.inpa.2019.11.001.

[97] S. Mardanisamani et al., "Crop Lodging Prediction From UAV-Acquired Images of Wheat and Canola Using a DCNN Augmented With Handcrafted Texture Features," 2019 IEEE/CVF Conference on Computer Vision and Pattern Recognition Workshops (CVPRW), 2019, pp. 2657-2664, doi: 10.1109/CVPRW.2019.00322.

[98] Montras Janer, Teresa & Knape, Jonas & Nilsson, Lovisa & Tombre, Ingunn & Pärt, Tomas & Månsson, Johan. (2019). Relating national levels of crop damage to the abundance of large grazing birds: Implications for management. Journal of Applied Ecology. 56. 10.1111/1365-2664.13457.

[99] Schlötelburg, A., Plekat, A., Bellingrath-Kimura, S. and Jacob, J. (2020), Self-service traps inspected by avian and terrestrial predators as a management option for rodents. Pest. Manag. Sci., 76: 103-110. https://doi.org/10.1002/ps.5550

[100] Kasinathan, Thenmozhi & Singaraju, Dakshayani & Reddy, U. Srinivasulu. (2020). Insect classification and detection in field crops using modern machine learning techniques. Information Processing in Agriculture. 10.1016/j.inpa.2020.09.006.

[101] Li, Weilu & Chen (陈鹏), Peng & Wang, Bing & Xie, Chengjun. (2019). Automatic Localization and Count of Agricultural Crop Pests Based on an Improved Deep Learning Pipeline. Scientific Reports. 9. 10.1038/s41598-019-43171-0.
Cuaran, Jose & Leon, Jose. (2021). Crop Monitoring using Unmanned Aerial Vehicles: A Review. Agricultural Reviews. 10.18805/ag.R-180.

[102] Yang, Haoxu & Gao, Lutao & tang, niansheng & Yang, Po. (2019). Experimental Analysis and Evaluation of Wide Residual Networks based Agricultural Disease Identification in Smart Agriculture System. EURASIP Journal on Wireless Communications and Networking. 2019. 10.1186/s13638-019-1613-z.

[103] SM, GOMEZ & Vergara, Alejandro & Ruiz, Henry & Safari, Nancy & Elayabalan, Sivalingam & Ocimati, Walter & Blomme, Guy. (2019). AI-powered banana diseases and pest detection. Plant Methods. 15. 10.1186/s13007-019-0475-z.

[104] Shang, Yifen & Hasn, Md.Kamrul & Ahammed, Golam Jalal & Li, Mengqi & Yin, Hanqin & Zhou, Jie. (2019). Applications of Nanotechnology in Plant Growth and Crop Protection: A Review. Molecules. 24. 2558. 10.3390/molecules24142558.

[105] Ceballos, Francisco & Kramer, Berber & Robles, Miguel. (2017). The Feasibility of Image-Based Insurance (PBI): Smartphone Images for Affordable Crop Insurance.

[106] Bebber, DP, Field, E, Gui, H, Mortimer, P, Holmes, T, Gurr, SJ. Many unreported crop pests and pathogens are probably already present. Glob Change Biol. 2019; 25: 2703– 2713. https://doi.org/10.1111/gcb.14698

[107] Larijani, MR, Asli-Ardeh, EA, Kozegar, E, Loni, R. Evaluation of image processing technique in identifying rice blast disease in field conditions based on KNN algorithm improvement by K-means. Food Sci Nutr. 2019; 7: 3922– 3930. https://doi.org/10.1002/fsn3.1251

[108] Rustia, DJA, Chao, J-J, Chiu, L-Y, et al. Automatic greenhouse insect pest detection and recognition based on a cascaded deep learning classification method. J Appl Entomol 2021; 145: 206– 222. https://doi.org/10.1111/jen.12834

[109] D. Lakmal, K. Kugathasan, V. Nanayakkara, S. Jayasena, A. S. Perera and L. Fernando, "Brown Planthopper Damage Detection using Remote Sensing and Machine Learning," 2019 18th IEEE International Conference On Machine Learning And Applications (ICMLA), 2019, pp. 97-104, doi: 10.1109/ICMLA.2019.00024.

[110] O. Kulkarni, "Crop Disease Detection Using Deep Learning," 2018 Fourth International Conference on Computing Communication Control and Automation (ICCUBEA), 2018, pp. 1-4, doi: 10.1109/ICCUBEA.2018.8697390.

[111] Q. Dai, X. Cheng, Y. Qiao and Y. Zhang, "Crop Leaf Disease Image Super-Resolution and Identification With Dual Attention and Topology Fusion Generative Adversarial Network," in IEEE Access, vol. 8, pp. 55724-55735, 2020, doi: 10.1109/ACCESS.2020.2982055.

[112] L. S. Puspha Annabel, T. Annapoorani and P. Deepalakshmi, "Machine Learning for Plant Leaf Disease Detection and Classification – A Review," 2019 International Conference on Communication and Signal Processing (ICCSP), 2019, pp. 0538-0542, doi: 10.1109/ICCSP.2019.8698004.

[113] Y. Dong et al., "Monitoring and forecasting for disease and pest in crop based on WebGIS system," 2019 8th International Conference on Agro-Geoinformatics (Agro-Geoinformatics), 2019, pp. 1-5, doi: 10.1109/Agro-Geoinformatics.2019.8820620.

[114] R. Hari Shankar, A. K. Veeraraghavan, Uvais, K. Sivaraman and S. S. Ramachandran, "Application of UAV for Pest, Weeds and Disease Detection using Open Computer Vision," 2018 International Conference on Smart Systems and Inventive Technology (ICSSIT), 2018, pp. 287-292, doi: 10.1109/ICSSIT.2018.8748404.

[115] R. Kamesaka and Y. Hoshino, "Development of a Prevention System for Beast Damage of Agricultural Products Using Deep Learning," 2018 Joint 10th International Conference on Soft Computing and Intelligent Systems (SCIS) and 19th International Symposium on Advanced Intelligent Systems (ISIS), 2018, pp. 747-752, doi: 10.1109/SCIS-ISIS.2018.00124.

[116] Rahman, M.S., Di, L., Yu, E. et al. Remote Sensing Based Rapid Assessment of Flood Crop Damage Using Novel Disaster Vegetation Damage Index (DVDI). Int J Disaster Risk Sci 12, 90–110 (2021). https://doi.org/10.1007/s13753-020-00305-7

[117] Jadhav, S.B., Udupi, V.R. & Patil, S.B. Identification of plant diseases using convolutional neural networks. Int. j. inf. tecnol. (2020). https://doi.org/10.1007/s41870-020-00437-5

[118] Cappa, F., Bani, L. & Meriggi, A. Factors affecting the crop damage by wild boar (Sus scrofa) and effects of population control in the Ticino and Lake Maggiore Park (North-western Italy). Mamm Biol (2021). https://doi.org/10.1007/s42991-021-00125-2

[119] Nuttall, JG, Perry, EM, Delahunty, AJ, O'Leary, GJ, Barlow, KM, Wallace, AJ. Frost response in wheat and early detection using proximal sensors. J Agro Crop Sci. 2019; 205: 220– 234. https://doi.org/10.1111/jac.12319

[120] Mohammadi, M., Darabi, H., Mirchooli, F. et al. Flood risk mapping and crop-water loss modeling using water footprint analysis in agricultural watershed, northern Iran. Nat Hazards 105, 2007–2025 (2021). https://doi.org/10.1007/s11069-020-04387-w

[121] Honda, Takeshi. (2020). Geographical personality gradient in herbivorous animals: Implications for selective culling to reduce crop damage. Ecological Research. 36. 10.1111/1440-1703.12186.

[122] Egerer, Monika & Liere, Heidi & Lucatero, Azucena & Philpott, Stacy. (2020). Plant damage in urban agroecosystems varies with local and landscape factors. Ecosphere. 11. e03074. 10.1002/ecs2.3074.

[123] Champ, Julien & Mora-Fallas, Adan & Goëau, Hervé & Mata-Montero, Erick & Bonnet, Pierre & Joly, Alexis. (2020). Instance segmentation for the fine detection of crop and weed plants by precision agricultural robots. Applications in Plant Sciences. 8. 10.1002/aps3.11373.

[124] Lee, Sheng-Hung & Lin, Shiou-Ruei & Chen, Shih-Fang. (2020). Identification of Tea Foliar Diseases and Pest Damages under Practical Field Conditions Using Convolutional Neural Network. Plant Pathology. 69. 10.1111/ppa.13251.

[125] R. Luciani, G. Laneve and M. JahJah, "Agricultural Monitoring, an Automatic Procedure for Crop Mapping and Yield Estimation: The Great Rift Valley of Kenya Case," in IEEE Journal of Selected Topics in Applied Earth Observations and Remote Sensing, vol. 12, no. 7, pp. 2196-2208, July 2019, doi: 10.1109/JSTARS.2019.2921437.

[126] A. Shelestov et al., "Cloud Approach to Automated Crop Classification Using Sentinel-1 Imagery," in IEEE Transactions on Big Data, vol. 6, no. 3, pp. 572-582, 1 Sept. 2020, doi: 10.1109/TBDATA.2019.2940237.

[127] J. Jiang et al., "HISTIF: A New Spatiotemporal Image Fusion Method for High-Resolution Monitoring of Crops at the Subfield Level," in IEEE Journal of Selected Topics in Applied Earth Observations and Remote Sensing, vol. 13, pp. 4607-4626, 2020, doi: 10.1109/JSTARS.2020.3016135.

[128] Z. Li, G. Chen and T. Zhang, "A CNN-Transformer Hybrid Approach for Crop Classification Using Multitemporal Multisensor Images," in IEEE Journal of Selected Topics in Applied Earth Observations and Remote Sensing, vol. 13, pp. 847-858, 2020, doi: 10.1109/JSTARS.2020.2971763.

[129] M. Rousi et al., "Semantically Enriched Crop Type Classification and Linked Earth Observation Data to Support the Common Agricultural Policy Monitoring," in IEEE Journal of Selected Topics in Applied Earth Observations and Remote Sensing, vol. 14, pp. 529-552, 2021, doi: 10.1109/JSTARS.2020.3038152.

[130] Z. Sun, L. Di, H. Fang and A. Burgess, "Deep Learning Classification for Crop Types in North Dakota," in IEEE Journal of Selected Topics in Applied Earth Observations and Remote Sensing, vol. 13, pp. 2200-2213, 2020, doi: 10.1109/JSTARS.2020.2990104.

[131] J. Quiros Vargas, L. R. Khot, R. T. Peters, A. K. Chandel and B. Molaei, "Low Orbiting Satellite and Small UAS-Based High-Resolution Imagery Data to Quantify Crop Lodging: A Case Study in Irrigated Spearmint," in IEEE Geoscience and Remote Sensing Letters, vol. 17, no. 5, pp. 755-759, May 2020, doi: 10.1109/LGRS.2019.2935830.

[132] A. Mestre-Quereda, J. M. Lopez-Sanchez, F. Vicente-Guijalba, A. W. Jacob and M. E. Engdahl, "Time-Series of Sentinel-1 Interferometric Coherence and Backscatter

for Crop-Type Mapping," in IEEE Journal of Selected Topics in Applied Earth Observations and Remote Sensing, vol. 13, pp. 4070-4084, 2020, doi: 10.1109/JSTARS.2020.3008096.

[133] W. Khan et al., "On the Performance of Temporal Stacking and Vegetation Indices for Detection and Estimation of Tobacco Crop," in IEEE Access, vol. 8, pp. 103020-103033, 2020, doi: 10.1109/ACCESS.2020.2998079.

[134] P. W. Khan, Y. -C. Byun and M. A. Latif, "Clifford Geometric Algebra-Based Approach for 3D Modeling of Agricultural Images Acquired by UAVs," in IEEE Access, vol. 8, pp. 226297-226308, 2020, doi: 10.1109/ACCESS.2020.3045443.

[135] P. Tang, P. Du, J. Xia, P. Zhang and W. Zhang, "Channel Attention-Based Temporal Convolutional Network for Satellite Image Time Series Classification," in IEEE Geoscience and Remote Sensing Letters, vol. 19, pp. 1-5, 2022, Art no. 8016505, doi: 10.1109/LGRS.2021.3095505.

[136] M. H. Asad and A. Bais, "Crop and Weed Leaf Area Index Mapping Using Multi-Source Remote and Proximal Sensing," in IEEE Access, vol. 8, pp. 138179-138190, 2020, doi: 10.1109/ACCESS.2020.3012125.

[137] Y. T. Solano-Correa, F. Bovolo, L. Bruzzone and D. Fernández-Prieto, "A Method for the Analysis of Small Crop Fields in Sentinel-2 Dense Time Series," in IEEE Transactions on Geoscience and Remote Sensing, vol. 58, no. 3, pp. 2150-2164, March 2020, doi: 10.1109/TGRS.2019.2953652.

[138] S. Liu, Z. Zhou, H. Ding, Y. Zhong and Q. Shi, "Crop Mapping Using Sentinel Full-Year Dual-Polarized SAR Data and a CPU-Optimized Convolutional Neural Network With Two Sampling Strategies," in IEEE Journal of Selected Topics in Applied Earth Observations and Remote Sensing, vol. 14, pp. 7017-7031, 2021, doi: 10.1109/JSTARS.2021.3094973.

[139] M. M. G. de Macedo, A. B. Mattos and D. A. B. Oliveira, "Generalization of Convolutional LSTM Models for Crop Area Estimation," in IEEE Journal of Selected Topics in Applied Earth Observations and Remote Sensing, vol. 13, pp. 1134-1142, 2020, doi: 10.1109/JSTARS.2020.2973602.

[140] C. Silva-Perez, A. Marino, J. M. Lopez-Sanchez and I. Cameron, "Multitemporal Polarimetric SAR Change Detection for Crop Monitoring and Crop Type

Classification," in IEEE Journal of Selected Topics in Applied Earth Observations and Remote Sensing, vol. 14, pp. 12361-12374, 2021, doi: 10.1109/JSTARS.2021.3130186.

[141] S. Yang, L. Gu, X. Li, F. Gao and T. Jiang, "Fully Automated Classification Method for Crops Based on Spatiotemporal Deep-Learning Fusion Technology," in IEEE Transactions on Geoscience and Remote Sensing, vol. 60, pp. 1-16, 2022, Art no. 5405016, doi: 10.1109/TGRS.2021.3113014.

[142] H. -W. Jo et al., "Deep Learning Applications on Multitemporal SAR (Sentinel-1) Image Classification Using Confined Labeled Data: The Case of Detecting Rice Paddy in South Korea," in IEEE Transactions on Geoscience and Remote Sensing, vol. 58, no. 11, pp. 7589-7601, Nov. 2020, doi: 10.1109/TGRS.2020.2981671.

[143] T. Lampert, B. Lafabregue, T. -B. -H. Dao, N. Serrette, C. Vrain and P. Gançarski, "Constrained Distance-Based Clustering for Satellite Image Time-Series," in IEEE Journal of Selected Topics in Applied Earth Observations and Remote Sensing, vol. 12, no. 11, pp. 4606-4621, Nov. 2019, doi: 10.1109/JSTARS.2019.2950406.

[144] J. Bell, E. Gebremichael, A. Molthan, L. Schultz, F. Meyer and S. Shrestha, "Synthetic Aperture Radar and Optical Remote Sensing of Crop Damage Attributed to Severe Weather in the Central United States," IGARSS 2019 - 2019 IEEE International Geoscience and Remote Sensing Symposium, 2019, pp. 9938-9941, doi: 10.1109/IGARSS.2019.8899775.

[145] S. Sawant, J. Mohite, M. Sakkan and S. Pappula, "Near Real Time Crop Loss Estimation using Remote Sensing Observations," 2019 8th International Conference on Agro-Geoinformatics (Agro-Geoinformatics), 2019, pp. 1-5, doi: 10.1109/Agro-Geoinformatics.2019.8820217.

[146] S. Jones and J. Saniie, "Using Deep Learning and Satellite Imagery to Assess the Damage to Civil Structures After Natural Disasters," 2019 IEEE International Conference on Electro Information Technology (EIT), 2019, pp. 189-193, doi: 10.1109/EIT.2019.8833724.

[147] Y. Sofue, C. Hongo, N. Manago, G. Sigit, K. Homma and B. Barus, "Estimation of Normal Rice Yield Considering Heading Stage Based on Observation Data and Satellite Imagery," 2021 IEEE International Geoscience and Remote Sensing

Symposium IGARSS, 2021, pp. 6439-6442, doi: 10.1109/IGARSS47720.2021.9554679.

[148] G. Sravan Kumar, S. Venkatramaphanikumar and K. Venkata Krishna Kishore, "Smart Farming - A Flexible Approach to Improve Crop Yield and Profit using Machine Learning Techniques," 2021 2nd International Conference for Emerging Technology (INCET), 2021, pp. 1-6, doi: 10.1109/INCET51464.2021.9456433.

[149] D. Lakmal, K. Kugathasan, V. Nanayakkara, S. Jayasena, A. S. Perera and L. Fernando, "Brown Planthopper Damage Detection using Remote Sensing and Machine Learning," 2019 18th IEEE International Conference On Machine Learning And Applications (ICMLA), 2019, pp. 97-104, doi: 10.1109/ICMLA.2019.00024.

[150] S. Haque, N. Rahman and M. Mostakim, "Classification Of Damaged Vegetation Areas Using Convolutional Neural Network Over Unlabelled Sentinel-2 Images," 2021 26th International Conference on Automation and Computing (ICAC), 2021, pp. 1-7, doi: 10.23919/ICAC50006.2021.9594269.